

ScreeNOT: Exact MSE-Optimal Singular Value Thresholding in Correlated Noise

David Donoho¹, Matan Gavish² and Elad Romanov¹

¹Department of Statistics, Stanford University, e-mail: donoho@stanford.edu; eromanov@stanford.edu

²School of Computer Science and Engineering, Hebrew University of Jerusalem, e-mail: gavish@cs.huji.ac.il

Abstract: We derive a formula for optimal hard thresholding of the singular value decomposition in the presence of correlated additive noise; although it nominally involves unobservables, we show how to apply it even where the noise covariance structure is not a-priori known or is not independently estimable. The proposed method, which we call **ScreeNOT**, is a mathematically solid alternative to Cattell’s ever-popular but vague Scree Plot heuristic from 1966. ScreeNOT has a surprising oracle property: it typically achieves *exactly*, in large finite samples, the lowest possible MSE for matrix recovery, on each given problem instance – i.e. the specific threshold it selects gives exactly the smallest achievable MSE loss among all possible threshold choices for *that* noisy dataset and *that* unknown underlying true low rank model. The method is computationally efficient and robust against perturbations of the underlying covariance structure. Our results depend on the assumption that the singular values of the noise have a limiting empirical distribution of compact support; this property, which is standard in random matrix theory, is satisfied by many models exhibiting either cross-row correlation structure or cross-column correlation structure, and also by many situations with more general, inter-element correlation structure. Simulations demonstrate the effectiveness of the method even at moderate matrix sizes. The paper is supplemented by ready-to-use software packages implementing the proposed algorithm: package **ScreeNOT** in Python (via PyPI) and R (via CRAN).

AMS 2000 subject classifications: Primary 62C20, 62H25; secondary 90C25, 90C22.

Keywords and phrases: Singular Value Thresholding, Optimal Threshold, Scree Plot, Low-rank Matrix Denoising, High-Dimensional Asymptotics.

1. Introduction

Across a wide variety of scientific and technical fields, practitioners have found many valuable applications of *singular value thresholding* (SVT). This procedure starts from the singular value decomposition (SVD), which represents the data matrix Y as

$$Y = \sum_{i=1}^{\min(n,p)} y_i \cdot \mathbf{u}_i \mathbf{v}_i^\top, \quad (1.1)$$

using the empirical singular values $\{y_i\}_{i=1}^{\min(n,p)}$, and the empirical left- and right- singular vectors of Y , denoted here \mathbf{u}_i and \mathbf{v}_i .

In such applications, it is generally claimed that the small singular values represent ‘noise’ and the large singular values ‘signal’; practitioners attempt to separate signal from noise by setting a threshold θ (say), and using, in place of Y , the partial reconstruction containing only would-be signal components:

$$\hat{X}_\theta = \sum_i y_i \mathbb{1}_{\{y_i > \theta\}} \cdot \mathbf{u}_i \mathbf{v}_i^\top. \quad (1.2)$$

How do practitioners determine the threshold θ ? Often, by eye. They plot the ordered singular values and spot ‘elbows’. Sometimes, they give this a scholarly veneer by saying they are using the ‘scree-plot method’; they might even formally cite the originator of this folk-tradition [12], which still gets more than 1000 citations yearly. According to the method prescribed in that paper, the practitioner plots the values $\{y_i\}$ and uses her *eyes* to distinguish between ‘signal’ and ‘noise’ singular values of Y .

How *should* they determine the threshold? Relevant theory and methodology literature spans multiple disciplines over multiple decades; we mention only a few entry points, including: [36, 21, 24, 16, 2, 1, 3,

23, 31, 19, 11, 28, 30, 13, 18, 14]. Progress has been made in our understanding of the underlying problem, and many valuable quantitative approaches have been developed - to which we here add one more. Our contribution relies on recent advances in random matrix theory which point, we think convincingly, to the method introduced here. This method typically offers the exact optimal loss available on each specific, finite dataset Y .

Our task formalization supposes that: (a) there is an underlying matrix X of fixed rank r - though X and even its rank r are unknown to us; (b) only a potentially loose upper bound on the signal rank r is known; (c) the data matrix Y has the signal+noise form $Y = X + Z$, where Z is a noise matrix with a general covariance structure - also unknown to us; (d) we use hard thresholding of singular values, exactly as in (1.2) above¹; (e) we adopt squared error *loss*²:

$$\text{SE}[X|\theta] = \|\hat{X}_\theta - X\|_F^2. \quad (1.3)$$

As goal, we literally aim to choose a loss-minimizing value $\theta_{\text{opt}} = \theta_{\text{opt}}(Y|X)$ solving:

$$\text{SE}[X|\theta_{\text{opt}}] = \min_{\theta} \text{SE}[X|\theta]. \quad (1.4)$$

Aiming for $\theta_{\text{opt}}(Y|X)$ may seem overambitious, as we know only the data matrix Y , and not X . Wait and see.

Essentially this problem was studied previously by two of the authors in the special case of white noise. [18] supposed that the underlying noise Z matrix has i.i.d Gaussian zero-mean entries and the problem is scaled so that the columns of Z have unit Euclidean squared norm in expectation, and considered a sequence of increasingly large problems. In the square case, when Y has as many rows as columns: the authors found results³ which, in light of our results below, say that, with eventually overwhelming probability, we have $\theta_{\text{opt}} = 4/\sqrt{3}$. Their analysis relied on then-recent advances in the ‘Johnstone spiked model’ of random matrix theory [22]; they proposed a method for white noise with unknown variance, where the threshold formula became $\theta_{\text{opt}} \approx 4/\sqrt{3} \cdot \frac{y_{\text{med}}}{\sqrt{n \cdot 6528}}$, where y_{med} denotes the median empirical singular value of Y .⁴

Understanding the white noise case cannot be the end of the story. Practitioners ordinarily don’t know that their noise is white, and in fact realistic noise models can include correlations between columns, rows, or even general row-column combinations. Fortunately, a broad range of noise models can be studied using appropriate advances that have been made in random matrix theory. In this broader context, as we show, a more general formula for the optimal threshold can be given, which of course reduces to $4/\sqrt{3}$ in the above ‘square-matrix in white noise’ case, but which is inevitably quite a bit more sophisticated in general.

Section 2 below describes **ScreeNOT**, our proposed deployment of this formula on actual data. The acronym NOT stands for *Noise-adaptive Optimal Thresholding*; ‘adaptive’ refers to the algorithm’s optimality across a wide range of unknown noise covariances. The prefix ‘Scree’ reminds us that, still today, in many cases, the alternative would simply be ‘eyeballing’ the Scree Plot [12]. Cattell and his many followers clearly believed that *something*, some visible feature, in the Scree Plot – namely, in the collection of data singular values $\{y_i\}$ – could tell us where the noise stopped and the signal began. But what exactly? In a very concrete sense, the ScreeNOT algorithm shows that the information needed to separate signal from noise truly *is* there in the distribution of empirical singular values, where Cattell and his followers all hoped it would be. However, the ScreeNOT algorithm and the approach we develop here quantitatively identify this information as a specific *functional of the CDF of singular values*.

The method, once implemented, surprised us by the *finite-sample* optimality it exhibited; in simulations at reasonable problem sizes it typically achieves the exact minimal loss (1.4) for the given dataset, even though the method is not entitled to know the underlying low-rank model X or specifics of the noise model on Z ; we initially expected a weaker and more ‘asymptotic’ optimality property, perhaps similar to the one shown in [18]. Our analysis below proves typicality of such exact optimality in finite samples. This strong optimality is partly due to the penetrating nature of random matrix theory; but also to the very specific task: minimizing squared error loss (1.3) of singular value thresholding (1.2).

¹And not some variant, such as soft thresholding or a more general shrinkage.

² $\|X\|_F^2 = \sum_{i,j} X_{i,j}^2$ denotes the squared Frobenius norm.

³That is, the authors of [18] adopted a slightly different viewpoint involving asymptotic MSE, and showed that $4/\sqrt{3}$ is optimal, whereas we consider here exact finite sample MSE loss, and show that with eventually overwhelming probability, $4/\sqrt{3}$ is exactly optimal *on each typical realization*.

⁴ $\sqrt{6528}$ is approximately the median of the standard quarter-circle law; see the original paper.

Underlying Analysis Hoping to make the paper helpful to prospective users of the proposed method, we have made the Introduction and also Section 2 mostly independent of the analysis to come; however, we now very briefly offer mathematically-oriented readers some insight about the approach being followed in later sections and the tools being developed there.

At heart, this paper concerns the asymptotic analysis of a sequence of matrix recovery problems where the problem sizes n and p grow to ∞ in a proportional fashion. We assume that the matrix X has r nonzero singular values x_1, \dots, x_r which are fixed independently of n and p . About the sequence of random noise matrices $Z = Z_{n,p}$, we assume that the sequence of empirical cumulative distribution functions (CDF's) of noise singular values converges to a compactly supported distribution F_Z with certain qualitative restrictions at boundary of the support.

Using results of Benaych-Georges and Nadakuditi [10], we obtain an expression for an asymptotically optimal hard threshold, as a *functional* $T(\cdot)$ of the limiting CDF of noise singular values F_Z . The functional is continuous and even differentiable in certain senses.

Admittedly, the limiting CDF of noise singular values F_Z is not observable to the statistician, as we only observe a sample of the signal+noise singular values mixed together. Performing a kind of amputation and prosthetic extension on the CDF F_Y of singular values of Y , which we do observe, we construct a modified empirical CDF \hat{F}_n which consistently estimates the limiting CDF of noise-only singular values. Applying the hard threshold selection functional to this modified empirical CDF \hat{F}_n gives our proposed method, in the form $\hat{\theta} = T(\hat{F}_n)$. As we show in Section 2, there is a quite explicit and computationally tractable algorithm for computing $T(\hat{F}_n)$, which we label **ScreeNOT**.

Owing to the continuity of the hard threshold functional $T(\cdot)$, and the consistency of the constructed CDF, the resulting method is a consistent estimator of the underlying asymptotically optimal threshold $T(F_Z)$. We also prove a finite-sample optimality of the method. Specifically, the ScreeNOT algorithm is shown to be exactly optimal for squared error loss with high probability, in large-enough finite samples, under very general model assumptions. For generic configurations of signal singular values $(x_i)_{i=1}^r$, there is, in large finite samples, an *optimal interval* of thresholds, all achieving the optimal MSE at that realization; the consistency of the optimal threshold estimator implies that eventually for large-enough n , with overwhelming probability, the proposed method achieves the exact optimal MSE loss.

Contributions The approach we develop selects an optimal threshold for singular values, and thus selects the “signal” singular values, based on the principle of minimizing SE. Indeed, minimizing squared error loss is a ubiquitous goal in statistical theory, and we are not the first to consider it as a goal for threshold selection in the context of singular values. In addition to our own just-cited work [18], prior citable work on squared-error-loss includes Perry [30], Shabalin and Nobel [32] and Nadakuditi [26], although much of this concerns singular value shrinkage rather than thresholding⁵. While our approach is implemented for SE loss, we note that it could in principle be used to develop optimal thresholding rules for other loss criteria, such as the operator norm.

We especially point to [14]; in this work Dobriban and Owen mainly study Parallel Analysis [17] — simulation-based significance testing for large singular values; they develop tools from Random Matrix Theory to derandomize Parallel Analysis⁶. Beyond this, they also mention in a final section that their tools could be adapted to produce a threshold selector minimizing the asymptotic mean-squared error of the resulting approximation; and their equation (6) provides a way to characterize such a functional.

In this paper, we make explicit (in Equation 4.5 below) the functional T for threshold selection with minimal asymptotic SE, and show that it is well-defined; we offer (in Section 2.3) an explicit construction of a modified CDF \hat{F}_n to plug in to T - the proposal involves singular value “ablation and prosthesis”; we develop a theoretical machinery, involving continuity properties of T and convergence properties of \hat{F}_n , and use the machinery to prove that $T(\hat{F}_n)$ achieves not just asymptotic optimal loss (Theorem 1), but also (Theorem 2) that in large finite samples it achieves the exact minimal loss with overwhelming probability.

Outline. This paper is organized as follows. In Section 2 we offer a practical, succinct description of the ScreeNOT algorithm, for the convenience of prospective users. In Section 3 we introduce the signal+noise

⁵Singular value shrinkage is considerably more involved as it changes the data singular values rather than select them. The best-possible relative improvement of shrinkage over thresholding was studied in [18] in the white noise case.

⁶Potential users of ScreeNOT should note that in many scientific projects the goal is determining the number of statistically significant factors, without particular regard to the quality of squared-error approximation; it is possible that for such a goal Parallel Analysis or its derandomized version [14] is preferred.

model used and survey relevant results from random matrix theory. In Section 4 we state our main results regarding the optimality and stability properties of ScreeNOT, both in finite matrix size and asymptotically as the matrix size grows to infinity. In Section 5 we demonstrate the mathematical results in various simulations and numerical examples; for space considerations only a handful of figures are shown, with most simulation results deferred to the supplementary article and available in the code supplement [15]. The results are proved in Section 6, with some proofs referred to the supplementary article.

Reproducibility advisory. Implementation of the proposed algorithm, scripts generating all figures in this paper, and many additional simulations have been permanently deposited and are available at the code supplement [15].

Code packages. Ready-to-use code packages, implementing the ScreeNOT procedure in various language are available. In **Python**: package **ScreeNOT** is available through PyPI; in **R**: package **ScreeNOT** is available through CRAN; and **Matlab** source code. For details, see the following GitHub repository: <https://github.com/eladromanov/ScreeNOT>. In addition, the source code has been permanently deposited and is available at the code supplement [15].

2. The ScreeNOT Procedure: User-level description

In this section we give a brief self-contained description of our proposed procedure.

2.1. Procedure API

ScreeNOT selects a hard threshold for singular values, which can in finite samples give the optimal MSE approximation of a low rank matrix from a noisy version; the noise may be correlated, and the threshold will adapt to that appropriately.

2.1.1. Inputs

The user provides these inputs to ScreeNOT:

- y**: the singular values $y_1 \dots, y_{\min(n,p)}$ of the data matrix Y ;
- n, p : size parameters of the data matrix Y .
- k : upper bound on the rank r of the underlying unknown signal matrix X which is to be recovered.
This upper bound may be very loose.

2.1.2. Outputs

ScreeNOT returns $\hat{\theta} = \hat{\theta}(Y)$, the value to be used in singular value thresholding.

To use the threshold, the user should reconstruct an approximation to the underlying signal matrix X using the empirical singular values y_i and the empirical singular vectors \mathbf{u}_i and \mathbf{v}_i as follows:

$$\hat{X} = \sum_i y_i \mathbb{1}_{\{y_i > \hat{\theta}\}} \cdot \mathbf{u}_i \mathbf{v}_i^\top.$$

In this reconstruction, the singular values smaller than $\hat{\theta}$ are judged to be noise and the corresponding singular decomposition components are ignored.

2.2. Example in a stylized application

We next construct a synthetic-data example, in which we know the ground truth for demonstration purposes. The synthetic data $Y = X + Z$ and the invocation of ScreeNOT are based on these ingredients.

Signal X : The underlying signal matrix, unbeknownst to the hypothetical user, has rank 10, with singular values $(x_{10}, \dots, x_1) = (1.0, 1.15, 1.3, \dots, 2.35)$.

Noise Z : The underlying noise, unbeknownst to the hypothetical user, follows an $AR(1)$ process in the row index, within each column. The $AR(1)$ process has parameter $\rho = 0.4$, and additionally each entry is divided by \sqrt{n} , so to have variance⁷ $1/n$.

Problem Size: $n = p = 1000$

Rank bound: $k = 15$. The user specifies a bound of $k = 15$ on the possible rank of the signal.

Figure 1 shows a so-called *Scree Plot* [12] of the first 30 empirical singular values y_i . For this particular instance, it is verified (by exhaustive search) that the minimal loss is attained by retaining the first three principal components of Y ; in other words, thresholding at any point $\theta \in (y_3, y_4)$ is optimal. The threshold $\hat{\theta}$ returned by the ScreenNOT procedure is indicated by the green horizontal line, and, indeed, it falls inside the optimal interval. The would-be “elbow” in the scree-plot, determined subjectively by the authors, is indicated by the grey (lower) horizontal line; it corresponds to retaining the top 6 principal components of the data matrix. This rule attains strictly sub-optimal SE: roughly 31.3, as opposed by 26.4 attained by ScreenNOT.

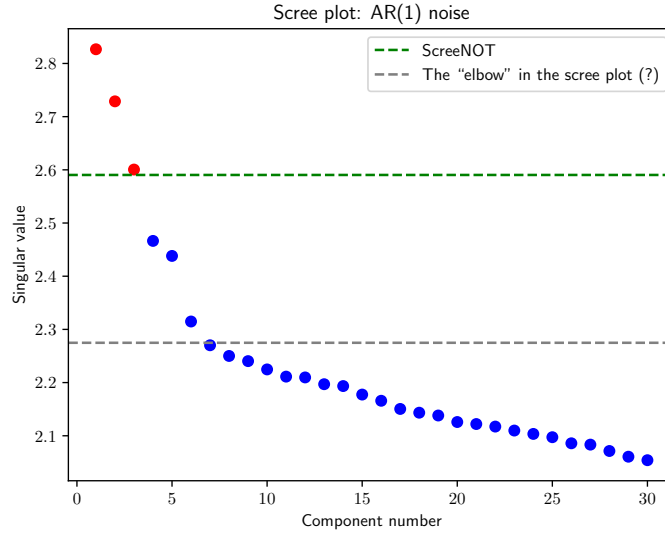


Fig 1: Scree Plot for the stylized example of Section 2.2. Horizontal axis: singular value index, where the singular values y_i of the data matrix Y are sorted in decreasing order. Vertical axis: singular values y_i . Dashed green (upper) line: the optimal threshold calculated by ScreenNOT. (Color online.)

2.3. Internals of the Procedure

We briefly describe the computational task performed by ScreenNOT.

Step 1. Sort the singular values in non-increasing order: $y_1 \geq \dots \geq y_p$.

Step 2. Compute the “pseudo singular values”:

$$\tilde{y}_i = y_{k+1} + \frac{1 - \left(\frac{i-1}{k}\right)^{2/3}}{2^{2/3} - 1} (y_{k+1} - y_{2k+1}) \quad \text{for } i = 1, \dots, k,$$

and set $\tilde{y}_i = y_i$ for $i = k+1, \dots, p$.⁸

Step 3. Define the four scalar functions $\varphi, \tilde{\varphi}, \varphi', \tilde{\varphi}'$ by

$$\varphi(y) = \frac{1}{p} \sum_{i=1}^n \frac{y}{y^2 - \tilde{y}_i^2}, \quad \varphi'(y) = -\frac{1}{p} \sum_{i=1}^n \frac{y^2 + \tilde{y}_i^2}{(y^2 - \tilde{y}_i^2)^2},$$

⁷That is, the columns of Z are independent and distributed as \mathbf{z}/\sqrt{n} , where the random vector \mathbf{z} has entries: $z_1 = \varepsilon_1$ and $z_i = \rho \cdot z_{i-1} + \sqrt{1 - \rho^2} \cdot \varepsilon_i$ for $2 \leq i \leq p$, where $\varepsilon_1, \dots, \varepsilon_p \stackrel{\text{iid}}{\sim} \mathcal{N}(0, 1)$.

⁸We assume $2k+1 < p$. Our proposed estimator is expected to perform poorly when k is large compared to p .

and

$$\tilde{\varphi}(y) = \gamma\varphi(y) + \frac{1-\gamma}{y}, \quad \tilde{\varphi}'(y) = \gamma\varphi'(y) - \frac{1-\gamma}{y^2}.$$

Now define

$$\Psi(y) = y \cdot \left(\frac{\varphi'(y)}{\varphi(y)} + \frac{\tilde{\varphi}'(y)}{\tilde{\varphi}(y)} \right).$$

Step 4. Assuming that $\tilde{y}_1, \dots, \tilde{y}_p$ are not all zero, the function $y \mapsto \Psi(y)$ can be shown to be continuous and strictly increasing for $y > \tilde{y}_1$. Moreover, $\lim_{y \searrow \tilde{y}_1} \Psi = -\infty$ and $\Psi(\infty) = -2$. The computed hard threshold is the unique value $\hat{\theta}$ satisfying

$$\Psi(\hat{\theta}) = -4. \quad (2.1)$$

This equation is then solved numerically, for example by binary search.⁹

Step 5. The algorithm returns the value $\hat{\theta}$.

Evidently, the procedure as stated costs $O(n \log(n))$ flops; the dominant cost is sorting the singular values; ordinarily of course, sorting is performed anyway as part of a standard SVD. In that situation, the additional computational effort is $O(n)$, which is unimportant compared to the cost of the underlying SVD.

2.4. How the procedure works on the stylized application

Figure 2(a) shows a plot of $\Psi(\theta)$ as a function of θ . The horizontal blue line indicates the desired level -4 . The vertical green line indicates the crossing point, $\hat{\theta}$, which is the value returned by ScreenNOT.

Figure 2(b) shows a plot of the loss $SE[\theta|X]$ versus θ . The red horizontal line shows the optimum achievable loss. The green vertical line shows the threshold selected by the procedure. It intersects the loss curve within the optimal level and the achieved loss is therefore optimal.

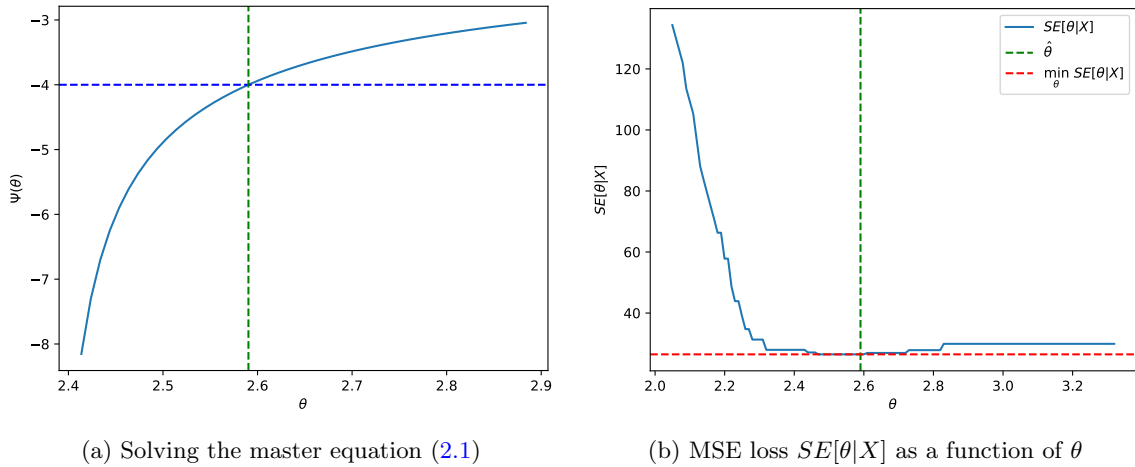


Fig 2: Calculation of the optimal threshold $\hat{\theta}$ on the stylized example of Section 2.2. (a) *Left panel:* Horizontal axis: candidate thresholds θ . Vertical axis: The function $\Psi(\theta)$. The ScreenNOT algorithm solves the equation $\Psi(\theta) = -4$ for θ . Vertical green line shows the solution, denoted by $\hat{\theta}$. This is the value returned by ScreenNOT. (b) *Right panel:* The MSE loss function $SE[\theta|X]$ for the stylized example of Section 2.2, plotted over candidate thresholds θ . There is an interval of values θ all achieving the lowest possible loss; The threshold $\hat{\theta}$ returned by ScreenNOT (shown by the vertical green line) is located inside this optimal interval. (Color online.)

⁹We remark that the computational cost of this search is not considerable. E.g., binary search requires a number of iterations which is only logarithmic in the required precision.

3. Setup and background from random matrix theory

The rest of this paper is dedicated to formal analysis of the ScreeNOT algorithm. To that end, we now define a precise signal+noise model and set up the necessary notation.

An asymptotic model for low-rank matrices observed in additive noise To recap, let X_n be an unknown n -by- p matrix, to be estimated. We observe a noisy measurement of X_n , $Y_n = X_n + Z_n$, where Z_n is a noise matrix, which is statistically independent of X_n . Our analysis employs an asymptotic framework originating in Random Matrix Theory, and considers a sequence of such problems $n, p \rightarrow \infty$, with the following generative assumptions.

1. **Limiting shape:** the dimensions n, p tend to infinity together at a fixed ratio $p/n \rightarrow \gamma$. More concretely, fix $\gamma \in (0, 1]$ and set $p = p_n = \lceil \gamma n \rceil$. Denoting $\gamma_n = p_n/n$, of course, $\gamma \leq \gamma_n < \gamma + \frac{1}{n}$ and $\gamma_n \rightarrow \gamma$ as $n \rightarrow \infty$.
2. **Fixed signal rank and singular values:** The matrix X_n has fixed rank $r = \text{rank}(X_n)$ and fixed singular values. Specifically, let r be constant, and fix r positive and distinct numbers $x_1 > \dots > x_r > 0$. X_n is the matrix

$$X_n = \sum_{i=1}^r x_i \mathbf{a}_{i,n} \mathbf{b}_{i,n}^\top,$$

where $\mathbf{a}_{i,n} \in \mathbb{R}^n$ (resp. $\mathbf{b}_{i,n} \in \mathbb{R}^p$) for $i = 1, \dots, r$ are sequences of left (resp. right) singular vectors of X_n , obeying a generative assumption as described next. We let $\mathbf{x} = (x_1, \dots, x_r)$ denote the vector of singular values and we refer to either the matrix X or just \mathbf{x} as the *signal*¹⁰.

3. **Incoherent signal singular vectors.** The vectors $\mathbf{a}_{1,n}, \dots, \mathbf{a}_{r,n}$ (resp. $\mathbf{b}_{i,n}$) constitute a random, uniformly distributed orthonormal r -frame in \mathbb{R}^n (resp. in \mathbb{R}^p).¹¹
4. **Compactly supported, limiting bulk distribution of noise singular values.** Each matrix Z_n is statistically independent of X_n . Let $z_{1,n}, \dots, z_{p,n}$ denote its singular values, with empirical CDF F_{Z_n} , $F_{Z_n}(z) = p^{-1} \sum_{i=1}^p \mathbb{1}_{\{z_{i,n} \leq z\}}$. There is a *limiting empirical CDF* (LECDF) F_Z such that $F_{Z_n} \rightarrow F_Z$ a.s. at continuity points.

Moreover, we assume that F_Z is compactly supported¹² and denote the upper edge of the support (sometimes called the *noise bulk edge*) by

$$\mathcal{Z}_+ \equiv \mathcal{Z}_+(F_Z) = \sup \{z : F_Z(z) < 1\}.$$

We also assume that F_Z is nontrivial (dF_Z is not a single atom at $z = 0$), in other words, $\mathcal{Z}_+(F_Z) > 0$. Note that neither the distribution F_Z nor its bulk edge $\mathcal{Z}_+(F_Z)$ are assumed to be known to the statistician.

5. **No outliers straying from the bulk.** Asymptotically, no singular values of Z_n can be found above the bulk edge:

$$z_{1,n} = \|Z_n\| \xrightarrow{\text{a.s.}} \mathcal{Z}_+(F_Z).$$

6. **Thickness of the bulk edge.** The following condition holds:

$$\lim_{y \rightarrow \mathcal{Z}_+(F_Z)} \int (y - z)^{-2} dF_Z(z) = \infty,$$

where the limit is taken from the right. That is, F_Z puts “sufficient” mass near the upper edge of its support. Under this condition, when the signal singular values x_i are sufficiently small, the amount

¹⁰The assumption that the x_i -s are all distinct is standard in the literature on singular value shrinkage in the spiked model. When there are multiplicities, the SVD of X_n is not uniquely defined and, consequently, some framing constructs we use in this paper become inapplicable. The reframings adapted to such degenerate situations are beyond our scope. At any rate, the distinctness condition is generic in the space of matrices.

¹¹In other words, $\mathbf{a}_{1,n}, \dots, \mathbf{a}_{r,n}$ are sampled from the $O(n)$ -invariant distribution on the Stiefel manifold $V_r(\mathbb{R}^n)$. Equivalently, one can assume that $\mathbf{a}_{i,n}$ and $\mathbf{b}_{i,n}$ are any arbitrary sequences of orthonormal r -frames, and the distribution of Z_n is invariant to multiplication by $O(n)$ to the left and by $O(p)$ to the right.

¹²This assumption might seem unnatural to many statisticians when they first encounter it; but note that if Z_n is a standard Gaussian white noise, then even though the distribution of matrix entries is not compactly supported, the limiting bulk distribution of singular values is compactly supported, in $[(1 - \sqrt{\gamma}), (1 + \sqrt{\gamma})]$.

of “information” one can obtain about the corresponding singular vectors $\mathbf{a}_{i,n}\mathbf{b}_{i,n}^\top$ from the leading singular vectors of Y_n also vanishes.

This assumption is by no means esoteric. For example, suppose that F_Z has a continuous density f_Z in a neighborhood of $z_+ = \mathcal{Z}_+(F_Z)$, where it behaves like $f_Z(z) \sim C(z - z_+)^\alpha$ as $z \rightarrow z_+$; here $\alpha > 0$ is some exponent. Then this condition holds whenever $\alpha \leq 1$. In Section 3.2, we mention a broad class of noise matrices Z_n for which this property holds with $\alpha = 1/2$.

Class of estimators and performance measure Our goal is to estimate X_n . We consider the family of singular value hard-thresholding estimators: $\hat{X}_\theta = \hat{X}_\theta(Y_n)$, where

$$\hat{X}_\theta = \sum_{i=1}^p y_{i,n} \mathbb{1}_{\{y_{i,n} > \theta\}} \cdot \mathbf{u}_{i,n} \mathbf{v}_{i,n}^\top, \quad (3.1)$$

where $Y_n = \sum_{i=1}^p y_{i,n} \mathbf{u}_{i,n} \mathbf{v}_{i,n}^\top$ is an SVD. To ensure that the vectors $\{\mathbf{u}_{i,n}, \mathbf{v}_{i,n}\}$ are well-defined, even when there are multiplicities in the spectrum, the right singular vectors $\mathbf{v}_{i,n}$ corresponding to a degenerate singular value of Y_n are chosen to be a random (Haar distributed) orthonormal basis for the corresponding (right) singular subspace. (Accordingly, the corresponding $\mathbf{u}_{i,n}$ -s constitute a random orthonormal basis for the corresponding left singular subspace.) We measure the error with respect to Frobenius norm (squared error)¹³, where we denote:

$$\text{SE}_n[\mathbf{x}|\theta] = \left\| X_n - \hat{X}_\theta(Y_n) \right\|_F^2. \quad (3.2)$$

Our task is to choose θ , so as to make $\text{SE}_n[\mathbf{x}|\theta]$ as small as possible, in an appropriate sense (note that $\text{SE}_n[\mathbf{x}|\theta]$ is a random variable - we *do not* take the expectation of X_n and Y_n). The best possible performance is given by the *Oracle Loss*

$$\text{SE}_n^*[\mathbf{x}] = \min_{\theta \geq 0} \text{SE}_n[\mathbf{x}|\theta], \quad (3.3)$$

which is the best loss one can achieve over the family of singular value hard-threshold estimators, *even knowing the true signal* X_n . Our goal in this paper is to develop a threshold-selector that, “typically for large n ”, attains the oracle loss $\text{SE}_n^*[\mathbf{x}]$. Note that the oracle loss $\text{SE}_n^*[\mathbf{x}]$ is also a random variable, and it is not a priori clear how to estimate it. An important observation is that the (random) function $\theta \mapsto \text{SE}_n[\mathbf{x}|\theta]$ is piecewise constant, with finitely many jumps (specifically, these are at the singular values of Y_n : $y_{1,n}, \dots, y_{p,n}$). In particular, the minimum of $\text{SE}_n[\mathbf{x}|\theta]$ is attained not strictly at a point, but on an *interval* (or a union of intervals).

3.1. Background from random matrix theory

The Spiked Model Our perspective on the matrix denoising problem extends the one proposed by Perry [30] and Shabalin and Nobel [32]. In the model they proposed, which was inspired by Johnstone’s Spiked Covariance model [22], one works under the same model $Y_n = X_n + Z_n$ as described above, but specifically assumes that the noise matrix Z_n is column-normalized and white, namely, that its entries are properly scaled *i.i.d* random variables. This model’s close sibling, the Spiked Model for high-dimensional covariance, has been extensively studied in the probability and statistics literature, to such an extent that we cannot point to all of the existing literature here. Seminal works such as [5, 9, 29] and others have shown that the randomness in the Spiked Model can be neatly described in terms of the so-called BBP phase transition, similar to the one discovered in [8]; and of the displacement of the sample eigenvalues relative to the population eigenvalues; and of the rotation of the sample eigenvectors relative to the populations eigenvectors.

In the matrix denoising setup we consider here, the model described by our assumptions above has been studied in [10], and the same three underlying phenomena were identified and quantified:

1. **BBP phase transition:** Let $z_+ = \mathcal{Z}_+(F_Z)$ denote the noise bulk edge. There is a functional $\mathcal{X}_+(F_Z, \gamma)$ that depends on the LECDF F_Z and the asymptotic shape γ that defines an important threshold

¹³Recall that for a matrix A , $\|A\|_F^2 = \sum_{i,j} |A_{i,j}|^2$.

phenomenon in the behavior of limiting empirical singular values. Setting $x_+ = \mathcal{X}_+(F_Z, \gamma)$, then for any $i = 1, \dots, r$ where $x_i \leq x_+$,

$$y_{i,n} \xrightarrow{a.s.} z_+, \quad n \rightarrow \infty. \quad (3.4)$$

In short, *sufficiently small signal singular values x_i do not produce outliers beyond the noise bulk edge*. As we are about to see, the situation for $x_i > x_+$ is quite different. The split between $x_i \geq x_+$ is sometimes called the Baik-Ben Arous-Péché (BBP) phase transition, after the original example of this type [8].

2. **Limiting location of outlier singular values:** The limiting value of $y_{i,n}$ is *not* its underlying population counterpart x_i . There is instead a functional $\mathcal{Y}(x; F_Z, \gamma)$, depending on F_Z and γ , describing this limiting behavior. The function of x obtained by fixing F_Z , and $\gamma - \mathcal{Y}(x) \equiv \mathcal{Y}(x; F_Z, \gamma) - \gamma$ explains how the asymptotic limit varies with theoretical singular value x . For any $i = 1, \dots, r$ where $x_i \geq x_+ \equiv \mathcal{X}_+$,

$$y_{i,n} \xrightarrow{a.s.} y_{i,\infty} = \mathcal{Y}(x_i), \quad n \rightarrow \infty. \quad (3.5)$$

The function $x \mapsto \mathcal{Y}(x)$ is strictly increasing and one-to-one between $[x_+, \infty)$ and $[z_+, \infty)$.

3. **No limiting cross-correlation of non-corresponding principal subspaces:** For $i \neq j$, the empirical dyad $\mathbf{u}_{n,i} \mathbf{v}_{n,i}^\top$ ultimately decorrelates from each of the non-corresponding population dyads $\mathbf{a}_{n,j} \mathbf{b}_{n,j}^\top$. For any $i, j = 1, \dots, r$ such that $i \neq j$,

$$\langle \mathbf{a}_{n,i}, \mathbf{u}_{n,j} \rangle \cdot \langle \mathbf{b}_{n,i}, \mathbf{v}_{n,j} \rangle \xrightarrow{a.s.} 0, \quad n \rightarrow \infty. \quad (3.6)$$

4. **Limiting cross-correlation of corresponding principal subspaces:** Suppose the signal singular values $(x_i)_{i=1}^r$ are distinct. The empirical dyad $\mathbf{u}_{n,i} \mathbf{v}_{n,i}^\top$ *does* correlate with its theoretical counterpart $\mathbf{a}_{n,i} \mathbf{b}_{n,i}^\top$, but not perfectly. The limit is described by a functional $\mathcal{C}(x; F_Z, \gamma)$ depending on x , F_Z and γ . Fixing once again F_Z and γ , we get a function of x , $\mathcal{C}(x) \equiv \mathcal{C}(x; F_Z, \gamma)$, such that, with $x_+ = \mathcal{X}_+(F_Z, \gamma)$,

$$\langle \mathbf{a}_{n,i}, \mathbf{u}_{n,i} \rangle \cdot \langle \mathbf{b}_{n,i}, \mathbf{v}_{n,i} \rangle \xrightarrow{a.s.} \begin{cases} \mathcal{C}(x_i) & x_i > x_+ \\ 0 & x_i \leq x_+ \end{cases}. \quad (3.7)$$

We now give formulas for \mathcal{X}_+ and the mappings $\mathcal{Y}(\cdot)$ and $\mathcal{C}(\cdot)$, as computed in [10]. For a CDF H , let

$$\varphi(y; H) = \int \frac{y}{y^2 - z^2} dH(z), \quad (3.8)$$

which defines a smooth function on $y > \mathcal{Z}_+(H)$. Its derivative is

$$\varphi'(y; H) = - \int \frac{y^2 + z^2}{(y^2 - z^2)^2} dH(z). \quad (3.9)$$

Also define

$$\tilde{\varphi}_\gamma(y; H) = \gamma \varphi(y; H) + \frac{(1 - \gamma)}{y}, \quad \tilde{\varphi}'_\gamma(y; H) = \gamma \varphi'(y; H) - \frac{1 - \gamma}{y^2}. \quad (3.10)$$

Note that $\tilde{\varphi}_\gamma(y; H)$ is simply $\varphi(y; \tilde{H}_\gamma)$, where $\tilde{H}_\gamma(z) = \gamma H(z) + (1 - \gamma) \mathbb{1}_{\{z \geq 0\}}$. This so-called *companion CDF* \tilde{H}_γ describes the same distribution of nonzero singular values as H , diluted by ‘zero padding’ and has the following interpretation: if Z_n is a sequence of n -by- p matrices with a limiting singular value distribution H , then Z_n^\top has a limiting singular value distribution \tilde{H}_γ ¹⁴. Let

$$\begin{aligned} \mathcal{D}_\gamma(y; H) &\equiv \varphi(y; H) \cdot \tilde{\varphi}_\gamma(y; H), \\ \mathcal{D}'_\gamma(y; H) &\equiv \varphi'(y; H) \cdot \tilde{\varphi}_\gamma(y; H) + \varphi(y; H) \cdot \tilde{\varphi}'_\gamma(y; H). \end{aligned} \quad (3.11)$$

¹⁴Practitioners will recognize that computer software often offers two options for SVD outputs, a ‘fat’ output with zero padding and a ‘thin’ output with those superfluous zeros stripped away. If H denotes the LECDF of the ‘thin’ output singular values, then \tilde{H} is the corresponding LECDF of the ‘fat’ outputs.

To ease the notation in coming paragraphs, we put for short $\mathcal{D}_\gamma(y) = \mathcal{D}_\gamma(y; F_Z, \gamma)$, and similarly for $\varphi(y)$, $\tilde{\varphi}_\gamma(y)$. Let $z_+ = \mathcal{Z}_+(F_Z)$ denote the bulk edge. The BBP phase transition location $x_+ = \mathcal{X}_+(F_Z, \gamma)$ is given by

$$x_+ = \lim_{y \rightarrow z_+} (\mathcal{D}_\gamma(y))^{-1/2}, \quad (3.12)$$

equivalently, $1/x_+^2 = \lim_{y \rightarrow z_+} \mathcal{D}_\gamma(y)$. It is easy to verify that $\varphi(y)$, $\tilde{\varphi}_\gamma(y)$ and $\mathcal{D}_\gamma(y)$ are non-negative, strictly decreasing functions of $y > z_+$, each tending to 0 as $y \rightarrow \infty$. Thus, $\mathcal{D}_\gamma(\cdot)$ maps the interval (z_+, ∞) bijectively into $(x_+, 0)$; denote by $\mathcal{D}_\gamma^{-1}(\cdot) \equiv \mathcal{D}_\gamma^{-1}(\cdot; F_Z)$ the inverse mapping.

We finally can give formulas for the fundamental phenomenological limits described earlier. The limiting empirical signal singular value $y_{i,\infty} = \mathcal{Y}(x_i) \equiv \mathcal{Y}(x_i; F_Z, \gamma)$ obeys

$$\mathcal{Y}(x) = \mathcal{D}_\gamma^{-1}\left(\frac{1}{x^2}\right), \quad \text{for } x > x_+, \quad (3.13)$$

equivalently, $\mathcal{D}_\gamma(\mathcal{Y}(x)) = 1/x^2$. The asymptotic cosine $\mathcal{C}(x) \equiv \mathcal{C}(x; F_Z, \gamma)$ is given by

$$\mathcal{C}(x) = -\frac{2}{x^3} \cdot \frac{1}{\mathcal{D}'_\gamma(\mathcal{Y}(x))}, \quad \text{for } x > x_+. \quad (3.14)$$

One may readily verify that $\mathcal{C}(x) \geq 0$ for all $x > x_+$.¹⁵

We sometimes adopt the implicit parameterization of $\mathcal{C}(x)$ in terms of $y = \mathcal{Y}(x)$:

$$\mathcal{C}(x) = -2 \cdot \frac{(\mathcal{D}_\gamma(y))^{3/2}}{\mathcal{D}'_\gamma(y)}, \quad \text{where } y = \mathcal{Y}(x) \text{ and } x > x_+. \quad (3.15)$$

Existence of a BBP phase transition Recall that $x_+ = \mathcal{X}_+(F_Z, \gamma)$ gives the threshold such that whenever $x_i \leq x_+$, one *does not* observe an outlier singular value away from the bulk of Y . Not all noise distributions display this phase transition phenomenon, i.e. they may not exhibit $x_+ > 0$: indeed, by Eq. (3.12), $\mathcal{X}_+ > 0$ if and only if $\lim_{y \rightarrow \mathcal{Z}_+(F_Z)} \mathcal{D}_\gamma(y; F_Z) < \infty$, equivalently, $\lim_{y \rightarrow \mathcal{Z}_+(F_Z)} \int (y-z)^{-1} dF_Z(z) < \infty$. This condition entails that near its own bulk edge, F_Z is not “thick”. For example, when F_Z has a density in a neighborhood of $z_+ = \mathcal{Z}_+(F_Z)$ that behaves as $f_Z(z) \sim C(z - z_+)^{\alpha}$, this condition is satisfied whenever $\alpha > 0$. For example, the family of noise distributions described in Section 3.2 is of this type (with $\alpha = 1/2$); they all display a BBP phase transition. Moreover, Assumption 6 gives $\lim_{y \rightarrow z_+} \mathcal{D}'_\gamma(y; F_Z) = -\infty$. From Eq. (3.15), this means that if $x_+ \equiv \mathcal{X}_+(F_Z, \gamma) > 0$, then $\mathcal{C}(x) = 0$ as $x \rightarrow x_+$ from the right. Curiously, when $x_+ = 0$, this does not have to be the case. For instance, when $dF_Z = \delta_1$ and $\gamma = 1$, an easy computation shows $x_+ = 0$ and $\mathcal{C}(x) = \frac{y^3}{y(y^2+1)}$, where $y = \mathcal{Y}(x)$ and $\mathcal{Z}_+(F_Z) = 1$. We see that $\lim_{x \rightarrow x_+} \mathcal{C}(x) = 1/2$: this means that an *arbitrarily small* signal already creates a very strong bias in the direction of the principal singular vectors of Y_n .

Notation Throughout the paper, we use the notation

$$y_{i,\infty} = \begin{cases} \mathcal{Y}(x_i) & \text{when } x_i > \mathcal{X}_+, \\ \mathcal{Z}_+(F_Z) & \text{when } x_i \leq \mathcal{X}_+. \end{cases}$$

By the results of [10], the singular values of Y_n , $y_{1,n} \geq \dots \geq y_{p,n}$, satisfy $y_{i,n} \xrightarrow{a.s.} y_{i,\infty}$ for any *fixed* index i (for $i > r$ this is an easy consequence of the interlacing inequality for singular values).

¹⁵Note that in [10], Eq. (3.7) is only stated as $|\langle \mathbf{a}_{n,i}, \mathbf{u}_{n,i} \rangle \cdot \langle \mathbf{b}_{n,i}, \mathbf{v}_{n,i} \rangle| \xrightarrow{a.s.} \mathcal{C}(x_i)$ (assuming $x_i > x_+$), with the absolute value. One may readily verify that the limiting cross-correlation must, in fact, be non-negative: Start with

$$y_{i,n} = \mathbf{u}_{i,n}^\top Y_n \mathbf{v}_{i,n} = \mathbf{u}_{i,n}^\top X_n \mathbf{v}_{i,n} + \mathbf{u}_{i,n}^\top Z_n \mathbf{v}_{i,n} \leq \mathbf{u}_{i,n}^\top X_n \mathbf{v}_{i,n} + \|Z_n\|.$$

By Eq. (3.6), $\mathbf{u}_{i,n}^\top X_n \mathbf{v}_{i,n} \sim x_i \langle \mathbf{a}_{n,i}, \mathbf{u}_{n,i} \rangle \cdot \langle \mathbf{b}_{n,i}, \mathbf{v}_{n,i} \rangle$, while $\|Z_n\| \rightarrow z_+$, $y_{i,n} \rightarrow y_{i,\infty} \geq z_+$. The conclusion follows.

3.2. Noise matrices with correlated columns

We conclude this section by mentioning an important family of noise matrices satisfying our assumptions, namely, noise matrices with independent rows, having cross-column correlations. We consider noise matrices of the form $Z_n = W_n S_n^{1/2}$, where (W_n) and (S_n) are sequences of matrices obeying:

- W_n is an n -by- p matrix with i.i.d elements. Specifically, let W denote a random variable with moments

$$\mathbb{E}(W) = 0, \quad \mathbb{E}(W^2) = 1, \quad \mathbb{E}(W^4) < \infty.$$

The entries of W_n are i.i.d, with law $(W_n)_{ij} \stackrel{d}{=} n^{-1/2}W$, that is, scaled to variance $1/n$. Finiteness of the fourth moment of W is essential; see [7].

- (S_n) is a sequence of non-random p -by- p matrices. Let $\lambda_1(S_n) \geq \dots \geq \lambda_p(S_n)$ be the eigenvalues of S_n , and denote by $F_{S_n}(\lambda) = p^{-1} \sum_{i=1}^p \mathbb{1}_{\{\lambda_i(S_n) \leq \lambda\}}$ the empirical CDF of its eigenvalues. We assume that the sequence (F_{S_n}) converges to a compactly supported LECDF F_S . Moreover, denoting the upper and lower edges of the support by

$$\lambda_+(F_S) = \sup\{\lambda : F_S(\lambda) < 1\}, \quad \lambda_-(F_S) = \inf\{\lambda : F_S(\lambda) > 0\},$$

we assume that $\lambda_1(S_n) \rightarrow \lambda_+(F_S)$ and $\lambda_p(S_n) \rightarrow \lambda_-(F_S)$.

We refer to a random matrix ensemble of the form above as a **noise matrix with correlated columns**. They appear, for example, in the following scenario: We observe n i.i.d p -dimensional samples $\mathbf{y}_i = \mathbf{x}_i + \mathbf{z}_i$, where \mathbf{x}_i are instances of a signal vector, assumed to be supported in an r -dimensional subspace, and $\mathbf{z}_i = S_n^{1/2} \mathbf{w}_i$ is a vector of correlated noise, with covariance $\text{Cov}(\mathbf{w}_i) = S_n$. Let Y_n be the n -by- p matrix, whose rows are $n^{-1/2} \mathbf{y}_i^\top$ (define X_n , W_n and Z_n similarly). Then $Y_n = X_n + Z_n = X_n + W_n S_n^{1/2}$, where $\text{rank}(X_n) \leq r$, by assumption. For any estimator $\hat{X} = \hat{X}(Y_n)$, let $\hat{\mathbf{x}}_1, \dots, \hat{\mathbf{x}}_n$ be the rows of the matrix $n \cdot \hat{X}$. Then the Frobenius loss is just the average L^2 loss in estimating the signal samples \mathbf{x}_i by the vectors $\hat{\mathbf{x}}_i$: $\|X_n - \hat{X}(Y_n)\|_F^2 = n^{-1} \sum_{i=1}^n \|\mathbf{x}_i - \hat{\mathbf{x}}_i\|_2^2$.

Much is known about the singular values of Z_n :

1. **Limiting singular value distribution:** F_{Z_n} converges weakly almost surely to a compactly supported law F_Z . This limiting law is defined in terms of its Stieltjes transform¹⁶, $m(y) = \int (z^2 - y)^{-1} dF_Z(z)$; $m(y)$ is the unique Stieltjes transform satisfying

$$m(y) = \int \frac{1}{t(1 - \gamma - \gamma y m(y)) - y} dF_S(t), \quad \text{for all } y \in \mathbb{C} \setminus \mathbb{R}.$$

2. **Extreme singular values:** The largest and smallest singular values of Z_n converge almost surely to the upper and lower edges of the support of the limiting law¹⁷ F_Z :

$$\mathcal{Z}_+(F_{Z_n}) \xrightarrow{a.s.} \mathcal{Z}_+(F_Z), \quad \mathcal{Z}_-(F_{Z_n}) \xrightarrow{a.s.} \mathcal{Z}_-(F_Z).$$

3. **Behavior at the edge of the bulk:** On $\mathbb{R} \setminus \{0\}$, the limiting law F_Z is absolutely continuous with respect to Lebesgue measure. Denoting by f_Z the corresponding density, we have $f_Z(z) \sim C \cdot \sqrt{|z - \mathcal{Z}_+(F_Z)|}$ as $z \nearrow \mathcal{Z}_+(F_Z)$. This is the same behavior as a Marčenko-Pastur law, corresponding to $S_n = I$. This edge behavior will motivate one of our strategies for estimating F_{Z_n} from the observed singular values F_{Y_n} (*imputation*, see Section 4.2); this is an important step in the ScreeNOT algorithm. Also, note that in particular, the limiting noise CDF F_Z satisfies Assumption 6.

4. **CLT for linear spectral statistics:** Denote

$$\underline{y} = (1 - \sqrt{\gamma})^2 \cdot \lambda_-(F_S), \quad \bar{y} = (1 + \sqrt{\gamma})^2 \cdot \lambda_+(F_S).$$

¹⁶ $m(y)$ is in fact the Stieltjes transform of the limiting eigenvalue distribution of $Z^\top Z$:

$$m(y) = \int (z - y)^{-1} dF_{Z^\top Z}(z) = \int (z^2 - y)^{-1} dF_Z(z).$$

¹⁷Below, $\mathcal{Z}_-(F_{Z_n})$ denotes the smallest singular value of Z_n . Recall that we assume $p \leq n$.

Note that $\underline{y}^{1/2} \leq \mathcal{Z}_-(F_Z) \leq \mathcal{Z}_+(F_Z) \leq \bar{y}^{1/2}$. Let g be analytic on an open domain in \mathbb{C} containing the closed interval $[\underline{y}, \bar{y}]$. Set

$$\Phi_n[g] = \int g(z^2) (dF_Z - dF_{Z_n})(z),$$

which is a random variable.¹⁸ Then the sequence $p \cdot \Phi_n[g]$ is tight. If, moreover, $\mathbb{E}(W^4) = 3$, then $p \cdot \Phi_n[g]$ converges in law to a Gaussian random variable.

For properties (1) and (2), we refer to [7] and the references therein (see also the book [4]). Property (3) is proved in [34]. Property (4) is proved in [6].

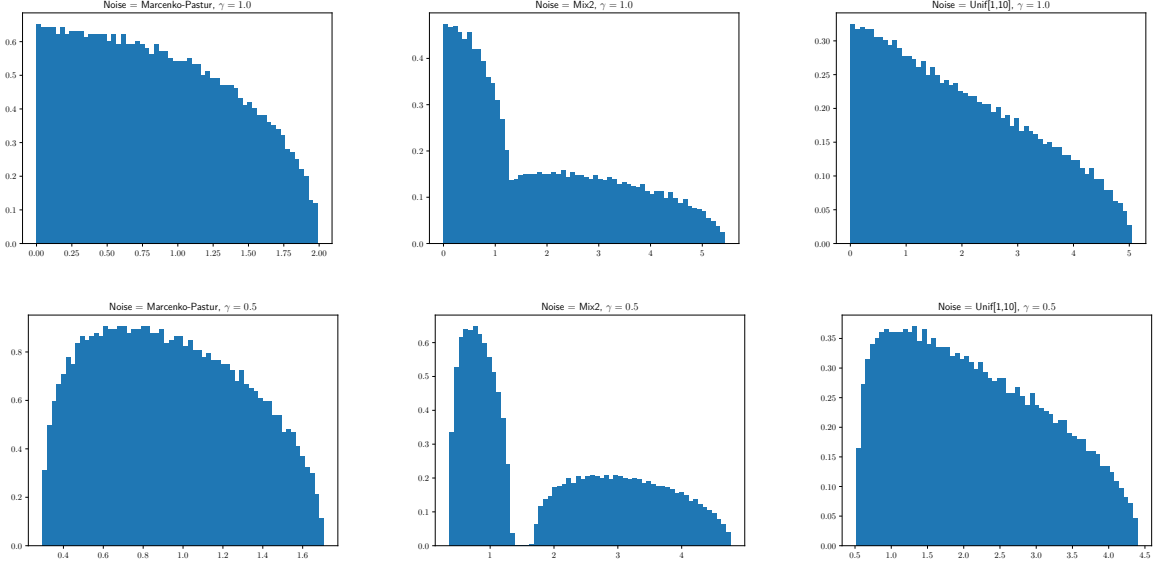


Fig 3: Several empirical noise singular value distributions that come from the model in Section 3.2. Left to right: covariance eigenvalue distribution: (i) $dF_S = \delta_1$ (giving a Marčenko-Pastur bulk); (ii) An equal mix of two atoms, $dF_S = \frac{1}{2}\delta_1 + \frac{1}{2}\delta_{10}$; (iii) F_S uniform on $[1, 10]$. Top: shape $\gamma = 1$; bottom: $\gamma = 0.5$. Each plot is the histogram of singular values from a single random $n \times p$ matrix, with $p = 3000$ and $n = p/\gamma$.

As a final remark, we mention that when the covariance matrix S_n is invertible and known (or can be consistently estimated with respect to the operator norm), estimating X_n using the leading singular vectors of Y_n is sub-optimal. Instead, it is better to first “whiten” the noise, that is, compute $Y_n^w = Y_n S_n^{-1/2} = X_n S_n^{-1/2} + W_n$. Letting $\mathbf{u}_{i,n}^w$ and $\mathbf{v}_{i,n}^w$ be respectively the left and right singular vectors of Y_n , we can “recolor” the right singular vectors, $\mathbf{v}_{i,n}^c = S_n^{1/2} \mathbf{v}_{i,n}^w / \|S_n^{1/2} \mathbf{v}_{i,n}^w\|$. Under a uniform prior on the signal singular vectors, as we assume in this paper, and when W_n is i.i.d Gaussian, the correlations between the signal singular vectors and empirical singular vectors can be shown to be *stronger* in the whiten-then-recolor scheme, see [25, 20] for details:

$$\lim_{n \rightarrow \infty} \langle \mathbf{a}_{i,n}, \mathbf{u}_{i,n}^w \rangle \langle \mathbf{b}_{i,n}, \mathbf{v}_{i,n}^c \rangle \geq \lim_{n \rightarrow \infty} \langle \mathbf{a}_{i,n}, \mathbf{u}_{i,n} \rangle \langle \mathbf{b}_{i,n}, \mathbf{v}_{i,n} \rangle.$$

4. Results

Outline We start by developing a theory for optimal hard thresholding, under the assumption that the noise singular value distribution F_Z is known. We show that there is an asymptotically uniquely admissible hard threshold $T_\gamma(F_Z)$, which is given as a certain functional T_γ of the asymptotic aspect ratio γ and the limiting noise CDF F_Z . Relying on the fact that $\text{SE}_n[\mathbf{x}|\theta]$ can only take a finite number of values as θ varies,

¹⁸A random variable of the form $\int h(z) F_{Z_n}(z) = p^{-1} \sum_{i=1}^n h(z_{i,n})$ is called a linear spectral statistic.

we show that thresholding at $T_\gamma(F_Z)$ has rather strong optimality properties: it in fact attains oracle loss, at finite n , with probability increasing to 1 as $n \rightarrow \infty$. We then move on to the practical setting of interest, in which F_Z is unknown. We propose a method for consistently estimating $T_\gamma(F_Z)$ from the observed data Y_n . We do this by applying the optimal threshold functional $T_{p/n}(\cdot)$ on a judiciously transformed version of F_{Y_n} , the empirical singular value distribution of Y_n . The continuity of the functional with respect to the CDF and the shape parameter then implies that the resulting quantity is a consistent estimator for $T_\gamma(F_Z)$; the optimality properties of the adaptive algorithm then follow from the previously developed theory. Unless otherwise stated, we always operate under assumptions (1)-(6) of Section 3.

4.1. A theory for optimal singular value thresholding

Consider the function $\theta \mapsto \text{ASE}[\mathbf{x}|\theta]$ defined for $\theta > 0$ by

$$\text{ASE}[\mathbf{x}|\theta] = \sum_{i=1}^r R(x_i|\theta), \quad \text{where} \quad R(x_i|\theta) = \mathbb{1}_{\{y_{i,\infty} \leq \theta\}} \cdot R_0(x_i) + \mathbb{1}_{\{y_{i,\infty} > \theta\}} \cdot R_1(x_i), \quad (4.1)$$

and

$$R_0(x) = x^2, \quad R_1(x) = \begin{cases} x^2 + \mathcal{Y}(x)^2 - 2x\mathcal{Y}(x)\mathcal{C}(x) & \text{if } x > x_+, \\ x^2 + z_+^2 & \text{if } x \leq x_+. \end{cases} \quad (4.2)$$

Recall that $y_{i,\infty} = z_+$ ($\equiv \mathcal{Z}_+(F_Z)$) when $x_i \leq x_+$ ($= \mathcal{X}_+(F_Z, \gamma)$) and $y_{i,\infty} = \mathcal{Y}(x_i)$ when $x > x_+$. Define also

$$\text{ASE}^*[\mathbf{x}] = \sum_{i=1}^r R^*(x_i), \quad \text{where} \quad R^*(x_i) = \min\{R_0(x_i), R_1(x_i)\}. \quad (4.3)$$

Clearly, $R^*(x) \leq R(x|\theta)$ for any x and θ , which means $\text{ASE}^*[\mathbf{x}] \leq \text{ASE}[\mathbf{x}|\theta]$.

It is easy to verify that for almost every $\theta > \mathcal{Z}_+(F_Z)$, the loss of thresholding at the fixed point θ converges: $\lim_{n \rightarrow \infty} \text{SE}_n[\mathbf{x}|\theta] = \text{ASE}[\mathbf{x}|\theta]$ almost surely; see Lemma 7 for a precise statement. We start by finding the threshold that attains minimum asymptotic loss.

Definition 1 (Optimal threshold functional). For a compactly supported CDF H and $\gamma \in (0, 1]$, let

$$\Psi_\gamma(y; H) = y \cdot \frac{\mathcal{D}'_\gamma(y; H)}{\mathcal{D}_\gamma(y; H)} = y \cdot \left(\frac{\varphi'(y; H)}{\varphi(y; H)} + \frac{\tilde{\varphi}'_\gamma(y; H)}{\tilde{\varphi}_\gamma(y; H)} \right); \quad (4.4)$$

this is well-defined for $y > \mathcal{Z}_+(H)$. Define the functional of H

$$T_\gamma(H) = \inf \{y : y > \mathcal{Z}_+(H) \text{ and } \Psi_\gamma(y; H) \geq -4\}. \quad (4.5)$$

We call this the **optimal threshold functional**.

Lemma 1. The following holds:

1. For any H and γ , $y \mapsto \Psi_\gamma(y; H)$ is negative and increasing, with $\Psi_\gamma(\infty) = -2$.
2. Assume that H is compactly supported and satisfies $\lim_{y \rightarrow \mathcal{Z}_+(H)} \int (y-z)^{-2} dH(z) = \infty$ (note that, by assumption, $H = F_Z$ satisfies this). Then $T_\gamma(H)$ is the unique number $> \mathcal{Z}_+(H)$ satisfying $\Psi_\gamma(T_\gamma(H); H) = -4$.
3. Thresholding at $\theta^* = T_\gamma(F_Z)$ minimizes the asymptotic loss:

$$\text{ASE}[\mathbf{x}|\theta^*] = \min_{\theta} \text{ASE}[\mathbf{x}|\theta] = \text{ASE}^*[\mathbf{x}].$$

Moreover, θ^* is the unique threshold for which the above holds **universally**, for all signals \mathbf{x} .

Lemma 1 is proved in Section 6.1.

Note that $\theta \mapsto \text{ASE}[\mathbf{x}|\theta]$ is piecewise constant, with jumps at $y_{1,\infty}, \dots, y_{r,\infty}$. This means that its minimum is actually attained on an *interval*:

Definition 2 (The asymptotic optimal interval). *Let*

$$\underline{\Theta}(\mathbf{x}) = \max \{y_{i,\infty} : y_{i,\infty} < T_\gamma(F_Z)\}, \quad \overline{\Theta}(\mathbf{x}) = \min \{y_{i,\infty} : y_{i,\infty} > T_\gamma(F_Z)\}. \quad (4.6)$$

Note that since $T_\gamma(F_Z) > z_+ = \mathcal{Z}_+(F_Z, \gamma)$ and $y_{r+1,\infty} = z_+$, we always have, by definition, $\underline{\Theta}(\mathbf{x}) \geq z_+$. Moreover, if $y_{1,\infty} \leq T_\gamma(F_Z)$ then we define $\overline{\Theta}(\mathbf{x}) = \infty$.

Lemma 2. *1. Throughout the interval $\theta \in (\underline{\Theta}(\mathbf{x}), \overline{\Theta}(\mathbf{x}))$, $\text{ASE}[\mathbf{x}|\theta]$ is constant. Moreover, it attains its minimum there; if $\theta_0 \in (\underline{\Theta}(\mathbf{x}), \overline{\Theta}(\mathbf{x}))$, then*

$$\text{ASE}[\mathbf{x}|\theta_0] = \min_{\theta \geq 0} \text{ASE}[\mathbf{x}|\theta] = \text{ASE}^*[\mathbf{x}].$$

2. Any $\theta_1 > \mathcal{Z}_+(F_Z)$ outside $[\underline{\Theta}(\mathbf{x}), \overline{\Theta}(\mathbf{x})]$ has

$$\text{ASE}[\mathbf{x}|\theta_1] > \text{ASE}^*[\mathbf{x}].$$

*3. **Unique asymptotic admissibility:** $T_\gamma(F_Z)$ is in the interior of the asymptotic optimal interval. In fact, it is the only threshold which has optimal asymptotic loss simultaneously for all signals \mathbf{x} :*

$$\bigcap_{\mathbf{x} \text{ signal}} (\underline{\Theta}(\mathbf{x}), \overline{\Theta}(\mathbf{x})) = \{T_\gamma(F_Z)\}.$$

Lemma 2 is proved in Section 6.1.

The Scree Plot heuristic: a quantitatively interpretation Under our signal model, one could think of a “natural” quantification of Cattell’s Scree Plot heuristic. Roughly, it hopes to threshold the data singular values slightly above the pure-noise bulk edge. If this hope is fulfilled, the excess ASE incurred, compared to the minimal attainable ASE, is

$$\lim_{\delta \rightarrow 0} \text{ASE}[\mathbf{x}|z_+ + \delta] - \text{ASE}^*[\mathbf{x}] = \sum_{i : y_{i,\infty} \in (z_+, T_\gamma(F_Z))} (R_1(x_i) - R_0(x_i)).$$

The excess ASE is proportional to the number of barely/moderately emergent signal singular values, namely, such that $y_{i,\infty} > z_+$ (so that they can be observed as outliers in the spectrum of Y_n) but $y_{i,\infty} < T_\gamma(F_Z)$ (meaning that the corresponding empirical singular vectors are too “noisy” so to be useful in estimating X_n). Clearly, in the worst-case scenario, the signal \mathbf{x} consists entirely of barely emergent singular values, so that the excess ASE is proportional to $r = \text{rank}(X_n)$. For a concrete example, consider \mathbf{x} that consists of r distinct singular values, located *just slightly* above x_+ ; in that case, the excess ASE is $r \cdot (R_1(x_+) - R_0(x_+)) = r \cdot z_+^2$.

It is clear at this point that thresholding at any point in the interior of the asymptotic optimal interval achieves the best asymptotic loss, among all other fixed hard thresholds. Our main result states that, remarkably, one **cannot** come up with a consistently better thresholding strategy, even if given access to the true unknown signal X_n :

Theorem 1. *1. Almost surely,*

$$\lim_{n \rightarrow \infty} \text{SE}_n^*[\mathbf{x}] = \text{ASE}^*[\mathbf{x}].$$

2. Let $\theta \in (\underline{\Theta}(\mathbf{x}), \overline{\Theta}(\mathbf{x}))$ be in the interior of the asymptotic optimal interval, and θ_n be any sequence of thresholds (possibly depending on Y_n) such that $\theta_n \xrightarrow{a.s.} \theta$. Then

$$\text{SE}_n[\mathbf{x}|\theta_n] \xrightarrow{a.s.} \text{ASE}^*[\mathbf{x}].$$

Our next result states that thresholding inside the asymptotic optimal interval in fact achieves oracle risk with high probability, **for finite n** :

Theorem 2. *Suppose that $T_\gamma(F_Z) \notin \{y_{1,\infty}, \dots, y_{r,\infty}\}$.¹⁹ Then:*

¹⁹We need to exclude the case $T_\gamma(F_Z) \in \{y_{1,\infty}, \dots, y_{r,\infty}\}$ for this reason: If $y_{i,\infty} = T_\gamma(F_Z)$ for some i , then thresholding either slightly above or below $y_{i,n}$ (but still inside the asymptotic optimal interval) will achieve the same (optimal) asymptotic risk. However, we cannot deduce that for finite n , one of those options is, necessarily, consistently better than the other, thereby achieving oracle risk exactly.

1. Let $\theta_0 \in (\underline{\Theta}(\mathbf{x}), \overline{\Theta}(\mathbf{x}))$ and θ_n be a sequence with $\theta_n \xrightarrow{a.s.} \theta_0$. Then

$$\mathbb{P} \{ \exists N \text{ s.t. } \forall n \geq N : \text{SE}_n[\mathbf{x}|\theta_n] = \text{SE}_n^*[\mathbf{x}] \} = 1.$$

2. Let $\theta_1 \notin (\underline{\Theta}(\mathbf{x}), \overline{\Theta}(\mathbf{x}))$ and $\theta_n \xrightarrow{a.s.} \theta_1$. There exists $\delta > 0$, $\delta = \delta(\mathbf{x}; F_Z, \gamma)$ such that

$$\mathbb{P} \{ \exists N \text{ s.t. } \forall n \geq N : \text{SE}_n[\mathbf{x}|\theta_n] > \text{SE}_n^*[\mathbf{x}] + \delta \} = 1.$$

Theorems 1 and 2 are proved in Section 6.2.

4.2. The ScreeNOT algorithm

In practice, the noise distribution F_Z is generally unknown to the statistician. Theorems 1 and 2, along with the unique admissibility property of Lemma 2, tell us that our goal should be to estimate the optimal threshold $T_\gamma(F_Z)$.

We start by showing that the functional $(\gamma, H) \mapsto T_\gamma(H)$ is continuous with respect to weak convergence of CDFs, with the additional requirement that the edge of the support converges as well:

Lemma 3 (Continuity of the optimal threshold functional). *Suppose that H is compactly supported and satisfies the condition $\lim_{y \rightarrow \mathcal{Z}_+(H)} \int (y - z)^{-2} dH(z) = \infty$. Let H_n be a sequence of CDFs such that*

1. H_n converges weakly to H , denoted $H_n \xrightarrow{d} H$.
2. $\mathcal{Z}_+(H_n) \rightarrow \mathcal{Z}_+(H)$.

Then $T_{p/n}(H_n) \rightarrow T_\gamma(H)$.

The proof of Lemma 3 appears in the supplementary material, Section D.

Recall that the empirical singular value distribution of the noise matrix, F_{Z_n} , converges, by assumption, weakly almost surely to F_Z , with $\mathcal{Z}_+(F_{Z_n}) \xrightarrow{a.s.} \mathcal{Z}_+(F_Z)$. The matrix noise Z_n , and consequently F_{Z_n} , is of course unknown to the statistician. However, since Y_n is a rank- r additive perturbation of Z_n , the interlacing inequalities for singular values imply for example the convergence of CDF's in Kolmogorov-Smirnov distance $\|F_{Y_n} - F_{Z_n}\|_{KS} \rightarrow 0$ (see, for example, the statement and proof of Lemma 4 below) and hence also in weak convergence. The obstacle preventing the would-be use of $T_{p/n}(F_{Y_n})$ to estimate $T_\gamma(F_Z)$ lies with the fact that T is not continuous in Kolmogorov-Smirnov metric convergence or other topologies involving CDF convergence such as weak convergence. More concretely, $T_{p/n}(F_{Y_n})$ can be very different than $T_\gamma(F_Z)$ because the top masspoints of F_{Y_n} do not converge to the bulk edge F_Z .²⁰ Indeed, recall that $\mathcal{Z}_+(F_{Y_n}) = y_{1,n} \xrightarrow{a.s.} y_{1,\infty}$, which is $> \mathcal{Z}_+(F_Z)$ when $x_1 > \mathcal{X}_+$.

To get a reasonable simulacrum of F_{Z_n} built from knowledge only of F_{Y_n} we perform “surgery” on F_{Y_n} , “amputating” the top k masspoints and fitting a “prosthesis” to replace them. Post-surgery, we get an estimate for the unknown empirical noise CDF F_{Z_n} .

As indicated in Section 2 above, the user of our proposed procedure supplies an upper bound (which can be potentially very loose) $k \geq r$ on the rank of the unknown low-rank matrix.

We could, in principle, propose any one of the following “pseudo-noise” CDFs, derived from F_{Y_n} :

- **Transport to zero:** We construct a CDF, $F_{n,k}^0$, obtained by removing the k largest singular values of Y_n , and adding k additional zeros. That is,

$$F_{n,k}^0(y) = \frac{1}{p} \sum_{i=k+1}^p \mathbb{1}_{\{y_{i,n} \leq y\}} + \frac{k}{p} \mathbb{1}_{\{y \geq 0\}}.$$

- **“Winsorization” (clipping):** As in the previous construction, we remove the leading k singular values. Instead of adding k zeroes, we add k copies of $y_{k+1,n}$. Equivalently, we “clip” the large singular values of Y_n to be at most the size of $y_{n,k+1}$. That is,

$$F_{n,k}^w(y) = \frac{1}{p} \sum_{i=k+1}^p \mathbb{1}_{\{y_{i,n} \leq y\}} + \frac{k}{p} \mathbb{1}_{\{y_{k+1,n} \leq y\}}.$$

²⁰Of course, this does not prevent convergence of ECDFs. Recall that $F_{Y_n} \xrightarrow{d} F_Z$ means that for **bounded and continuous** functions f , $\int f(z) dF_{Y_n}(z) \rightarrow \int f(z) dF_Z(z)$.

- **“Imputation” (reconstruction of the missing upper tail):** After removing the top k singular values of Y_n , we try to construct the noise tail in a principled way. Recall that when Z_n is a noise matrix with correlated columns, as described in Section 3.2, F_Z has a density near $z_+ = \mathcal{Z}_+(F_Z)$ that behaves as $f_Z(z) \sim C(z_+ - z)^{1/2}$ as $z \rightarrow z_+$ ([34]). Using the heuristic²¹

$$\frac{\ell - 1}{p} \approx \int_{z_{\ell,n}}^{\mathcal{Z}_+(F_Z)} f_Z(z) dz \approx \int_{z_{\ell,n}}^{z_+} C(z_+ - z)^{1/2} dz = C'(z_+ - z_{\ell,n})^{3/2},$$

we can estimate the distance between singular values in the upper tail as

$$z_{\ell,n} - z_{t,n} \approx C'' \left[\left(\frac{t-1}{p} \right)^{2/3} - \left(\frac{\ell-1}{p} \right)^{2/3} \right].$$

Taking $y_{\ell,n} \approx z_{\ell,n}$ for $\ell \geq r+1$, we propose to estimate the unknown constant as:

$$C'' = \frac{y_{2k+1,n} - y_{k+1}}{(2k/p)^{2/3} - (k/p)^{2/3}},$$

assuming $2k+1 < p$ (when k is not very small compared to p , there is no reason to believe this heuristic should give good results). We “reconstruct” the missing upper tail as

$$\tilde{y}_{i,n} = y_{k+1,n} + C'' \left[\left(\frac{k}{p} \right)^{2/3} - \left(\frac{i-1}{p} \right)^{2/3} \right] = y_{k+1,n} + \frac{1 - \left(\frac{i-1}{k} \right)^{2/3}}{2^{2/3} - 1} (y_{2k+1,n} - y_{k+1,n}).$$

The CDF we use is then

$$F_{n,k}^i(y) = \frac{1}{p} \sum_{i=k+1}^p \mathbb{1}_{\{y_{i,n} \leq y\}} + \frac{1}{p} \sum_{i=1}^k \mathbb{1}_{\{\tilde{y}_{i,n} \leq y\}}.$$

The label i on $F_{n,k}^i$ stands for ‘imputation’, a standard terminology in statistical practice for filling in utterly missing data with plausible pseudo-data. Numerical results in Section 5 suggest that in many cases, the ‘imputation’ method gives significantly better results than truncation or Winsorization at finite n . It is also more psychologically “supportive”, which is why we recommended it to practitioners in Section 2 above. However, our formal results hold for all three methods. Importantly, the list of strategies above is by no means exhaustive. Indeed, any sequence of CDFs F_n^* that satisfies the conditions of Lemma 3 may be used instead, yielding an asymptotically consistent estimate of the optimal threshold. Furthermore, our ‘imputation’ procedure is not claimed to be optimal; possibly, other strategies will outperform those we suggest in finite problem sizes.

Lemma 4. *Suppose that $k = k_n$ satisfies $k_n \geq r$ and $k_n/p \rightarrow 0$ (in particular, k can be any constant $\geq r$). Then for any choice $\star \in \{0, w, i\}$:*

1. *Almost surely, $F_{n,k}^\star \xrightarrow{d} F_Z$.*
2. $\mathcal{Z}_+(F_{n,k}^\star) \xrightarrow{a.s.} \mathcal{Z}_+(F_Z)$.
3. *We have the following bound on the Kolmogorov-Smirnov distance between $F_{n,k}^\star$ and F_{Z_n} :*

$$\|F_{n,k}^\star - F_Z\|_{\text{KS}} = \sup_z |F_{n,k}^\star(z) - F_{Z_n}(z)| \leq \frac{k}{p}.$$

The proof of Lemma 4 is deferred to the supplementary material, Section D.

The following theorem states the optimality properties of the proposed ScreeNOT algorithm. It is an immediate corollary of Theorems 1, 2 and Lemma 4:

²¹The exponent $\alpha = 1/2$ was chosen as typical of bulk-edge distributions in random matrix theory. If there is reason to believe that the behavior at the bulk edge follows a different power law $f_Z(z) \sim (z_+ - z)^\alpha$, a correspondingly different exponent can be used instead.

Theorem 3. Suppose that $k = k_n$ satisfies $k_n \geq r$ and $k_n/p \rightarrow 0$. For any $\star \in \{0, w, i\}$, $\hat{\theta}_n = T_{p/n}(F_{n,k}^\star)$ satisfies:

1. $\hat{\theta}_n \xrightarrow{a.s.} T_\gamma(F_Z)$.
2. $\text{SE}_n[\mathbf{x}|\hat{\theta}_n] \xrightarrow{a.s.} \text{ASE}^\star[\mathbf{x}]$.
3. Assume that $T_\gamma(F_Z) \notin \{y_{1,\infty}, \dots, y_{r,\infty}\}$. Then

$$\mathbb{P}\{\exists N \text{ s.t. } \forall n \geq N : \text{SE}_n[\mathbf{x}|\theta_n] = \text{SE}_n^\star[\mathbf{x}]\} = 1.$$

Regarding the assumption in item 3 above, we note the following.

Lemma 5. The condition $T_\gamma(F_Z) \notin \{y_{1,\infty}, \dots, y_{r,\infty}\}$ is **generic**, i.e., in the space of possible singular value r -vectors \mathbf{x} , this condition holds on an open dense set.

Proof. Fix the noise bulk F_Z ; then $\theta^\star = T_\gamma(F_Z)$ is a constant not varying as the underlying signal \mathbf{x} changes. Moreover, it always strictly exceeds the bulk edge $\mathcal{Z}_+(F_Z)$. So $x^\star = \mathcal{Y}^{-1}(\theta^\star; F_Z, \gamma)$ is a uniquely defined constant which exceeds $\mathcal{X}_+(F_Z, \gamma)$. The set of vectors \mathbf{x} with all entries distinct from x^\star is open and dense. \square

4.3. Stability of ScreeNOT

One wonders how fast $T_{p/n}(F_{n,k}^\star)$ converges to the limit $T_\gamma(F_Z)$. We show that for noise matrices with correlated columns, the model described in Section 3.2, the typical deviations are of order $\mathcal{O}(k/p)$. We start with a “quantitative” version of Lemma 3:

Lemma 6. Adopt the setting of Lemma 3. Set

$$\Delta_{1,n} = |\varphi(T_\gamma(H); H) - \varphi(T_\gamma(H); H_n)|, \quad \Delta_{2,n} = |\varphi'(T_\gamma(H); H) - \varphi'(T_\gamma(H); H_n)|,$$

where φ and φ' are given in Eqs (3.8) and (3.9). Then

$$|T_\gamma(H) - T_{p/n}(H_n)| = \mathcal{O}\left(\Delta_{1,n} + \Delta_{2,n} + \left|\frac{p}{n} - \gamma\right|\right).$$

Lemma 6, along with the Kolmogorov-Smirnov distance bound from Lemma 4 and the tightness result for linear spectral statistics from [6] (see Section 3.2), gives the following:

Proposition 1. Suppose that (Z_n) is a sequence of noise matrices with correlated columns, as described in Section 3.2; and let F_S denote the LECDF of eigenvalues of the cross-column covariances S_n . Assume, in addition, that $T_\gamma(F_Z) > \bar{y}^{1/2} = (1 + \sqrt{\gamma}) \cdot \sqrt{\lambda_+(F_S)}$.²² Suppose that $k \geq r$ with $k/p \rightarrow 0$. Then for any $\star \in \{0, w, i\}$,

$$|T_\gamma(F_Z) - T_{p/n}(F_{n,k}^\star)| = \mathcal{O}_{\mathbb{P}}\left(\frac{k+1}{p}\right).$$

Lemma 6 and Proposition 1 are proved in the supplementary material, Section D.

5. Numerical experiments

The supplementary article contains comprehensive experiments conducted on a large variety of noise distributions. For space constraints, we include just a sample of these results - specifically, for white noise (Marčenko-Pastur LECDF) with $\gamma = 0.5$. Simulation results and code reproducing all figures here and in the supplementary article is available at [15]. See Section E of the supplementary article for full details on each experiment reported here.

In Figure 4a, we plot the function $\theta \mapsto \text{SE}_n[\mathbf{x}|\theta]$ for a single fixed problem instance. The vertical lines correspond to thresholds θ , taken to be either the true optimal threshold $\theta = T_\gamma(F_Z)$, its estimated versions $\theta = T_\gamma(F_{n,k}^\star)$, $\star \in \{0, w, i\}$, or the noise (asymptotic) bulk edge, $\theta = \mathcal{Z}_+(F_Z)$, which is the “natural” implementation of Cattell’s scree-plot heuristic in the spiked model. The error landscape $\text{SE}_n[\mathbf{x}|\theta]$ is seen to be a step function, and on this particular instance, all the proposed thresholding strategies fall inside the

²²This additional assumption is used due to a technical requirement in the results of [6]. We suspect that it can be removed.

interval where it attains its global minimum; hence, they attain the oracle risk. In contrast, thresholding at the bulk edge results in a strictly suboptimal squared error.

Figures 4b and 4c compare the relative efficacy of the proposed threshold estimation strategies. In both experiments, thresholding at the exact optimal threshold $\theta = T_\gamma(F_Z)$ (which is a priori unknown) yields the best results; among the proposed strategies, “imputation” $\theta = T_\gamma(F_{n,k}^i)$ appears to give the best results for finite problem dimensions. Figure 4d demonstrates the superior finite- n error of “imputation” in estimating the optimal threshold $T_\gamma(F_Z)$.

6. Proofs

6.1. The asymptotic loss at a fixed threshold

To simplify notation, throughout this section F_Z and γ will be held fixed, and left implicit in the notation where possible. In particular, we set $z_+ = \mathcal{Z}_+(F_Z)$, $x_+ = \mathcal{X}_+(F_Z, \gamma)$ throughout, and we suppress mention of F_Z and γ in entities like \mathcal{C} , \mathcal{Y} , \mathcal{D} .

We start by investigating $\lim_{n \rightarrow \infty} \text{SE}_n[\mathbf{x}|\theta]$ for fixed θ . Note that when $\theta < z_+$, it is clear that $\lim_{n \rightarrow \infty} \text{SE}_n[\mathbf{x}|\theta] = \infty$; the reason being that, for small enough $\epsilon > 0$, with probability 1, $(1 - F_Z(\theta + \epsilon)) \cdot n = \Omega(n)$ empirical singular values $y_{i,n}$ exceed the threshold θ , so that $\text{rank}(\hat{X}_\theta(Y_n))$ increases indefinitely. (This argument will be made more precise later.)

The following is an easy calculation:

Lemma 7. *For any $\theta > z_+$, almost surely:*

1.

$$\liminf_{n \rightarrow \infty} \text{SE}_n[\mathbf{x}|\theta] \geq \text{ASE}^*[\mathbf{x}].$$

2. *If, in addition, $\theta \notin \{y_{1,\infty}, \dots, y_{r,\infty}\}$, then*

$$\lim_{n \rightarrow \infty} \text{SE}_n[\mathbf{x}|\theta] = \text{ASE}[\mathbf{x}|\theta].$$

The quantities $\text{ASE}[\mathbf{x}|\theta]$ and $\text{ASE}^*[\mathbf{x}]$ appear in Eqs. (4.1) and (4.3) respectively.

Proof. Since $\theta > z_+$ and $y_{r+1,n} \xrightarrow{a.s.} y_{r+1,\infty} = z_+$, we see that with probability 1, for large enough n , $\hat{X}_t(Y_n) = \sum_{i=1}^r y_{i,n} \mathbf{1}_{\{y_{i,n} > \theta\}} \cdot \mathbf{u}_{i,n} \mathbf{v}_{i,n}^\top$. Thus, for large enough n ,

$$\begin{aligned} \text{SE}_n[\mathbf{x}|\theta] &= \left\| \sum_{i=1}^r x_i \cdot \mathbf{a}_{i,n} \mathbf{b}_{i,n}^\top - \sum_{i=1}^r y_{i,n} \mathbf{1}_{\{y_{i,n} > \theta\}} \cdot \mathbf{u}_{i,n} \mathbf{v}_{i,n}^\top \right\|_F^2 \\ &= \sum_{i=1}^2 (x_i^2 + y_{i,n}^2 \mathbf{1}_{\{y_{i,n} > \theta\}}) + \sum_{i=1}^r \sum_{j=1}^r x_i y_{j,n} \mathbf{1}_{\{y_{i,n} > \theta\}} \cdot \langle \mathbf{a}_{i,n}, \mathbf{u}_{j,n} \rangle \langle \mathbf{b}_{i,n}, \mathbf{v}_{j,n} \rangle. \end{aligned}$$

The lemma follows by recalling (i) that $y_{i,n} \xrightarrow{a.s.} y_{i,\infty}$ for all $i = 1, \dots, r$, where $y_{i,\infty} = \mathcal{Y}(x_i)$ if $x_i > x_+$ and $y_{i,\infty} = z_+ < \theta$ whenever $x_i \leq x_+$, (ii) that

$$\langle \mathbf{a}_{i,n}, \mathbf{u}_{j,n} \rangle \langle \mathbf{b}_{i,n}, \mathbf{v}_{j,n} \rangle \rightarrow \begin{cases} \mathcal{C}(x_i) & \text{when } i = j \text{ and } x_i > x_+ \\ 0 & \text{otherwise} \end{cases}$$

and (iii) that $\mathbf{1}_{\{y_{i,n} > \theta\}} \xrightarrow{a.s.} \mathbf{1}_{\{y_{i,\infty} > \theta\}}$ whenever $\theta \neq y_{i,\infty}$. \square

Our goal for the moment is to characterize the minimum of $\text{ASE}[\mathbf{x}|\theta]$ with respect to thresholds θ strictly above the noise bulk edge, $\theta > z_+$. This will give us the optimal *fixed* threshold, in the sense of minimal asymptotic loss (though, at this point, we cannot exclude the possibility that thresholding precisely at $\theta = z_+$ might achieve better asymptotic risk).

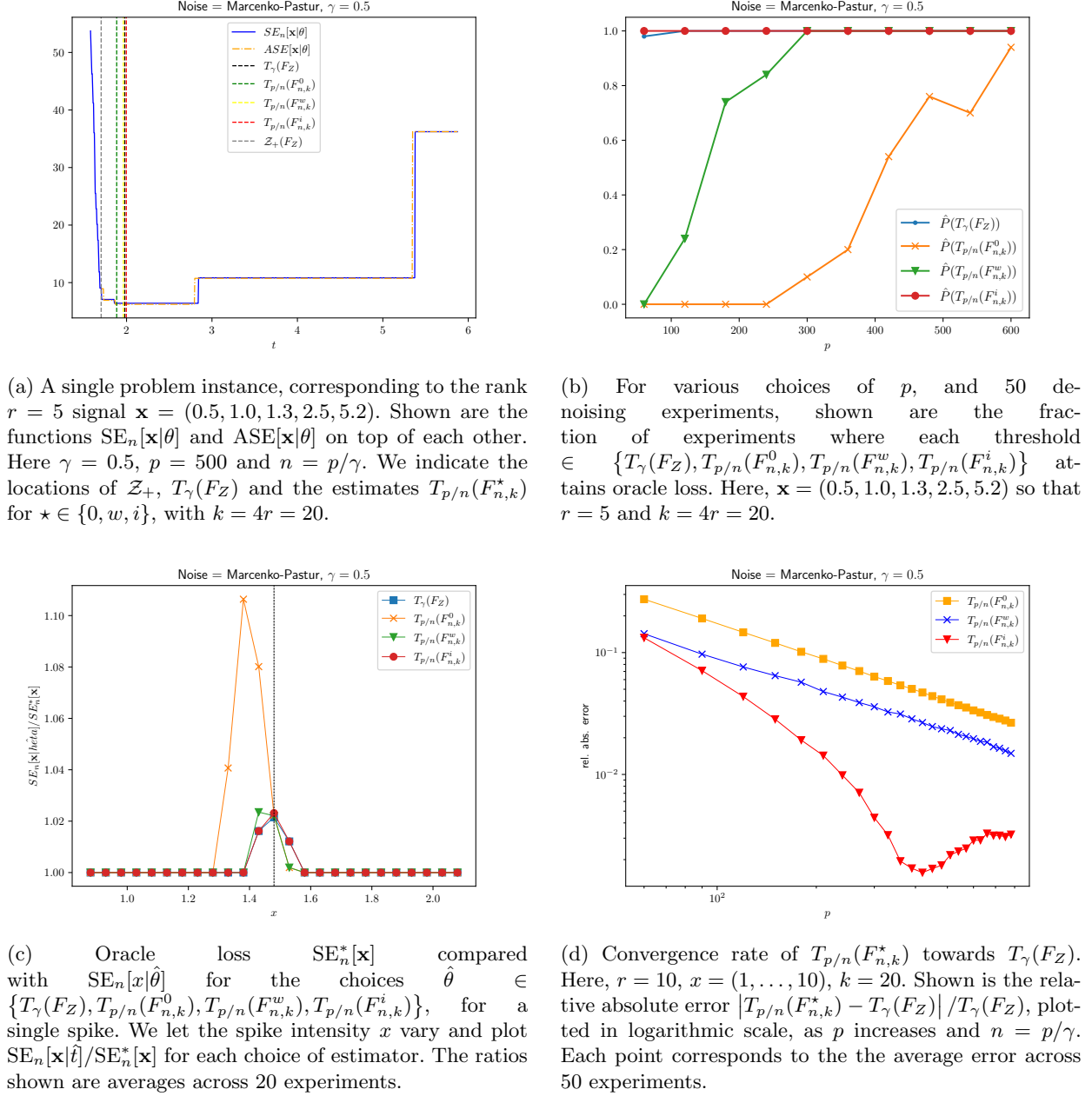


Fig 4: Monte-Carlo simulation results

Recall, by Eqs. (4.1) and (4.3), that the asymptotic loss decouples across the signal spikes as

$$\text{ASE}[\mathbf{x}|\theta] = \sum_{i=1}^r R(x_i|\theta), \quad \text{ASE}^*[\mathbf{x}] = \sum_{i=1}^r R^*(x_i).$$

Assuming that $\theta > z_+$, we have $R(x|\theta) = R^*(x) = x^2$ when $x \leq x_+$, while for $x > x_+$,

$$R(x|\theta) = \mathbb{1}_{\{\mathcal{Y}(x) \leq \theta\}} \cdot R_0(x) + \mathbb{1}_{\{\mathcal{Y}(x) > \theta\}} \cdot R_1(x), \quad R^*(x) = \min\{R_0(x), R_1(x)\},$$

with

$$R_0(x) = x^2, \quad R_1(x) = x^2 + \mathcal{Y}(x)^2 - 2x\mathcal{Y}(x)\mathcal{C}(x).$$

If we were able to find $\theta > z_+$ such that $R(x|\theta) = R^*(x)$ for all $x > x_+$, then, clearly, it achieves minimal asymptotic loss. To do that, it is convenient to introduce a re-parameterization $y = \mathcal{Y}(x)$, where recall that $\mathcal{Y}(\cdot)$ is an increasing bijection, mapping (x_+, ∞) to (z_+, ∞) . Using Eqs. (3.13) and (3.14), assuming $x > x_+$, we get

$$x^2 = (\mathcal{D}(y))^{-1}, \quad \mathcal{C}(x) = -2 \frac{(\mathcal{D}(y))^{3/2}}{\mathcal{D}'(y)},$$

so that

$$R_1(x) - R_0(x) = y^2 - 2xy\mathcal{C}(x) = y^2 + 4y \cdot \frac{\mathcal{D}(y)}{\mathcal{D}'_\gamma(y)} = y^2 \left(1 + \frac{4}{\Psi_\gamma(y)}\right),$$

where

$$\Psi_\gamma(y) = y \cdot \frac{\mathcal{D}'(y)}{\mathcal{D}(y)}$$

is as defined in Eq. (4.4). Since $\Psi_\gamma(\cdot)$ is negative (\mathcal{D} is positive and decreasing), we conclude that

$$R^*(x) = \mathbb{1}_{\{\Psi_\gamma(y) \leq -4\}} \cdot R_0(x) + \mathbb{1}_{\{\Psi_\gamma(y) > -4\}} \cdot R_1(x). \quad (6.1)$$

The next lemma establishes some essential properties of $\Psi_\gamma(y)$:

Lemma 8. *Let H be a compactly supported CDF, with $\mathcal{Z}_+(H) > 0$. Let $\gamma \in (0, 1]$, and let $\Psi_\gamma(y; H)$ be defined as in Eq. (4.4). Then*

1. *The function $y \mapsto \Psi_\gamma(y; H)$ is strictly increasing on $y \in (\mathcal{Z}_+(H), \infty)$, with $\lim_{y \rightarrow \infty} \Psi_\gamma(y; H) = -2$.*
2. *Assume that*

$$\lim_{y \rightarrow \mathcal{Z}_+(F_Z)} \int (y - z)^{-2} dH(z) = \infty.$$

(This is Assumption 6 for $H = F_Z$). Then $\lim_{y \rightarrow \mathcal{Z}_+(H)} \Psi_\gamma(y; H) = -\infty$, and there is a unique point $y^ \in (\mathcal{Z}_+(F_Z), \infty)$ such that $\Psi_\gamma(y; H) = -4$.*

The proof of Lemma 8 appears in Section A of the supplementary article . An illustration of this Lemma and its consequences appears in Figure 5 below.

Proof of Lemma 1 The lemma follows as a straightforward corollary of Lemma 8. Lemma 8 implies that there is a unique number $T_\gamma(F_Z) > \mathcal{Z}_+(F_Z)$ such that $\Psi_\gamma(T_\gamma(F_Z); F_Z) = -4$. Since $y \mapsto \Psi_\gamma(y; F_Z)$ is increasing, plugging into Eq. (6.1),

$$R^*(x) = R(x|T_\gamma(F_Z)) = \mathbb{1}_{\{y \leq T_\gamma(F_Z)\}} \cdot R_0(x) + \mathbb{1}_{\{y > T_\gamma(F_Z)\}} \cdot R_1(x), \quad (6.2)$$

where $x > \mathcal{X}_+$ and $y = \mathcal{Y}(x)$. We conclude that $\text{ASE}^*[\mathbf{x}] = \text{ASE}[\mathbf{x}|T_\gamma(F_Z)]$. This is the minimum of $\text{ASE}[\mathbf{x}|\theta]$ over all $\theta \geq 0$ since, clearly, $\text{ASE}[\mathbf{x}|\theta] \geq \text{ASE}^*[\mathbf{x}]$ by definition. Moreover, for any $\theta \neq T_\gamma(F_Z)$, we can find some $y > \mathcal{Z}_+(F_Z)$ such that either $\theta < y < T_\gamma(F_Z)$ or $T_\gamma(F_Z) < y < \theta$. Taking $x = \mathcal{Y}^{-1}(y)$, we find that $R(x|\theta) > R(x|T_\gamma(F_Z)) = R^*(x)$, since there is a **unique** crossing point $x > \mathcal{X}_+$ with $R_0(x) = R_1(x)$ (because $y \mapsto \Psi_\gamma(y; F_Z)$ is strictly increasing). Thus, we can construct a signal \mathbf{x} for which $\text{ASE}[\mathbf{x}|\theta] > \text{ASE}^*[\mathbf{x}]$, and therefore $T_\gamma(F_Z)$ is the unique threshold which minimizes $\text{ASE}[\mathbf{x}|\theta]$ universally for all \mathbf{x} .

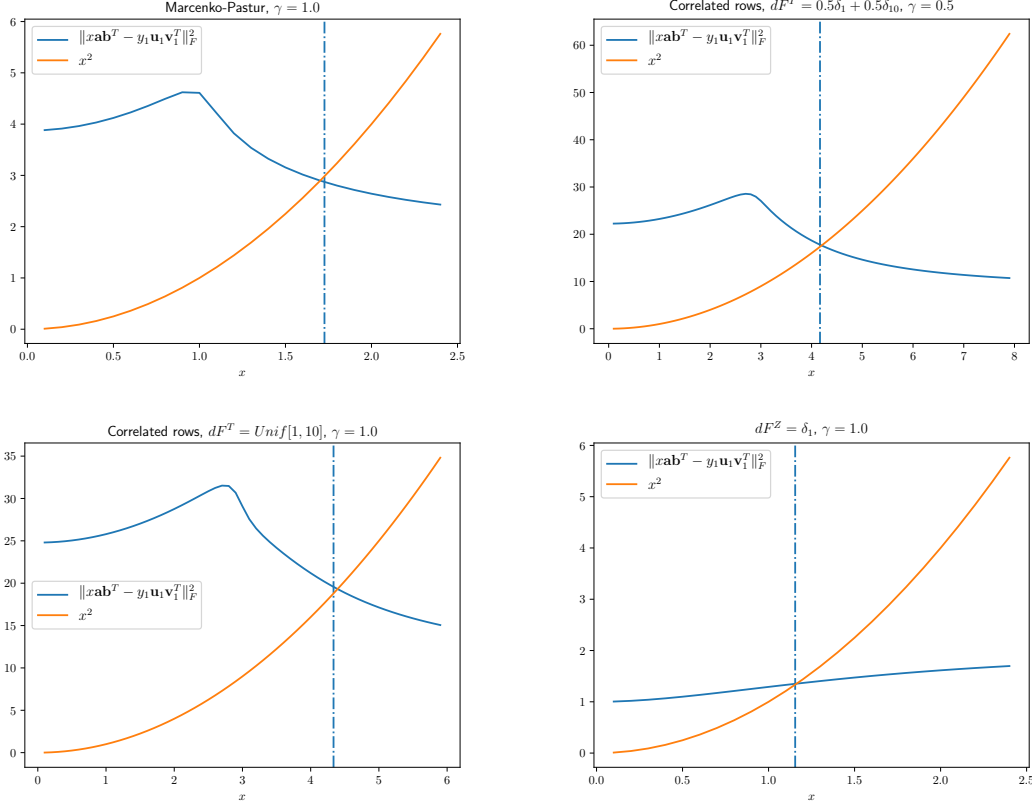


Fig 5: A numerical illustration of Lemma 8 and its consequences. Assuming a rank-1 signal $X = x \cdot \mathbf{a}_{1,n} \mathbf{b}_{1,n}^\top$, set $R_0(x) = \|X\|_F^2 = x^2$ and $R_1(x) = \lim_{n \rightarrow \infty} \|X - y_{1,n} \mathbf{a}_{1,n} \mathbf{b}_{1,n}^\top\|_F^2$. The point $x^* = \mathcal{Y}^{-1}(T_\gamma(F_Z))$ is the unique crossing point $R_0(x^*) = R_1(x^*)$. When $x < x^*$, the principal components of Y are “too noisy”, so that estimating $\hat{X} = 0$ gives better squared error; when $x > x^*$, the situation reverses. At each plot, $R_0(x)$ and $R_1(x)$ are plotted as x varies, for finite n , fixed signal components $\mathbf{a}_{1,n} \mathbf{b}_{1,n}^\top$ and a single instance of Z_n . The dashed vertical line is an estimate of x^* , obtained by applying the functional $T_{p/n}(\cdot)$ on F_{Z_n} , as well as computing the inverse map $\mathcal{Y}^{-1}(T_{p/n}(F_{Z_n}))$ numerically from F_{Z_n} . In all cases, $p = 500$ and $n = p/\gamma$. From left to right, top to bottom: (i) Marčenko-Pastur law with shape $\gamma = 1$; (ii) Noise matrix with correlated columns, with $F_S = \frac{1}{2}\delta_1 + \frac{1}{2}\delta_{10}$ and $\gamma = 0.5$; (iii) Likewise, with $F_S = \text{Unif}[1, 10]$; (iv) $F_Z = \delta_1$ and $\gamma = 1$ (specifically, $Z_n = I$).

Proof of Lemma 2 Part (1) of Lemma 2 follows from Lemma 1, along with the observation that if $\mathcal{Y}(x) = T_\gamma(F_Z)$, then $R_0(x) = R_1(x) = R^*(x)$; this means that regardless of whether we threshold slightly above or below $\mathcal{Y}(x)$, we get the same asymptotic loss. Part (2) follows by the same argument as in the proof of Lemma 1, in the paragraph above. Finally, part (3) follows right from the definition of $\underline{\Theta}(\mathbf{x})$ and $\overline{\Theta}(\mathbf{x})$.

6.2. Achieving oracle loss

We move on to study the oracle loss $\text{SE}_n^*[\mathbf{x}]$. This random variable depends on both X_n and the noise Z_n . Denote

$$\hat{X}_{[k]} = \sum_{i=1}^k y_{n,i} \mathbf{u}_{i,n} \mathbf{v}_{i,n}^\top, \quad k = 0, \dots, p. \quad (6.3)$$

That is, $\hat{X}_{[k]}$ is obtained from Y by keeping only the top $k = 0, \dots, p$ singular values (equivalently, hard thresholding at $t = y_{k+1,n}$, in case one has $y_{k+1,n} < y_{k,n}$). Any hard thresholding estimator \hat{X}_θ obviously corresponds to some $\hat{X}_{[k]}$ (however if there are multiplicities, possibly not every $\hat{X}_{[k]}$ is representable by some threshold θ); thus,

$$\text{SE}_n^*[\mathbf{x}] \geq \min_{0 \leq k \leq p} \|X - \hat{X}_{[k]}\|_F^2.$$

We first show that keeping too many singular values is consistently sub-optimal:

Lemma 9. Set $M = r + 1 + \left\lceil \frac{\text{ASE}^*[\mathbf{x}]}{z_+^2} \right\rceil$. Then

$$\mathbb{P} \left\{ \exists N \text{ s.t. } \forall n \geq N : \text{SE}_n^*[\mathbf{x}] < \min_{k \geq M} \|X - \hat{X}_{[k]}\|_F^2 \right\} = 1.$$

The proof of Lemma 9 is deferred to the supplementary article, Section B. Lemma 9 tells us that to study the oracle loss $\text{SE}_n^*[\mathbf{x}]$ as $n \rightarrow \infty$, we only need, essentially, to study the risk of a *fixed* collection of estimators, the number of whom does not depend on n ; specifically, $\hat{X}_{[k]}$ for $0 \leq k < M$. obtain formulas for $\lim_{n \rightarrow \infty} \|X_n - \hat{X}_{[k]}\|_F^2$, we need to compute the limiting correlations between the underlying signal dyads, $\mathbf{a}_{1,n} \mathbf{b}_{1,n}^\top, \dots, \mathbf{a}_{r,n} \mathbf{b}_{r,n}^\top$ and the corresponding empirical dyads $\mathbf{u}_{i,n} \mathbf{v}_{i,n}^\top$, for all $1 \leq i < M$. For empirical spikes up to $i = r$, these limiting correlations are computed in [10] (recall Eq. (3.7)).

The next result shows that, as one would expect, the j -th singular vectors of Y , for any bounded $j \geq r+1$, are asymptotically uncorrelated with the signal singular vectors:

Proposition 2. For any $1 \leq i \leq r$ and fixed $j \neq i$ (not necessarily $j \leq r$), one has

$$\langle \mathbf{a}_{n,i}, \mathbf{u}_{n,j} \rangle \cdot \langle \mathbf{b}_{n,i}, \mathbf{v}_{n,j} \rangle \xrightarrow{a.s.} 0.$$

The proof of Proposition 2 is deferred to Section C of the supplementary article. Note that Proposition 2 implies that for any *fixed* M (meaning M cannot depend on n), the event

$$\{\forall 1 \leq i \leq r, 1 \leq j \leq M, j \neq i, \quad : \quad \langle \mathbf{a}_{n,i}, \mathbf{u}_{n,j} \rangle \cdot \langle \mathbf{b}_{n,i}, \mathbf{v}_{n,j} \rangle \longrightarrow 0\}$$

holds with probability 1. The following Lemma is an immediate corollary:

Lemma 10. For any $k \geq r$,

$$\|X - \hat{X}_{[k]}\|_F^2 \xrightarrow{a.s.} \sum_{i=1}^r [x_i^2 + y_{i,\infty}^2 - 2x_i \cdot y_{i,\infty} \cdot \mathcal{C}(x_i)] + (k-r)z_+^2,$$

where, by way of notation, we use $\mathcal{C}(x_i) = 0$ for $x_i \leq x_+$. In particular,

$$\mathbb{P} \left\{ \exists N \text{ s.t. } \forall n \geq N : \text{SE}_n^*[\mathbf{x}] < \min_{k \geq r+1} \|X - \hat{X}_{[k]}\|_F^2 \right\} = 1.$$

Proof. The calculation is straightforward, as in the proof of Lemma 7. For the last part, simply recall that

$$\text{SE}_n[\mathbf{x}|T_\gamma(F_Z)] \xrightarrow{a.s.} \text{ASE}^*[\mathbf{x}] \leq \sum_{i=1}^r [x_i^2 + y_{i,\infty}^2 - 2x_i \cdot y_{i,\infty} \cdot \mathcal{C}(x_i)] .$$

□

We are ready to prove Theorems 1 and 2.

Proof of Theorem 1 By Lemmas 9 and 10, almost surely, there exists N such that $\forall n \geq N$,

$$\text{SE}_n^*[\mathbf{x}] \geq \min_{0 \leq k \leq r} \|X - \hat{X}_{[k]}\|_F^2 .$$

Part (1) then follows from the observation that $\min_{0 \leq k \leq r} \|X - \hat{X}_{[k]}\|_F^2 \xrightarrow{a.s.} \text{ASE}^*[\mathbf{x}]$, as can be deduced from the calculations of Section 6.1, together with $\text{SE}_n[\mathbf{x}|T_\gamma(F_Z)] \xrightarrow{a.s.} \text{ASE}^*[\mathbf{x}]$. We now prove (2). Let's assume, for ease of notation, that $T_\gamma(F_Z) \notin \{y_{1,\infty}, \dots, y_{r,\infty}\}$. In that case, the asymptotic optimal interval is just the interval between two consecutive spikes, say,

$$\underline{\Theta}(\mathbf{x}) = y_{k^*+1,\infty} , \quad \overline{\Theta}(\mathbf{x}) = y_{k^*,\infty} ,$$

where $y_{0,\infty} = \infty$. Note that if $T_\gamma(F_Z) = y_{k,\infty}$ for some $k \geq 1$, then $\underline{\Theta}(\mathbf{x}) = y_{k+1,\infty}$, $\overline{\Theta}(\mathbf{x}) = y_{k-1,\infty}$. With probability one, for large enough n , $X_{\theta_n} = \hat{X}_{[k^*]}$. Now, recall that $\|X_n - \hat{X}_{[k^*]}\|_F^2 \xrightarrow{a.s.} \text{ASE}^*[\mathbf{x}]$.

Proof of Theorem 2 Let k^* be as in the proof of Theorem 1. We know, from Lemmas 9, 10 and the definition of the asymptotic optimal interval, that $\|X - \hat{X}_{[k^*]}\|_F^2 \xrightarrow{a.s.} \text{ASE}^*[\mathbf{x}]$ and that almost surely, $\liminf_{n \rightarrow \infty} \min_{k \neq k^*} \|X - \hat{X}_{[k]}\|_F^2 > \text{ASE}^*[\mathbf{x}]$ (here is where we assume that there is no $y_{i,\infty}$ that equals $T_\gamma(F_Z)$). Thus,

$$\mathbb{P} \left\{ \exists N \text{ s.t. } \forall n \geq N : \text{SE}_n^*[\mathbf{x}] = \|X - \hat{X}_{[k^*]}\|_F^2 < \min_{k \neq k^*} \|X - \hat{X}_{[k]}\|_F^2 \right\} = 1 .$$

The proof follows by noting that: (i) If $\theta \in (\underline{\Theta}(\mathbf{x}), \overline{\Theta}(\mathbf{x}))$, then with probability 1, for all large enough n , $\hat{X}_{\theta_n} = \hat{X}_{[k^*]}$; (ii) If $\theta \notin [\underline{\Theta}(\mathbf{x}), \overline{\Theta}(\mathbf{x})]$ then with probability 1, for large enough n , $\hat{X}_{\theta_n} \neq \hat{X}_{[k^*]}$.

Acknowledgments

We are grateful to the anonymous reviewers for their thoughtful comments, which have helped improve this manuscript considerably.

Funding

DD was supported in part by NSF DMS 1407813, 1418362, and 1811614. This work was made possible by United States – Israel Binational Science Foundation (BSF) Grant 2016201 “Frontiers of Matrix Recovery”. ER was affiliated with the School of Computer Science and Engineering, the Hebrew University of Jerusalem, and supported in part by Israel Science Foundation grant no. 1523/16 and an Einstein-Kaye Fellowship from the Hebrew University of Jerusalem.

References

- [1] ACHLIOPTAS, D. and MCSHERRY, F. (2001). Fast Computation of Low Rank Matrix Approximations. In *Proceedings of the thirty-third annual ACM symposium on Theory of computing* 611–618.
- [2] ALTER, O., BROWN, P. O. and BOTSTEIN, D. (2000). Singular value decomposition for genome-wide expression data processing and modeling. *Proceedings of the National Academy of Sciences* **97** 10101–10106.

- [3] AZAR, Y., FIAT, A., KARLIN, A. R., MCSHERRY, F. and SAIA, J. (2001). Spectral Analysis of Data. In *Proceedings of the thirty-third annual ACM symposium on Theory of computing* 619–626.
- [4] BAI, Z. and SILVERSTEIN, J. W. (2010). *Spectral analysis of large dimensional random matrices* **20**. Springer.
- [5] BAI, Z. and YAO, J.-F. (2008). Central limit theorems for eigenvalues in a spiked population model. *Annales de l'Institut Henri Poincaré (B) Probability and Statistics* **44** 447–474.
- [6] BAI, Z. D. and SILVERSTEIN, J. W. (2004). CLT for linear spectral statistics of large-dimensional sample covariance matrices. *Ann. Probab.* **32** 553–605.
- [7] BAI, Z.-D., SILVERSTEIN, J. W. et al. (1998). No eigenvalues outside the support of the limiting spectral distribution of large-dimensional sample covariance matrices. *The Annals of Probability* **26** 316–345.
- [8] BAIK, J., BEN AROUS, G. and PÉCHÉ, S. (2005). Phase transition of the largest eigenvalue for nonnull complex sample covariance matrices. *The Annals of Probability* **33** 1643–1697.
- [9] BAIK, J. and SILVERSTEIN, J. W. (2006). Eigenvalues of large sample covariance matrices of spiked population models. *Journal of Multivariate Analysis* **97** 1382–1408.
- [10] BENAYCH-GEORGES, F. and NADAKUDITI, R. R. (2012). The singular values and vectors of low rank perturbations of large rectangular random matrices. *Journal of Multivariate Analysis* **111** 120–135.
- [11] BICKEL, P. J. and LEVINA, E. (2008). Covariance regularization by thresholding. *The Annals of Statistics* **36** 2577–2604.
- [12] CATTELL, R. B. (1966). The scree test for the number of factors. *Multivariate Behavioral Research* **1** 245–276.
- [13] CHATTERJEE, S. (2015). Matrix estimation by universal singular value thresholding. *Annals of Statistics* **43** 177–214.
- [14] DOBRIBAN, E. and OWEN, A. B. (2019). Deterministic parallel analysis: an improved method for selecting factors and principal components. *Journal of the Royal Statistical Society: Series B (Statistical Methodology)* **81** 163–183.
- [15] DONOHO, D. L., GAVISH, M. and ROMANOV, E. (2020). Code supplement for “ScreeNOT: Exact MSE-Optimal Singular Value Thresholding in Correlated Noise”. <https://purl.stanford.edu/py196rk3919>.
- [16] EDFORS, O. and SANDELL, M. (1998). OFDM channel estimation by singular value decomposition. *IEEE Transactions on Communications* **46** 931–939.
- [17] FRANKLIN, S. B., GIBSON, D. J., ROBERTSON, P. A., POHLMANN, J. T. and FRALISH, J. S. (1995). Parallel analysis: a method for determining significant principal components. *Journal of Vegetation Science* **6** 99–106.
- [18] GAVISH, M. and DONOHO, D. L. (2014). The Optimal Hard Threshold for Singular Values is $4/\sqrt{3}$. *IEEE Transactions on Information Theory* **60** 5040–5053.
- [19] HOFF, P. D. (2007). Model averaging and dimension selection for the singular value decomposition. *Journal of the American Statistical Association* **102** 674–685.
- [20] HONG, D., BALZANO, L. and FESSLER, J. A. (2018). Asymptotic performance of PCA for high-dimensional heteroscedastic data. *Journal of Multivariate Analysis* **167** 435–452.
- [21] JACKSON, D. A. (1993). Stopping rules in principal components analysis: a comparison of heuristical and statistical approaches. *Ecology*.
- [22] JOHNSTONE, I. M. (2001). On the distribution of the largest eigenvalue in principal components analysis. *Annals of Statistics* **29** 295–327.
- [23] JOLLIFFE, I. (2005). *Principal Component Analysis*, 2nd ed. Springer, New York.
- [24] LAGERLUND, T. D., SHARBROUGH, F. W. and BUSACKER, N. E. (1997). Spatial filtering of multichannel electroencephalographic recordings through principal component analysis by singular value decomposition. *Journal of Clinical Neurophysiology* **14** 73–82.
- [25] LEEB, W. and ROMANOV, E. (2021). Optimal spectral shrinkage and PCA with heteroscedastic noise. *IEEE Transactions on Information Theory* **67** 3009–3037.
- [26] NADAKUDITI, R. R. (2014). OptShrink: An algorithm for improved low-rank signal matrix denoising by optimal, data-driven singular value shrinkage. *IEEE Transactions on Information Theory* **60** 3002–3018.
- [27] NADLER, B. (2008). Finite sample approximation results for principal component analysis: A matrix perturbation approach. *The Annals of Statistics* **36** 2791–2817.
- [28] OWEN, A. B. and PERRY, P. O. (2009). Bi-cross-validation of the SVD and the nonnegative matrix

- factorization. *The Annals of Applied Statistics* **3** 564–594.
- [29] PAUL, D. (2007). Asymptotics of Sample Eigenstructure for a Large Dimensional Spiked Covariance Model. *Statistica Sinica* **17** 1617–1642.
 - [30] PERRY, P. O. (2009). Cross validation for unsupervised learning, PhD thesis, Stanford University.
 - [31] PRICE, A. L., PATTERSON, N. J., PLENGE, R. M., WEINBLATT, M. E., SHADICK, N. A. and REICH, D. (2006). Principal components analysis corrects for stratification in genome-wide association studies. *Nature Genetics* **38** 904–9.
 - [32] SHABALIN, A. A. and NOBEL, A. B. (2013). Reconstruction of a low-rank matrix in the presence of Gaussian noise. *Journal of Multivariate Analysis* **118** 67–76.
 - [33] SILVERSTEIN, J. W. (1985). The limiting eigenvalue distribution of a multivariate F matrix. *SIAM Journal on Mathematical Analysis* **16** 641–646.
 - [34] SILVERSTEIN, J. W. and CHOI, S.-I. (1995). Analysis of the limiting spectral distribution of large dimensional random matrices. *Journal of Multivariate Analysis* **54** 295–309.
 - [35] WACHTER, K. W. et al. (1980). The limiting empirical measure of multiple discriminant ratios. *The Annals of Statistics* **8** 937–957.
 - [36] WOLD, S. (1978). Cross-Validatory Estimation of the Number of Components in Factor and Principal Components Components Models. *Technometrics* **20** 397–405.
 - [37] YIN, Y., BAI, Z. and KRISHNAIAH, P. (1983). Limiting behavior of the eigenvalues of a multivariate F matrix. *Journal of Multivariate Analysis* **13** 508–516.

Supplementary Article to *ScreeNOT*: Exact MSE-Optimal Singular Value Thresholding in Correlated Noise

David Donoho¹, Matan Gavish² and Elad Romanov¹

¹Department of Statistics, Stanford University, e-mail: donoho@stanford.edu; eromanov@stanford.edu

²School of Computer Science and Engineering, Hebrew University of Jerusalem, e-mail: gavish@cs.huji.ac.il

Appendix A: Proof of Lemma 8

Define the probability distribution $d\tilde{H} = \gamma dH + (1 - \gamma)\delta_0$, so that, by definition, $\tilde{\varphi}_\gamma(y; H) = \varphi(y; \tilde{H})$. Since

$$\Psi(y; H) = y \cdot \frac{\mathcal{D}'(y; H)}{\mathcal{D}(y; H)} = y \cdot \left(\frac{\varphi'(y; H)}{\varphi(y; H)} + \frac{\varphi'(y; \tilde{H})}{\varphi(y; \tilde{H})} \right),$$

to show that Ψ is increasing, it suffices to show that $y \mapsto y \cdot \frac{\varphi'(y; H)}{\varphi(y; H)}$ is increasing for any CDF H and $y > \mathcal{Z}_+(H)$.

Introduce a change of variables $w = \log(y)$ and set $\psi(w) = \phi(e^w; H)$. We have

$$y \cdot \frac{\varphi'(y; H)}{\varphi(y; H)} = y \cdot \frac{d}{dy} (\log \varphi(y; H)) = y \cdot \frac{d}{dw} (\log \varphi(e^w; H)) \cdot \frac{dw}{dy} = \frac{d}{dw} (\log \psi(w)).$$

Since w is strictly increasing in y , it remains to show that $w \mapsto (\log \psi(w))'$ is increasing, equivalently, that $w \mapsto \psi(w)$ is log-convex. Write

$$\psi(w) = \int \psi_z(w) dH(z), \quad \text{where} \quad \psi_z(w) = \frac{e^w}{e^{2w} - z^2}.$$

Since a convex combination of log-convex functions is log-convex, it suffices to verify that each $\psi_z(w)$ is log-convex, whenever $y^2 = e^{2w} > z^2$. A straightforward calculation gives:

$$(\log \psi_z(w))' = 1 - \frac{2e^{2w}}{e^{2w} - z^2} = -\frac{z^2 + e^{2w}}{e^{2w} - z^2} = -1 - \frac{2z^2}{e^{2w} - z^2},$$

which is negative and clearly increasing in w . Thus, $\psi_z(w)$ is log-convex, and so we conclude that $y \mapsto \mathcal{D}(y; H)$ is strictly increasing. For the limit as $y \rightarrow \infty$, write

$$\varphi(y; H) = \int \frac{y}{y^2 - z^2} dH(z) = \frac{1}{y} + o\left(\frac{1}{y^2}\right), \quad \varphi(y; H) = - \int \frac{y^2 + z^2}{(y^2 - z^2)^2} dH(z) = -\frac{1}{y^2} + o\left(\frac{1}{y^3}\right),$$

as $y \rightarrow \infty$. Thus, $\Psi_\gamma(y; H) = -2 + o(1)$ as $y \rightarrow \infty$.

For part (2), observe that the additional assumption on H implies that $\frac{\varphi'(y; H)}{\varphi(y; H)} \rightarrow -\infty$ as $y \rightarrow \mathcal{Z}_+(H)$ from the right, hence $\Psi(y) \rightarrow -\infty$. Now, since $\Psi(y)$ is continuous on $y \in (\mathcal{Z}_+(H), \infty)$, it must attain $\Psi(y^*) = -4$ for some y^* . This y^* must be unique since, as we have proved in (1), $\Psi(y; H)$ is strictly increasing.

Appendix B: Proof of Lemma 9

Recall that for any matrix $A \in \mathbb{R}^{n \times p}$ with SVD $A = \sum_{i=1}^p \sigma_i \mathbf{u}_i \mathbf{v}_i^\top$, its best rank- r approximation with respect to Frobenius norm is obtained by taking its r leading principal components. Since X has rank r , for any $k \geq M$,

$$\|X - \hat{X}_{[k]}\|_F^2 \geq \min_{\text{rank}(B)=r} \|B - \hat{X}_{[k]}\|_F^2 = \sum_{i=r+1}^k y_{i,n}^2 \geq \sum_{i=r+1}^M y_{i,n}^2.$$

Recall that any fixed $i \geq r + 1$ satisfies $y_{i,n} \xrightarrow{a.s.} y_{i,\infty} = z_+$. Since M is constant, and satisfies $M > r + \text{ASE}^*[\mathbf{x}]/z_+^2$, we obtain that

$$\sum_{i=r+1}^M y_{i,n}^2 \xrightarrow{a.s.} (M - r)z_+^2 > \text{ASE}^*[\mathbf{x}].$$

Since $\text{SE}_n^*[\mathbf{x}] \leq \text{SE}_n[\mathbf{x}|T_\gamma(F_Z)] \xrightarrow{a.s.} \text{ASE}^*[\mathbf{x}]$, we conclude that almost surely, for all large enough n , $\text{SE}_n^*[\mathbf{x}] < \min_{k \geq M} \|X - \hat{X}_{[k]}\|_F^2$.

Appendix C: Proof of Proposition 2

This proposition asserts the asymptotic de-cross-correlation between principal ($j \leq r$) population singular vectors and non-principal ($j > r$) empirical (sample) singular vectors. We assume distinct population principal singular values. Results on the asymptotic de-cross-correlation between “off diagonal” combinations of population principal and empirical principal singular vectors have already been discussed in the main text near (3.6), where they follow for example [10], and also in several earlier works on the spiked covariance model. In contrast, in Proposition 2 only one of the two vectors being compared is principal, and the other is sub-principal.

Our argument relies on the “arrowhead representation” of the spiked covariance eigenproblem; see (C.1) below. We learned of this representation from [27].

Recall that our data matrix is $Y_n = \sum_{\ell=1}^r x_\ell \mathbf{a}_{\ell,n} \mathbf{b}_{\ell,n}^\top + Z_n$. Our goal is to show that for every fixed $1 \leq i \leq r$ and $j \neq i$, one has

$$\langle \mathbf{a}_{n,i}, \mathbf{u}_{n,j} \rangle \cdot \langle \mathbf{b}_{n,i}, \mathbf{v}_{n,j} \rangle \xrightarrow{a.s.} 0,$$

with $\mathbf{u}_{n,j}, \mathbf{v}_{n,j}$ being, respectively, the left and right j -th singular vectors of Y_n . For notational convenience, let us assume, without loss of generality, that $i = 1$. We will show that $\langle \mathbf{b}_{n,i}, \mathbf{v}_{n,j} \rangle \xrightarrow{a.s.} 0$, which (since the inner products are bounded) clearly suffices. Recall also that $\mathbf{v}_{n,j}$ is the j -th eigenvector of the p -by- p matrix $Y_n^\top Y_n$. Note that we may also assume without loss of generality that the eigenvalues of $Y_n^\top Y_n$ (equivalently, the p singular values of Z_n) are all distinct.¹ We may further assume throughout the proof that the distribution of Z_n is orthogonally invariant (both from the left and right); this is because $(\mathbf{a}_{n,1}, \dots, \mathbf{a}_{n,r})$ and $(\mathbf{b}_{n,1}, \dots, \mathbf{b}_{n,r})$ have an orthogonally-invariant distribution and are independent of Z_n (and, of course, the inner products we would like to compute are invariant to a global orthogonal transformation applied to both the population spikes and Y_n).

Let $P_n = I - \mathbf{b}_{1,n} \mathbf{b}_{1,n}^\top$ be the projection onto the orthogonal complement of $\mathbf{b}_{1,n}$, and set

$$\tilde{Z}_n = \sum_{\ell=2}^r x_\ell \mathbf{a}_{\ell,n} \mathbf{b}_{\ell,n}^\top + Z_n,$$

so that $Y_n = x_1 \mathbf{a}_{1,n} \mathbf{b}_{1,n}^\top + \tilde{Z}_n$. Let $\mathbf{q}_{2,n}, \dots, \mathbf{q}_{p,n}$ be an orthonormal basis of $\text{Range}(P_n)$, that diagonalizes the linear operator $P_n \tilde{Z}_n^\top \tilde{Z}_n P_n \Big|_{\text{Range}(P_n)}$ (that is, the restriction of the matrix $P_n \tilde{Z}_n^\top \tilde{Z}_n P_n$ onto the linear subspace $\text{Range}(P_n)$). Importantly, observe that the vectors $\mathbf{q}_{2,n}, \dots, \mathbf{q}_{p,n}$ do not depend on the population left singular vectors $\mathbf{a}_{1,n}, \dots, \mathbf{a}_{r,n}$; moreover, they remain unchanged when \tilde{Z}_n is multiplied from the left by any orthogonal matrix. Let $\mu_{2,n}, \dots, \mu_{p,n}$ be the corresponding eigenvalues, that is,

$$(P_n \tilde{Z}_n^\top \tilde{Z}_n P_n) \mathbf{q}_{\ell,n} = \mu_{\ell,n} \mathbf{q}_{\ell,n}, \quad 2 \leq \ell \leq p.$$

Denote the p -by- p orthogonal matrix $\mathcal{U} = [\mathbf{b}_{1,n}, \mathbf{q}_{2,n}, \dots, \mathbf{q}_{p,n}]$, whose columns consists of the aforementioned orthonormal basis. The change of basis \mathcal{U} has been explicitly chosen so that, in this basis, $Y_n^\top Y_n$ has the

¹Otherwise, one could add to Y_n an orthogonally-invariant but very weak independent perturbation W_n (e.g., an i.i.d. Gaussian matrix); doing so will only infinitesimally change the corresponding singular value correlations, and in the limit $\|W_n\| \rightarrow 0$ the resulting SVD of $Y_n + W_n$ will produce singular values with the same distribution at those of Y_n (we defined that $\mathbf{v}_{i,n}/\mathbf{u}_{i,n}$ -s that correspond to multidimensional singular spaces are uniformly random on these subspaces).

very particular form of a so-called *arrowhead matrix*, which have known useful exact closed-form expressions for eigenvalues and eigenvectors. That is, upon conjugation by \mathcal{U} ,

$$\mathcal{U}(Y_n^\top Y_n)\mathcal{U}^\top = \begin{bmatrix} \alpha_n & \mathbf{w}_n^\top \\ \mathbf{w}_n & \text{diag}(\mu_{2,n}, \dots, \mu_{p,n}) \end{bmatrix}, \quad (\text{C.1})$$

where

$$\alpha_n = \mathbf{b}_{1,n}^\top (Y_n^\top Y_n) \mathbf{b}_{1,n}, \quad (\text{C.2})$$

and $\mathbf{w}_n = (w_{2,n}, \dots, w_{p,n})$ is a $(p-1)$ -dimensional column vector:

$$w_{\ell,n} = \mathbf{b}_{1,n}^\top (Y_n^\top Y_n) \mathbf{q}_{\ell,n}, \quad 2 \leq \ell \leq p. \quad (\text{C.3})$$

Importantly, the bottom-right $(p-1)$ -by- $(p-1)$ minor of (C.1) is diagonal. It is known [27] that the eigenvectors of a matrix of the form (C.1), denoted $\mathbf{p}_{1,n}, \dots, \mathbf{p}_{p,n}$ are, up to normalization:

$$\mathbf{p}_{\ell,n} = \left(1, \frac{w_{2,n}}{\lambda_\ell - \mu_{2,n}}, \dots, \frac{w_{p,n}}{\lambda_\ell - \mu_{p,n}} \right), \quad 1 \leq \ell \leq p, \quad (\text{C.4})$$

where λ_ℓ is the corresponding eigenvalue. Recalling Eq. (C.1), the eigenvalues and eigenvectors of the arrowhead matrix are related to those of $Y_n^\top Y_n$:

$$\lambda_\ell = y_{\ell,n}^2, \quad \mathbf{v}_{\ell,n} = \pm \mathcal{U} \mathbf{p}_{\ell,n} / \|\mathcal{U} \mathbf{p}_{\ell,n}\|. \quad (\text{C.5})$$

In particular, combining with Eq. (C.4),

$$|\langle \mathbf{b}_{1,n}, \mathbf{v}_{j,n} \rangle| = |(\mathcal{U}^\top \mathbf{v}_{j,n})_1| = \frac{|(\mathbf{p}_{j,n})_1|}{\|\mathbf{p}_{j,n}\|} = \left(1 + \sum_{\ell=2}^p \frac{w_{\ell,p}^2}{(y_{j,n}^2 - \mu_{\ell,n})^2} \right)^{-1/2}. \quad (\text{C.6})$$

The RHS of (C.6) has an exact closed form that allows the argument for Proposition 2 to be completed by Lemma 11 below. \square

Lemma 11. *One has*

$$\sum_{\ell=2}^p \frac{w_{\ell,p}^2}{(y_{j,n}^2 - \mu_{\ell,n})^2} \xrightarrow{a.s.} \infty. \quad (\text{C.7})$$

Towards the proof of Lemma 11, we start with a simpler claim:

Lemma 12. *One has*

$$\frac{1}{p-1} \sum_{\ell=2}^p \frac{\mu_{\ell,n}}{(y_{j,n}^2 - \mu_{\ell,n})^2} \xrightarrow{a.s.} \infty. \quad (\text{C.8})$$

Proof. (Of Lemma 12.) It is suggestive to write the LHS of (C.8) as

$$\frac{1}{p-1} \sum_{\ell=2}^p \frac{\mu_{\ell,n}}{(y_{j,n}^2 - \mu_{\ell,n})^2} = \int \frac{\mu}{(y_{j,n}^2 - \mu)^2} dF_{P_n \tilde{Z}_n^\top \tilde{Z}_n P_n}(\mu), \quad (\text{C.9})$$

where $dF_{P_n \tilde{Z}_n^\top \tilde{Z}_n P_n}(\mu) = \frac{1}{p-1} \sum \frac{1}{p-1} \delta(\mu - \mu_{\ell,n})$ is the empirical eigenvalue distribution (counting measure) of $P_n \tilde{Z}_n^\top \tilde{Z}_n P_n$.

We know by [10] that $y_{j,n}^2 \xrightarrow{a.s.} \mathcal{Z}_+(F_{Z^\top Z})$, where $F_{Z^\top Z}$ denotes the limiting eigenvalue distribution² of $Z_n^\top Z_n$. Moreover, recall that by assumption 6,

$$\lim_{t \rightarrow \mathcal{Z}_+(F_{Z^\top Z})} \int \frac{\mu}{(t - \mu)^2} dF_{Z^\top Z}(\mu) = \infty.$$

Consequently, the proof of Lemma 12 is concluded once one shows that $F_{P_n \tilde{Z}_n^\top \tilde{Z}_n P_n} \xrightarrow{d} F_{Z^\top Z}$ almost surely. To see this, it suffices to note that:

²Recall: F_Z is the limiting distribution of *singular values* of Z_n ; they are related to the eigenvalues of $Z_n^\top Z_n$ by $\lambda_\ell(Z_n^\top Z_n) = \sigma_\ell^2(Z_n)$.

1. $P_n \tilde{Z}_n^\top \tilde{Z}_n P_n$ is a $(p-1)$ -by- $(p-1)$ minor of $\tilde{Z}_n^\top \tilde{Z}_n$, and therefore by eigenvalue interlacing, they have the same limiting eigenvalue distribution.
2. $\tilde{Z}_n = Z_n + \sum_{\ell=2}^r x_\ell \mathbf{a}_{\ell,n} \mathbf{b}_{\ell,n}^\top$ is a finite-rank additive perturbation of Z_n ; hence by singular value interlacing, it has the same limiting singular value distribution as Z_n (with at most $r-1$ outlying singular values); thus, the limiting eigenvalue distribution of $\tilde{Z}_n^\top \tilde{Z}_n$ is $F_{Z^\top Z}$.

□

Equipped with Lemma 12, we now prove Lemma 11.

Proof. (Of Lemma 11) Let us analyze the weights $w_{\ell,n}^2$ in (C.7). Recalling (C.3),

$$\begin{aligned} w_{\ell,n} &= \mathbf{b}_{1,n}^\top (\tilde{Z}_n^\top + x_1 \mathbf{b}_{1,n} \mathbf{a}_{1,n}^\top) (\tilde{Z}_n + x_1 \mathbf{a}_{1,n} \mathbf{b}_{1,n}^\top) \mathbf{q}_{\ell,n} \\ &= (\mathbf{b}_{1,n}^\top \tilde{Z}_n^\top + x_1 \mathbf{a}_{1,n}^\top) \tilde{Z}_n \mathbf{q}_{\ell,n} \\ &= \mathbf{b}_{1,n}^\top (\tilde{Z}_n^\top \tilde{Z}_n) \mathbf{q}_{\ell,n} + x_1 \mathbf{a}_{1,n}^\top \tilde{Z}_n \mathbf{q}_{\ell,n}, \end{aligned}$$

where we used $\mathbf{b}_{1,n} \perp \mathbf{q}_{\ell,n}$ (by construction). Note that we may assume with loss of generality that $\mathbf{b}_{1,n}^\top (\tilde{Z}_n^\top \tilde{Z}_n) \mathbf{q}_{\ell,n} \geq 0$ (since we may a priori replace any \mathbf{q} by $-\mathbf{q}$), and therefore,

$$w_{\ell,n}^2 \geq x_1^2 (\mathbf{a}_{1,n}^\top \tilde{Z}_n \mathbf{q}_{\ell,n})^2 \mathbb{1}_{\{\mathbf{a}_{1,n}^\top \tilde{Z}_n \mathbf{q}_{\ell,n} \geq 0\}}. \quad (\text{C.10})$$

Recall that by their definition, the vectors $\{\tilde{Z}_n \mathbf{q}_{\ell,n}\}_{2 \leq \ell \leq p}$ are orthogonal to one another, with $\|\tilde{Z}_n \mathbf{q}_{\ell,n}\|^2 = \mu_{\ell,n}$. Let us, for the moment, make the simplifying assumption $r = 1$. In that case, $\tilde{Z}_n = Z_n$, hence $\{\tilde{Z}_n \mathbf{q}_{\ell,n}\}_{2 \leq \ell \leq p}$ are independent of $\mathbf{a}_{1,n}$. Since $\mathbf{a}_{1,n}$ is uniformly distributed on the n -dimensional unit sphere, we may write $\mathbf{a}_{1,n} = \mathbf{g}/\|\mathbf{g}\|$ for $\mathbf{g} \sim \mathcal{N}(0, I_n)$. Then $\{\mathbf{g}^\top \tilde{Z}_n \mathbf{q}_{\ell,n}\}_{2 \leq \ell \leq p}$ are independent (univariate) Gaussians, being the projections of a Gaussian vector onto orthogonal directions. To wit, the following equality in distribution holds:

$$\left(\mathbf{a}_{1,n}^\top \tilde{Z}_n \mathbf{q}_{2,n}, \dots, \mathbf{a}_{1,n}^\top \tilde{Z}_n \mathbf{q}_{p,n} \right) \stackrel{d}{=} \left(\frac{\mu_{2,n}^{1/2}}{\|\mathbf{g}\|} g_2, \dots, \frac{\mu_{p,n}^{1/2}}{\|\mathbf{g}\|} g_p \right).$$

Using (C.10), $n^{-1} \|\mathbf{g}\|^2 \xrightarrow{a.s.} 1$, and the strong law of large numbers,

$$\begin{aligned} \sum_{\ell=2}^p \frac{w_{\ell,p}^2}{(y_{j,n}^2 - \mu_{\ell,n})^2} &\geq \frac{x_1^2}{\|\mathbf{g}\|^2} \sum_{\ell=2}^p \frac{\mu_{\ell,n}}{(y_{j,n}^2 - \mu_{\ell,n})^2} g_\ell^2 \mathbb{1}_{\{g_\ell \geq 0\}} \\ &\approx x_1^2 \cdot \frac{p-1}{n} \cdot \frac{1}{p-1} \sum_{\ell=2}^p \frac{\mu_{\ell,n}}{(y_{j,n}^2 - \mu_{\ell,n})^2} \cdot \mathbb{E}[g_\ell^2 \mathbb{1}_{\{g_\ell \geq 0\}}] \xrightarrow{a.s.} \infty, \end{aligned}$$

where the last limit follows from Lemma 12. This proves Lemma 11 assuming $r = 1$.

Let us now adapt the above argument for any fixed $r \geq 1$. The difficulty in doing so lies with the fact that $\mathbf{a}_{1,n}$ is no longer independent of $\{\tilde{Z}_n \mathbf{q}_{\ell,n}\}_{2 \leq \ell \leq p}$, since $\tilde{Z}_n = \sum_{\ell=2}^r x_\ell \mathbf{a}_{\ell,n} \mathbf{b}_{\ell,n}^\top + Z_n$, and $\mathbf{a}_{1,n}$ is orthogonal to $\mathbf{a}_{2,n}, \dots, \mathbf{a}_{r,n}$. The key fact is that this dependence is rather weak, as we will show.

Let us condition on $\mathbf{a}_{2,n}, \dots, \mathbf{a}_{r,n}$, and let \mathcal{P}_A be the projection onto their orthogonal complement. Then we can write the conditional distribution of $\mathbf{a}_{1,n}$ as $\mathbf{a}_{1,n} \stackrel{d}{=} \mathcal{P}_A(\mathbf{g})/\|\mathcal{P}_A(\mathbf{g})\|$, where $\mathbf{g} \sim \mathcal{N}(0, I_n)$. Since \mathcal{P}_A projects onto a subspace of dimension $n-r$, with r constant, $\|\mathcal{P}_A(\mathbf{g})\|^2/n \xrightarrow{a.s.} 1$. Denote $\zeta_{\ell,n} = \tilde{Z}_n \mathbf{q}_{\ell,n}/\mu_{\ell,n}^{1/2}$, $2 \leq \ell \leq p$, which are $p-1$ orthonormal vectors. We have, as was before,

$$\sum_{\ell=2}^p \frac{w_{\ell,p}^2}{(y_{j,n}^2 - \mu_{\ell,n})^2} \gtrsim x_1^2 \cdot \frac{p-1}{n} \cdot \frac{1}{p-1} \sum_{\ell=2}^p \frac{\mu_{\ell,n}}{(y_{j,n}^2 - \mu_{\ell,n})^2} \cdot (\zeta_{\ell,n}^\top \mathcal{P}_A \mathbf{g})^2 \mathbb{1}_{\{\zeta_{\ell,n}^\top \mathcal{P}_A \mathbf{g} \geq 0\}}.$$

Since we assumed that the distribution of \tilde{Z}_n is orthogonally invariant from the left (see beginning of this section), and since the eigenvectors $\mathbf{q}_{2,n}, \dots, \mathbf{q}_{p,n}$ are not dependent on such orthogonal left multiplication, the random signs $\{\text{sign}(\zeta_{\ell,n}^\top \mathcal{P}_A \mathbf{g})\}_{2 \leq \ell \leq p}$ are i.i.d. $\text{Ber}(1/2)$ and independent of the moduli $(\zeta_{\ell,n}^\top \mathcal{P}_A \mathbf{g})^2$.

Consequently, in light of Lemma 12, it suffices to prove that for any $\varepsilon > 0$, there is constant C_ε such that

$$\frac{1}{p} \sum_{\ell=2}^{\lfloor \varepsilon p \rfloor} (\zeta_{\ell,n}^\top \mathcal{P}_A \mathbf{g})^2 \geq C_\varepsilon$$

holds asymptotically almost surely as $p \rightarrow \infty$. The above sum has a simple geometric interpretation: one first projects \mathbf{g} onto the complement of $\mathbf{a}_{2,n}, \dots, \mathbf{a}_{r,n}$, and then projects the result onto the span of $\zeta_{2,n}, \dots, \zeta_{\lfloor \varepsilon p \rfloor, n}$; the sum is the remaining energy (squared L_2 norm). Let $\mathcal{W} = \text{span}(\mathbf{a}_{2,n}, \dots, \mathbf{a}_{r,n}, \{\zeta_{2,n}, \dots, \zeta_{\lfloor \varepsilon p \rfloor, n}\}^\perp) \subseteq \mathbb{R}^p$, so that $\dim(\mathcal{W}) \leq r + p - \lfloor \varepsilon p \rfloor + 1$. Certainly, $\frac{1}{p} \sum_{\ell=2}^{\lfloor \varepsilon p \rfloor} (\zeta_{\ell,n}^\top \mathcal{P}_A \mathbf{g})^2 \geq \frac{1}{p} \|\mathcal{P}_{\mathcal{W}^\perp} \mathbf{g}\|^2$, where $\mathcal{P}_{\mathcal{W}^\perp}$ is the projection onto the complement of \mathcal{W} . Since r is constant, $\dim(\mathcal{W}^\perp) \geq p(\varepsilon - o(1))$, and consequently, $\frac{1}{p} \|\mathcal{P}_{\mathcal{W}^\perp} \mathbf{g}\|^2 \gtrsim \varepsilon$ almost surely as $p \rightarrow \infty$. Thus, the proof is concluded. \square

Appendix D: Estimating $T_\gamma(F_Z)$: Auxiliary Lemmas

D.1. Proof of Lemma 3

Let $\epsilon > 0$ be small. By assumption, $T_\gamma(H) > \mathcal{Z}_+(H)$, and it is the unique number satisfying $\Psi_\gamma(T_\gamma(H); H) = -4$. Let $y_1 = T_\gamma(H) - \epsilon/2$, $y_2 = T_\gamma(H) + \epsilon/2$, where ϵ was chosen small enough so that $\mathcal{Z}_+(H) < y_1 < y_2$. Note that $\Psi_\gamma(y_1; H) < -4 < \Psi_\gamma(y_2; H)$, as $\Psi(\cdot; H)$ is increasing. Since $H_n \xrightarrow{d} H$ (and $|p/n - \gamma| \leq 1/n \rightarrow 0$) we find that for all large enough n , $\Psi_{p/n}(y_1; H_n) < -4 < \Psi_{p/n}(y_2; H_n)$, since $\Psi_{p/n}(y_1; H_n) \rightarrow \Psi_{p/n}(y_1; H)$ and $\Psi_{p/n}(y_2; H_n) \rightarrow \Psi_{p/n}(y_2; H)$. Since also $\mathcal{Z}_+(H_n) \rightarrow \mathcal{Z}_+(H) < y_1$, we deduce that for large enough n , $y_1 < T_{p/n}(H_n) < y_2$, that is, $|T_{p/n}(H_n) - T_\gamma(H)| < \epsilon$.

D.2. Proof of Lemma 4

Part (1) will follow from (3), since convergence in KS distance implies weak convergence, and $F_{Z_n} \xrightarrow{d} F_Z$ almost surely. For part (3), denote by $z_{i,n}$, $i = 1, \dots, p$, the singular values of Z_n . By Weyl's interlacing inequality, since $Y_n = X_n + Z_n$ and $\text{rank}(X) = r \leq k$,

$$z_{i,n} \leq y_{i,n} \leq z_{i-k,n}, \quad \text{for } i = k+1, \dots, p.$$

Fix some y , and let j be the smallest index $j \geq k+1$ such that $y_{j,n} \leq y$ (set $j = 0$ if no such index exists). The interlacing inequality states that $z_{j,n} \leq y$ as well. If $j = k+1$, then at worst the interval contains all of $z_{k,n}, \dots, z_{1,n}$, and none of the additional “pseudo-singular values” we have introduced. Hence, in that case, $|F_{Z_n}(y) - F_{n,k}^*(y)| \leq k/p$. Now, suppose that $j > k+1$. Since $y_{j+1,n} > y$, the interlacing inequality gives $z_{j+1-k,n} \geq y_{j+1,n} > y$, hence in addition to $z_{p,n}, \dots, z_{j,n}$, the interval $(-\infty, y]$ contains at most k additional singular values of Z_n , specifically $z_{j+1,n}, \dots, z_{j-k}$. In the worst case, we have added no “pseudo-singular values” with $\leq y$, hence again $|F_{Z_n}(y) - F_{n,k}^*(y)| \leq k/p$. Lastly, to prove (2), note that for any $\epsilon > 0$, $F_Z(\mathcal{Z}_+(F_Z) - \epsilon) < 1$, which means that almost surely, for large enough n , there are $\Omega(n)$ singular values of Z_n bigger than $\mathcal{Z}_+(F_Z) - \epsilon$. By interlacing, for any $m_n = o(n)$ with $r < m_n$, $y_{m_n,n} \geq z_{m_n,n}$, and $z_{m_n,n}$ must eventually be among those singular values bigger than $\mathcal{Z}_+(F_Z) - \epsilon$. But this is true for any $\epsilon > 0$, meaning that $y_{m_n} \xrightarrow{a.s.} \mathcal{Z}_+(F_Z)$ whenever $r < m_n = o(n)$.

D.3. Proof of Lemma 6

Fix any a satisfying $\mathcal{Z}_+(H) < a < T_\gamma(H)$. Observe that one can find a neighborhood \mathcal{N} of $T_\gamma(H)$ and $c_1, c_2 > 0$ such that $c_2 < \Psi'_{\gamma'}(y; G) < c_1$ for all $y \in \mathcal{N}$ and any distribution G supported on $[0, a]$ and γ' (to see this, simply follow calculations in the proof of Lemma 8). Now, since $T_{p/n}(H_n) \rightarrow T_\gamma(H)$, we see that $T_{p/n}(H_n) \in \mathcal{N}$ for all large enough n . Consequently, by the mean value theorem,

$$c_2(T_{p/n}(H_n) - T_\gamma(H)) < \Psi_{p/n}(T_{p/n}(H_n); H_n) - \Psi_{p/n}(T_\gamma(H); H_n) \leq c_1(T_{p/n}(H_n) - T_\gamma(H)).$$

Using $\Psi_\gamma(T_\gamma(H); H) = \Psi_{p/n}(T_{p/n}(H_n); H_n) = -4$, and the fact that Ψ is increasing, we conclude that

$$\begin{aligned} |T_{p/n}(H_n) - T_\gamma(H)| &\leq \max(1/c_1, 1/c_2) \cdot |\Psi_{p/n}(T_{p/n}(H_n); H_n) - \Psi_{p/n}(T_\gamma(H); H_n)| \\ &= \max(1/c_1, 1/c_2) \cdot |\Psi_\gamma(T_\gamma(H); H) - \Psi_{p/n}(T_\gamma(H); H_n)|. \end{aligned}$$

The right-hand-side is now $\mathcal{O}(\Delta_{1,n} + \Delta_{2,n} + |p/n - \gamma|)$.

D.4. Proof of Proposition 1

By Lemma 6, we need to show that

$$|\varphi(T_\gamma(F_Z); F_Z) - \varphi(T_\gamma(F_Z); F_{n,k}^*)|, |\varphi'(T_\gamma(F_Z); F_Z) - \varphi'(T_\gamma(H); F_{n,k}^*)| = \mathcal{O}_{\mathbb{P}}(k/p)$$

(by definition, $|\gamma_n - \gamma| \leq 1/n$). Write

$$\begin{aligned} \varphi(T_\gamma(F_Z); F_Z) - \varphi(T_\gamma(F_Z); F_{n,k}^*) &= [\varphi(T_\gamma(F_Z); F_Z) - \varphi(T_\gamma(F_Z); F_{Z_n})] \\ &\quad + [\varphi(T_\gamma(F_Z); F_{Z_n}) - \varphi(T_\gamma(F_Z); F_{n,k}^*)], \end{aligned}$$

we bound each bracket separately (the argument when φ is replaced by φ' is the same). The expression $\varphi(T_\gamma(F_Z); F_Z) = \int \frac{T_\gamma(F_Z)}{T_\gamma(F_Z)^2 - z^2} dF_Z(z)$ is a linear spectral statistic, and satisfies the requirement of [6], by assumption - see Section 3.2. Hence,

$$|\varphi(T_\gamma(F_Z); F_Z) - \varphi(T_\gamma(F_Z); F_{Z_n})| = \mathcal{O}_{\mathbb{P}}(1/p).$$

For the second term, recall that if F_1 and F_2 are CDFs supported on the interval I and $g : I \rightarrow \mathbb{R}$ is bounded and continuously differentiable, then

$$\left| \int g(t)(dF_1(t) - dF_2(t)) \right| \leq (\|g\|_{L^\infty(I)} + \|g'\|_{L^1(I)}) \cdot \|F_1 - F_2\|_{\text{KS}}.$$

Since both $\mathcal{Z}_+(F_{Z_n}), \mathcal{Z}_+(F_{n,K}^*) \xrightarrow{a.s.} \mathcal{Z}_+(F_Z)$, by Lemma 4, almost surely,

$$|\varphi(T_\gamma(F_Z); F_{Z_n}) - \varphi(T_\gamma(F_Z); F_{n,k}^*)| = \mathcal{O}(k/p).$$

Appendix E: Additional numerical experiments

In this section we provide extensive numerical experiments validating different aspects of our results under various noise distributions.

E.1. Noise distributions

We have conducted experiments using the following noise distributions:

- **Marčenko-Pastur**: the matrix Z is an i.i.d Gaussian matrix, so that F_Z is a Marčenko-Pastur with shape parameter γ .
- **Chi10**: A noise matrix with correlated columns, such that W is i.i.d Gaussian and F_S is the law of a χ -squared random variable with 10 degrees of freedoms, normalized to have variance 1: $T = \frac{1}{10} \sum_{i=1}^{10} g_i$ where $g_1, \dots, g_{10} \sim \mathcal{N}(0, 1)$.
- **Mix2**: A noise matrix with correlated columns, such that W is i.i.d Gaussian, and F_S is an equal mixture of two atoms: $dF_S = \frac{1}{2}\delta_1 + \frac{1}{2}\delta_{10}$.
- **Unif[1,10]**: A noise matrix with correlated columns, such that W is i.i.d Gaussian, and F_S is the uniform distribution on $[1, 10]$.
- **Fisher3n**: Z has the form $Z = W_1 S_2^{-1/2}$ where $W_1 \in \mathbb{R}^{n \times p}$ is i.i.d Gaussian $\mathcal{N}(0, 1/n)$, and $S_2 = W_2^\top W_2$ where $W_2 \in \mathbb{R}^{3p \times p}$ is an i.i.d Gaussian matrix with entries $\mathcal{N}(0, 1/(3n))$. Matrices of this form have been studied in the literature under the name F-matrices (also F-ratios, Fisher matrices). Their limiting singular value distribution is given by Wachter's law [35], see also [37, 33, 4].

- **PaddedIdentity:** All the singular values of Z are 1, that is, $dF_Z = \delta_1$. Specifically, Z is the matrix $Z = [\mathbf{I}_{p \times p}, \mathbf{0}_{p \times (n-p)}]^\top$, that is, a p -by- p identity matrix, padded by zeros.

In the table below, one can find some useful quantities corresponding to the distributions above (with select choices of γ): the bulk edge $\mathcal{Z}_+(F_Z)$, the location of the BBP PT \mathcal{X}_+ , optimal threshold $T_\gamma(F_Z)$ and $x^* = \mathcal{Y}^{-1}(T_\gamma(F_Z))$. All these quantities are estimated by sampling a large noise matrix Z (specifically, we take $p = 3000$ and $n = p/\gamma$) and estimating all the necessary functionals by their plugin estimates, putting F_{Z_n} in place of F_Z , and rounding all numbers to 2 digits after the decimal point. Estimating \mathcal{X}_+ in this manner is especially problematic, since for any counting measure H , in our case $H = F_{Z_n}$, $\mathcal{X}_+(H) = \lim_{y \rightarrow \mathcal{Z}_+(H)} (D_{p/n}(y; H))^{-1/2} = 0$, since $\mathcal{D}(\cdot; H)$ has $1/y$ singularity near $\mathcal{Z}_+(H)$. For our purposes, we use the heuristic $\mathcal{X}_+ \approx (D_{p/n}(\mathcal{Z}_+(F_{Z_n}) + 0.01; F_{Z_n}))^{-1/2}$, which may be somewhat off from the true PT location.³ In the case of **PaddedIdentity**, it is obvious that $\mathcal{X}_+ = 0$, and this is what we give below.

Distribution:	γ	$\mathcal{Z}_+(F_Z)$	$\mathcal{X}_+(F_Z)$	$T_\gamma(F_Z)$	$\mathcal{Y}^{-1}(T_\gamma(F_Z))$
Marčenko-Pastur	0.5	1.7	0.91	1.98	1.48
	1.0	2.0	1.07	2.31	1.73
Chi10	0.5	2.11	1.59	2.17	1.7
	1.0	2.26	1.5	2.46	1.89
Fisher3n	0.5	1.99	1.19	2.23	1.7
	1.0	2.28	1.36	2.57	1.95
Mix2	0.5	4.76	2.73	5.34	4.16
	1.0	5.44	3.13	6.08	4.73
Unif[1,10]	0.5	4.4	2.48	4.96	3.79
	1.0	5.04	2.72	5.7	4.36
PaddedIdentity	0.5	1.0	0.0	1.62	1.11
	1.0	1.0	0.0	1.73	1.15

E.2. Description of experiments

For each noise distribution we conduct the following experiments:

- **Hist:** We give a histogram singular values of a large noise matrix, in the case where the description of F_Z is not trivial. We do this to get a some sense for how the noise bulk looks like. Specifically, the noise matrix we sample has dimensions $p = 3000$ and $n = p/\gamma$.
- **R0-vs-R1:** We compare the functions $R_0(x)$ and $R_1(x)$ from Lemma 8, and demonstrate that $x^* = \mathcal{Y}^{-1}(T_\gamma(F_Z))$ is their unique crossing point $x > \mathcal{X}_+$; this is done in the following way: we consider a rank 1 signal $X = x\mathbf{a}\mathbf{b}^\top$ and $Y = X + Z$, where the signal directions \mathbf{a}, \mathbf{b} and noise matrix Z are sampled once, and we let the intensity x vary. The dimensions used are $p = 500$ and $n = p/\gamma$. We plot the quantities $R_0(x) = \|X\|_F^2 = x^2$ (the error of the estimator $\hat{X} = 0$) and $\hat{R}_1(x) = \|X - y_1 \mathbf{u}\mathbf{v}^\top\|_F^2$, the error obtained by for estimating X using the principal component of Y . The theory states that $\hat{R}_1(x)$ converges to $R_1(x)$, and we also plot this, as well as show that x^* is the unique intersection point of $R_0(x)$ and $R_1(x)$. Thresholding at the intersection of $\hat{R}_1(x)$ and $R_0(x)$ is optimal (for this problem instance), and we see that indeed this intersection point is quite close to x^* .
- **SE-vs-ASE:** Our theory states that as n, p grow, the random function $\theta \mapsto \text{SE}_n[\mathbf{x}|\theta]$ tends to the deterministic function $\theta \mapsto \text{ASE}[\mathbf{x}|\theta]$, when $\theta > \mathcal{Z}_+(F_Z)$. We illustrate this phenomenon. We consider a single problem instance, corresponding to the rank $r = 5$ signal $\mathbf{x} = (0.5, 1.0, 1.3, 2.5, 5.2)$, and plot the function $\text{SE}_n[\mathbf{x}|\theta]$ and $\text{ASE}[\mathbf{x}|\theta]$ on top of each other (we plot $\text{SE}_n[\mathbf{x}|\theta]$ for very few thresholds $\theta \leq y_{r+1, n}$; as the rank of X_t grows, the MSE blows up quickly). We use dimensions $p = 500$ and $n = p/\gamma$. We indicate the locations of z_+ , $T_\gamma(F_Z)$ and the estimates $T_{p/n}(F_{n, k}^*)$ for $\star \in \{0, w, i\}$, where we use $k = 4r = 20$. We see that for a “typical” problem instance, $\text{ASE}[\mathbf{x}|\theta]$ is indeed a good proxy for $\text{SE}_n[\mathbf{x}|\theta]$.

³For instance, when the noise is Marčenko-Pastur, exact expressions are available, see e.g. [18], and $\mathcal{X}_+ = \gamma^{1/4}$. This is quite off from the expression in the table!

- **OracleAttainment:** We test Theorems 2 and 3, whereby the probability that thresholding at $T_{p/n}(F_{n,k}^*)$ attains oracle loss with probability tending to 1 as $n, p \rightarrow \infty$. For various choices of p , we run $T = 50$ denoising experiments, and report the fraction of experiments where each threshold $\in \{T_\gamma(F_Z), T_{p/n}(F_{n,k}^0), T_{p/n}(F_{n,k}^w), T_{p/n}(F_{n,k}^i)\}$ attains oracle loss ($T_\gamma(F_Z)$ is computed as described in experiment **R0-vs-R1**). In all experiments, we use the signal $\mathbf{x} = (0.5, 1.0, 1.3, 2.5, 5.2)$ which has rank $r = 5$ (the same signal as in experiment **SE-vs-ASE**), and the upper bound $k = 4r = 20$. Note that we have chosen the spikes x_i to be all far from $x^* = \mathcal{Y}^{-1}(T_\gamma(F_Z))$, in accordance with the condition in Theorem 2.
- **Regret:** We compare the oracle loss $\text{SE}_n[\mathbf{x}]$ with $\text{SE}_n[x|\hat{\theta}]$ for the choices

$$\hat{\theta} \in \{T_\gamma(F_Z), T_{p/n}(F_{n,k}^0), T_{p/n}(F_{n,k}^w), T_{p/n}(F_{n,k}^i)\},$$

in the single-spiked setup, as described in experiment **R0-vs-R1** above. We let the spike intensity x vary and plot $\text{SE}_n[\mathbf{x}|\hat{\theta}]/\text{SE}_n^*[\mathbf{x}]$ for each choice of estimator. We expect the choice of estimator to especially matter when x is close to $x^* = \mathcal{Y}^{-1}(T_\gamma(F_Z))$ (indicated in the plots by a dashed vertical line), and this can indeed be seen in the plots. The ratios we report are averages across $T = 20$ experiments.

- **ConvergenceRate:** We study the rate of convergence of $T_{p/n}(F_{n,k}^*)$ towards $T_\gamma(F_Z)$. To that end, we consider a rank $r = 10$ signal $x = (1, \dots, 10)$, set $k = 20$ and plots the relative absolute error $|T_{p/n}(F_{n,k}^*) - T_\gamma(F_Z)|/T_\gamma(F_Z)$ as p varies and $n = p/\gamma$. We plot the error in a logarithmic scale, to get a sense of its polynomial rate of decay in p . Note that by Proposition 1, we expect the slope in most cases to be, roughly, $\lesssim 1$. We find that almost always, $T_{p/n}(F_{n,k}^i)$ (imputation) approximates $T_\gamma(F_Z)$ much better than $T_{p/n}(F_{n,k}^w)$ (winsorization) or $T_{p/n}(F_{n,k}^0)$ (transport to zero). All points on the plots are generated by averaging the error of $T = 50$ experiments.

E.3. Distribution: Marčenko-Pastur, $\gamma = 1.0$

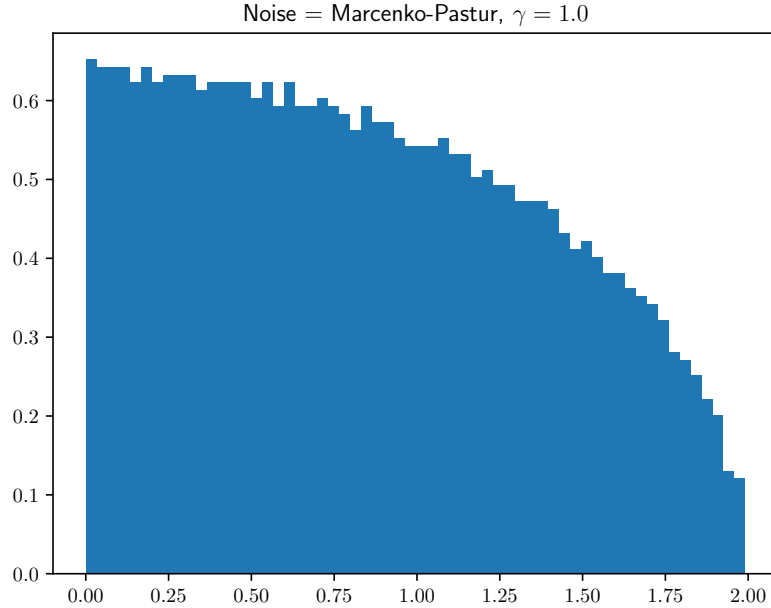
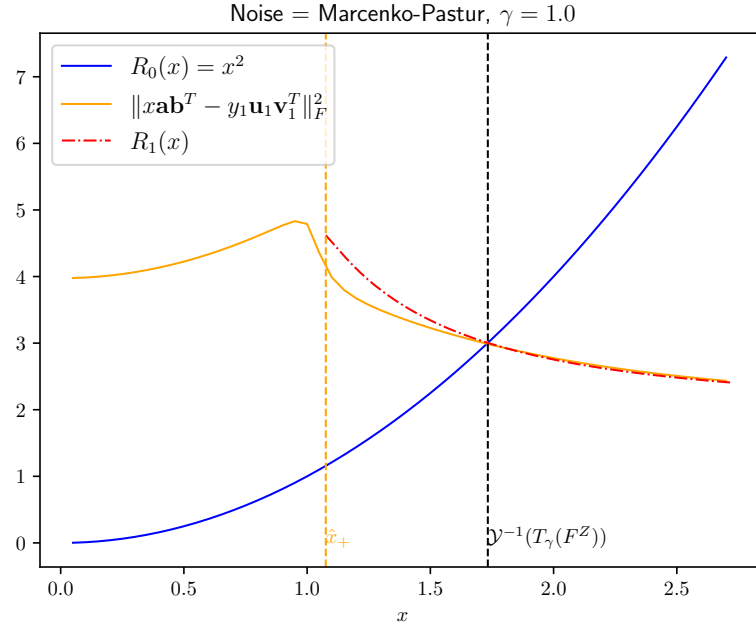
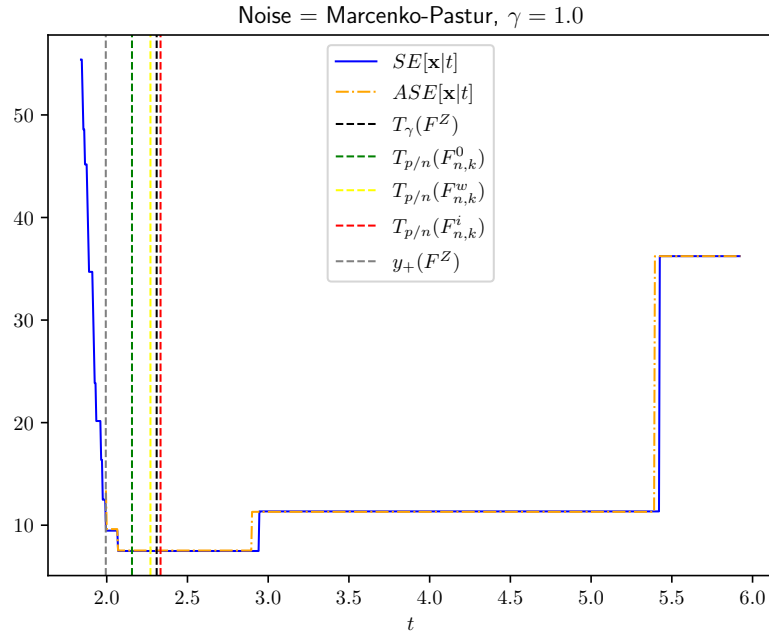
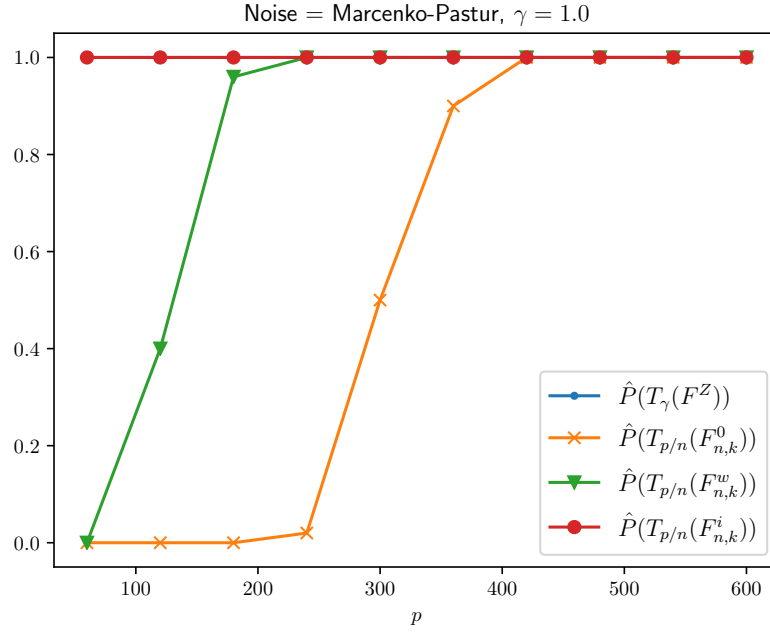
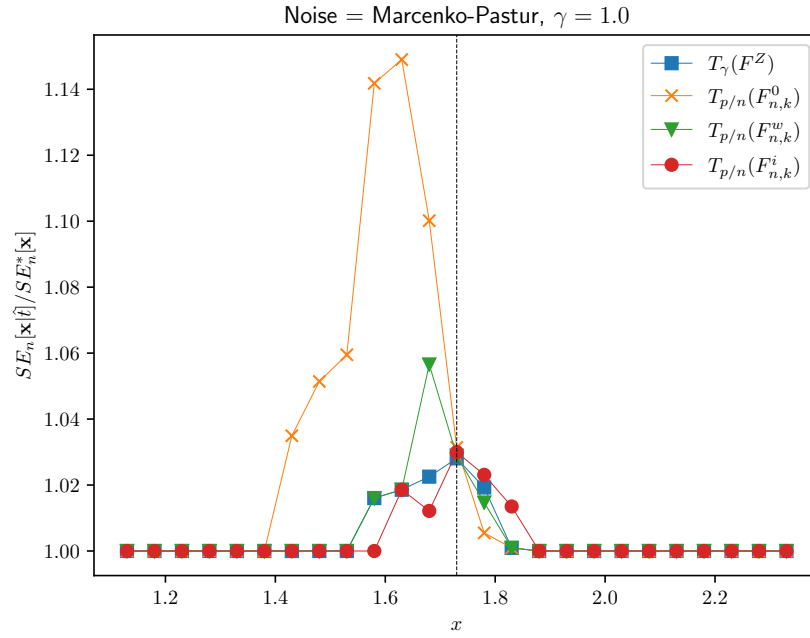
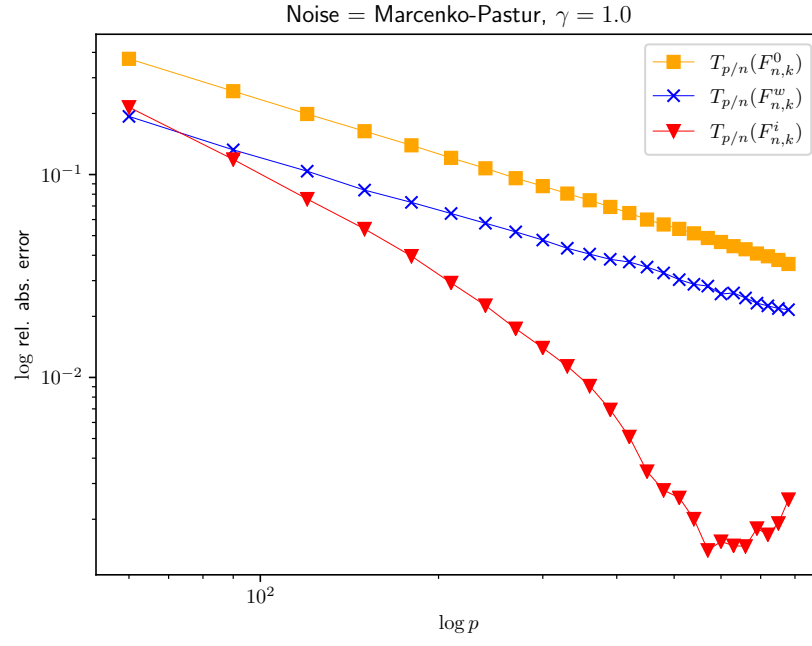


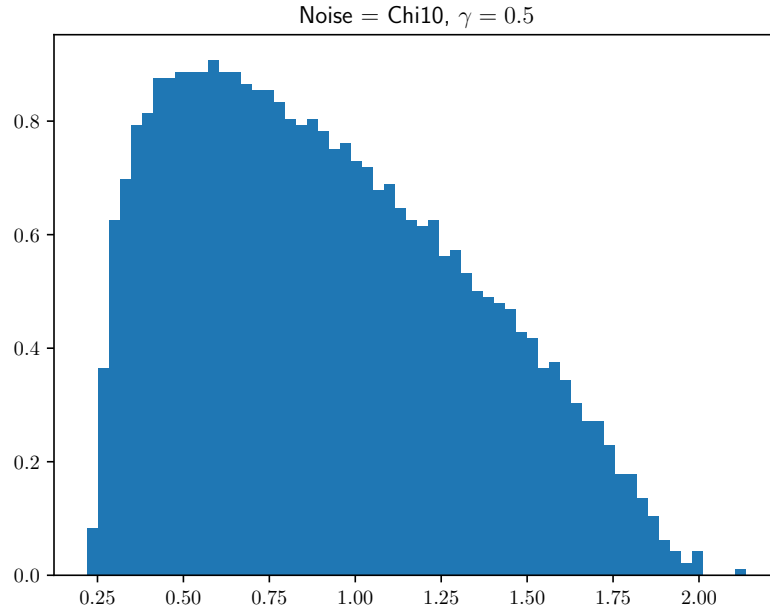
Fig 6: Experiment: **Hist**

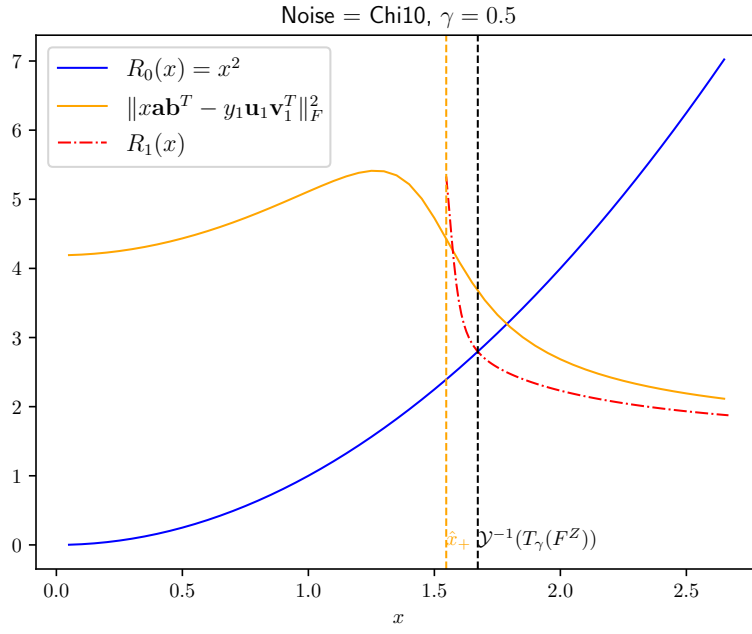
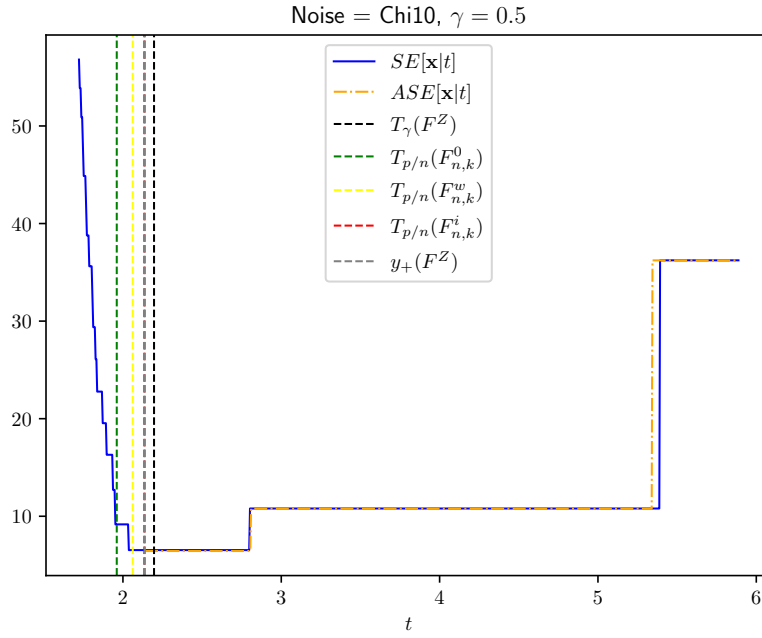
Fig 7: Experiment: **R0-vs-R1**Fig 8: Experiment: **SE-vs-ASE**

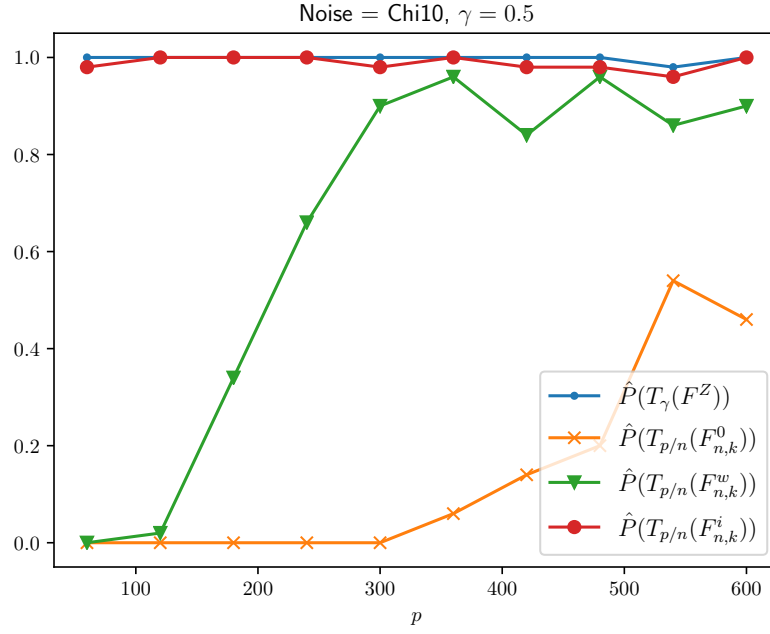
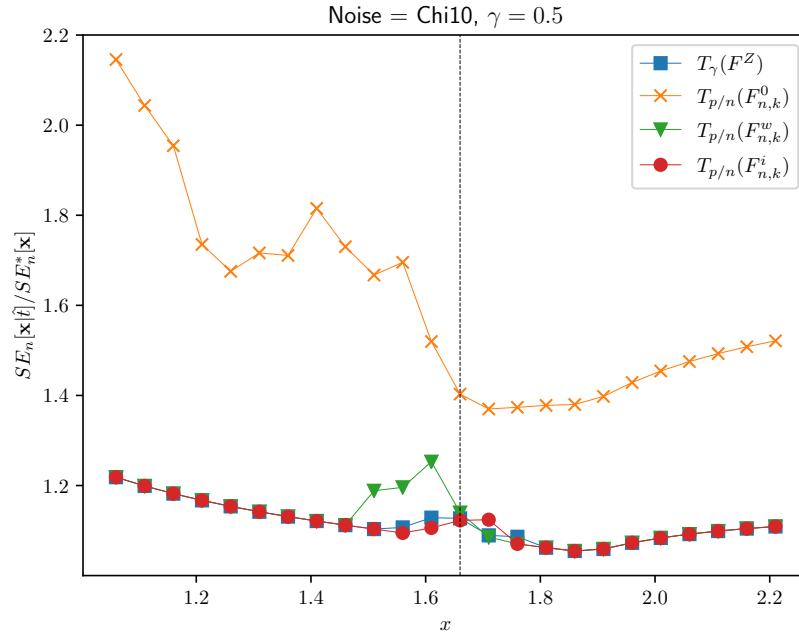
Fig 9: Experiment: **OracleAttainment**Fig 10: Experiment: **Regret**

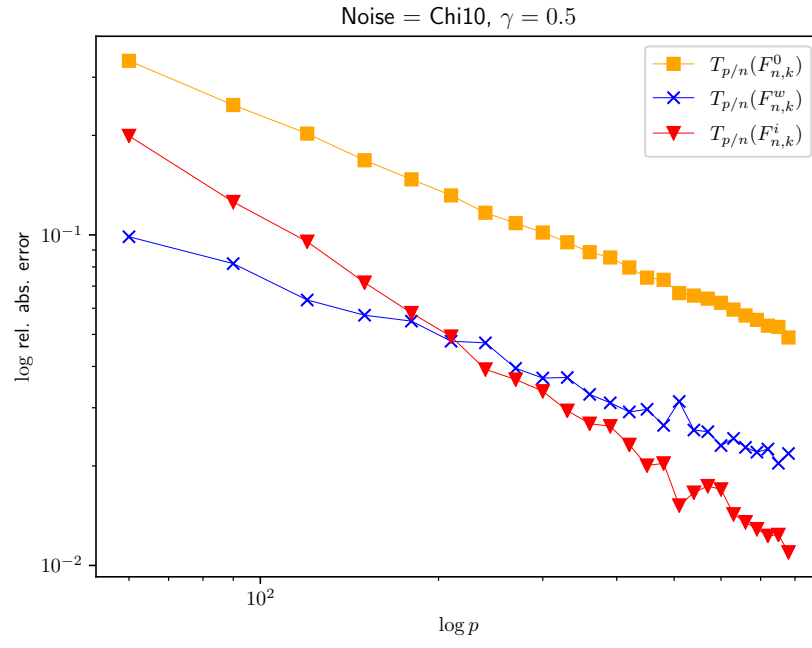
Fig 11: Experiment: **ConvergenceRate**

E.4. Distribution: *Chi10*, $\gamma = 0.5$

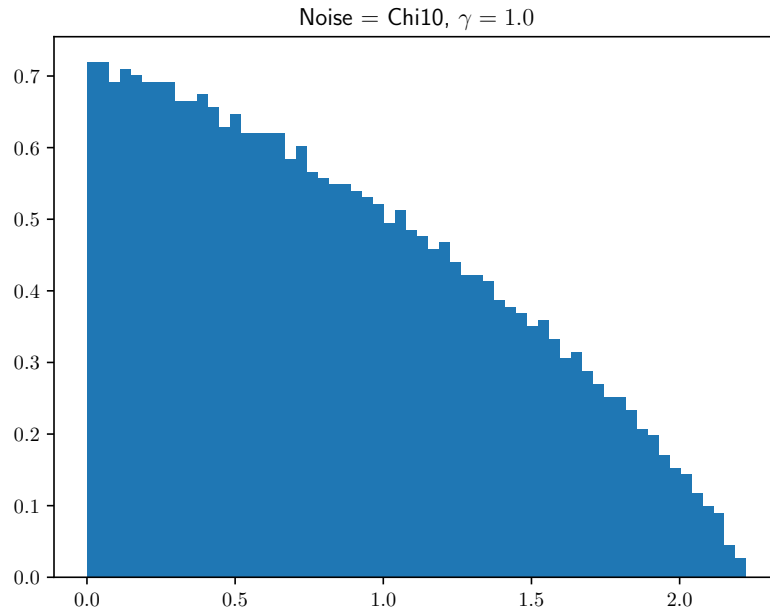
Fig 12: Experiment: **Hist**

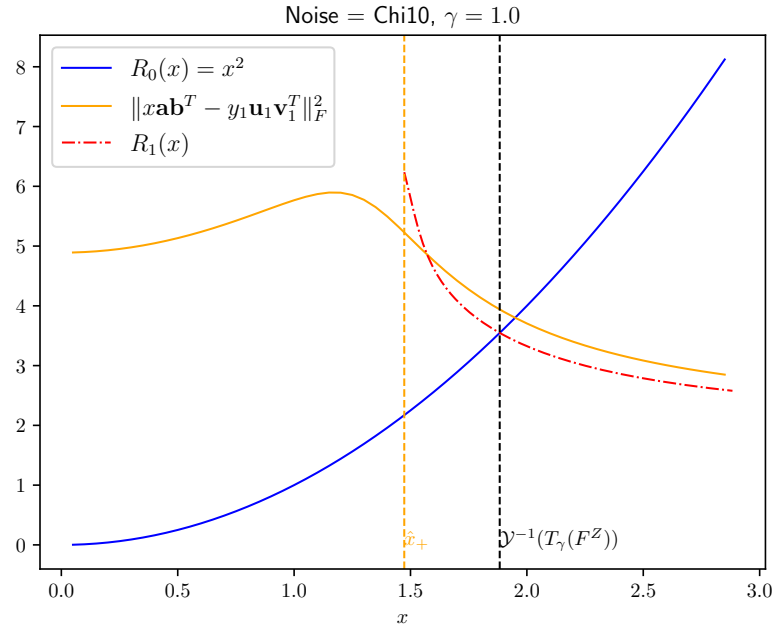
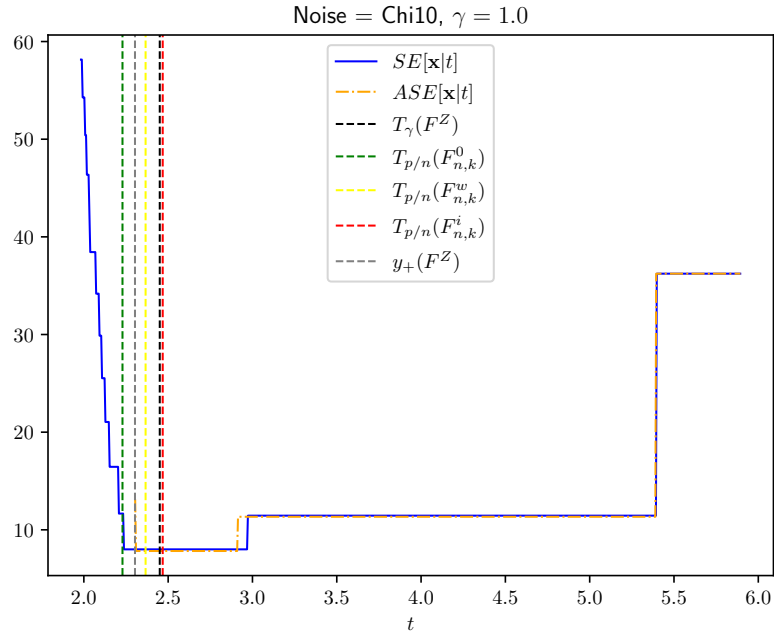
Fig 13: Experiment: **R0-vs-R1**Fig 14: Experiment: **SE-vs-ASE**

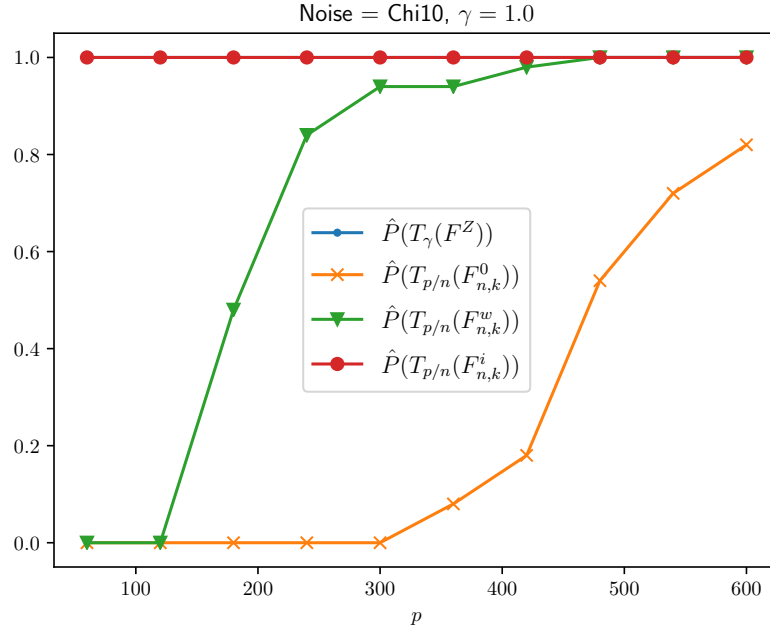
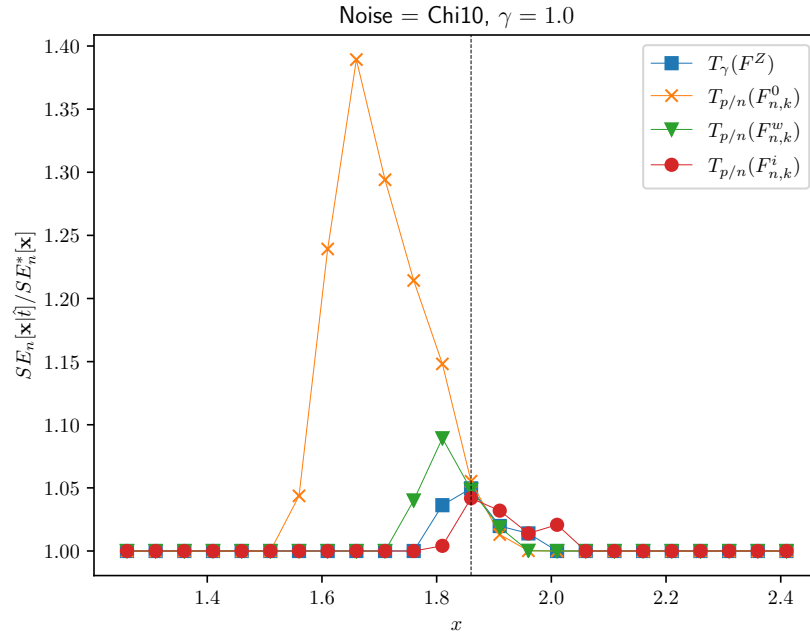
Fig 15: Experiment: **OracleAttainment**Fig 16: Experiment: **Regret**

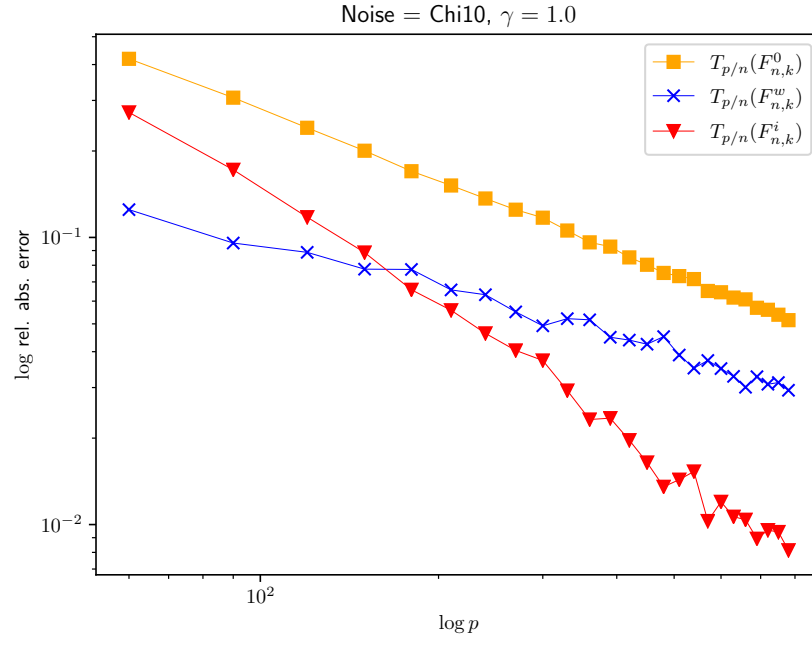
Fig 17: Experiment: **ConvergenceRate**

E.5. Distribution: Chi10, $\gamma = 1.0$

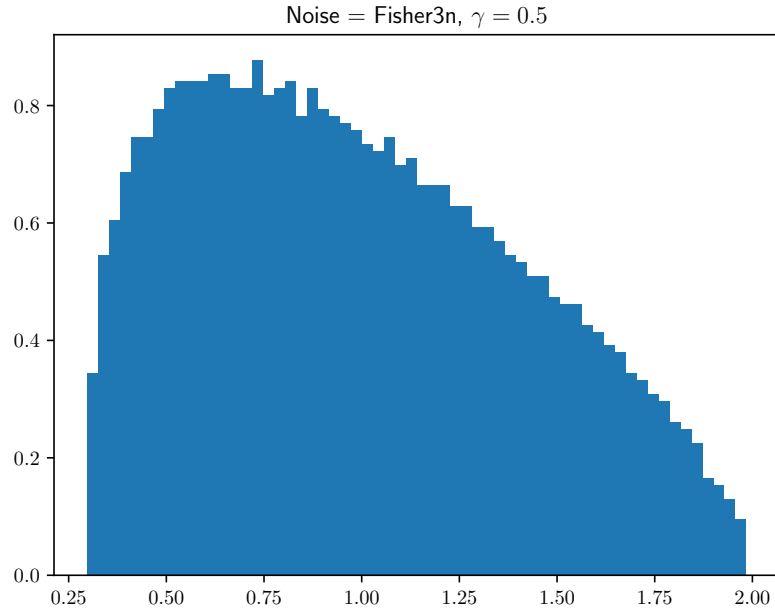
Fig 18: Experiment: **Hist**

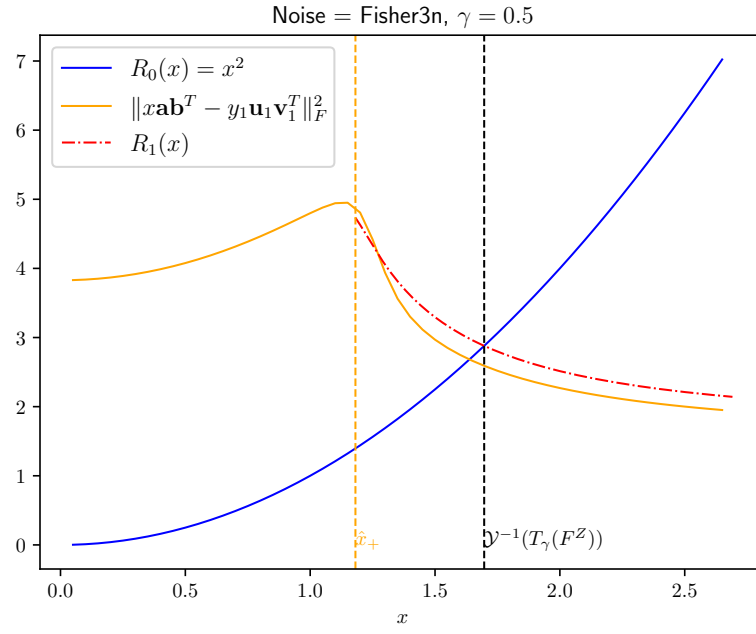
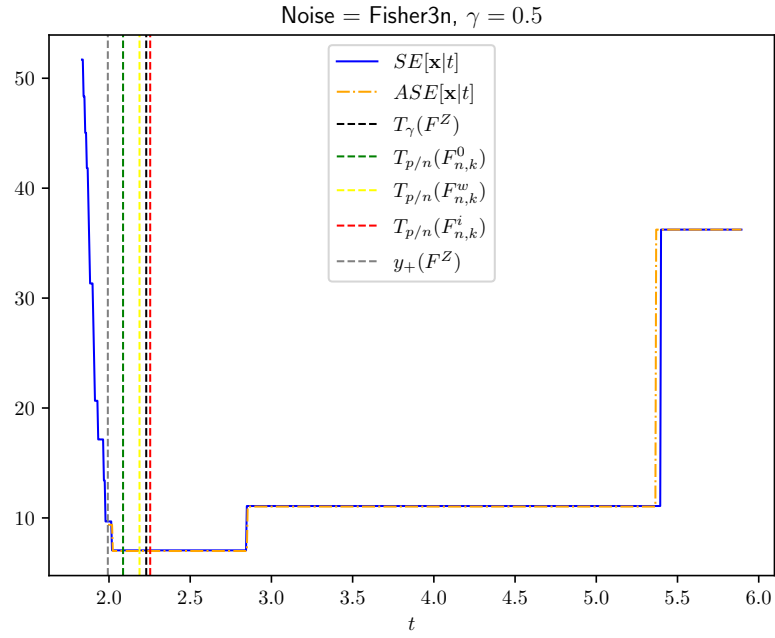
Fig 19: Experiment: **R0-vs-R1**Fig 20: Experiment: **SE-vs-ASE**

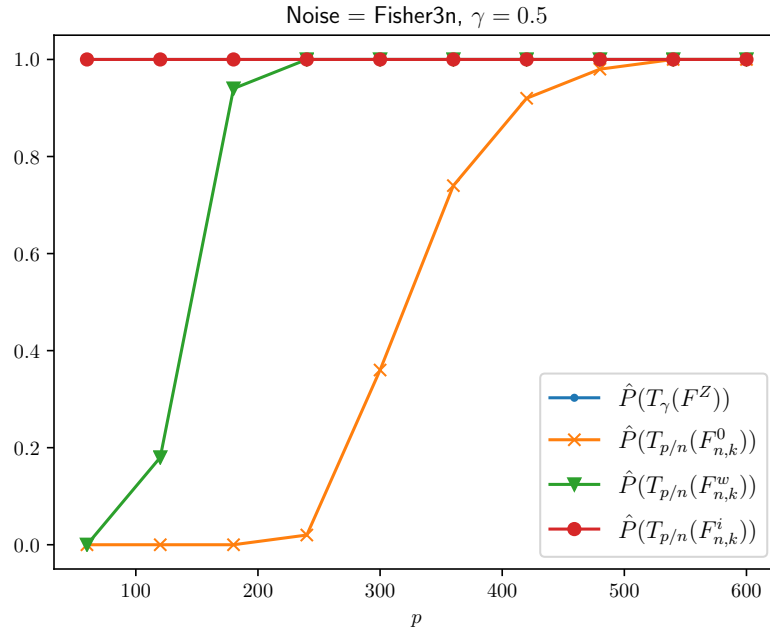
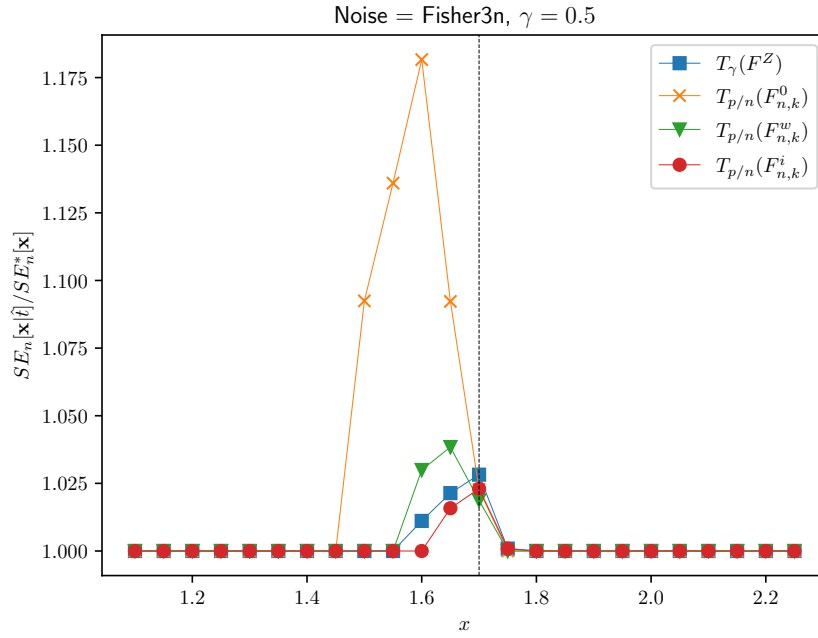
Fig 21: Experiment: **OracleAttainment**Fig 22: Experiment: **Regret**

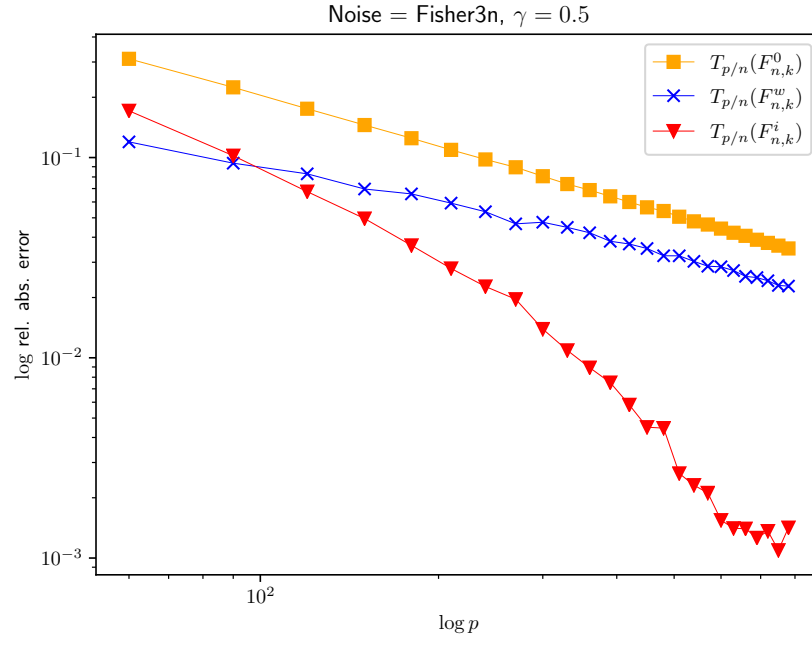
Fig 23: Experiment: **ConvergenceRate**

E.6. Distribution: Fisher3n, $\gamma = 0.5$

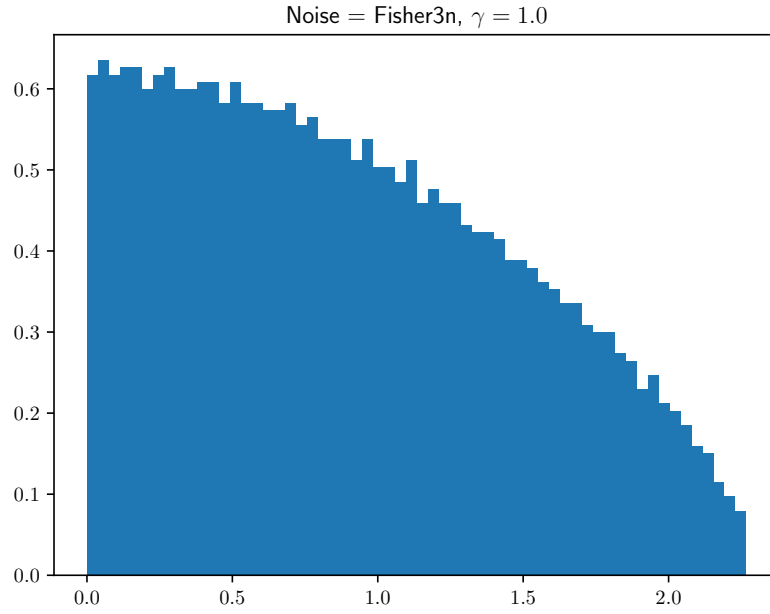
Fig 24: Experiment: **Hist**

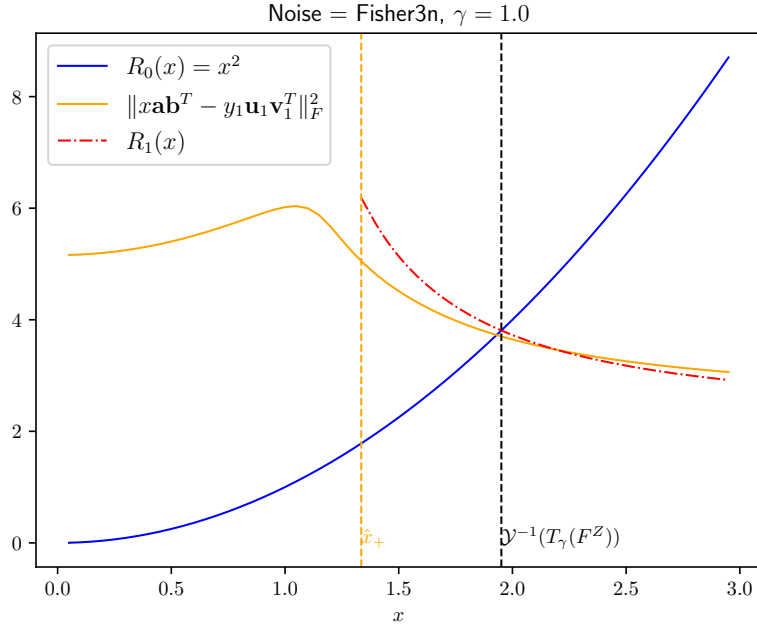
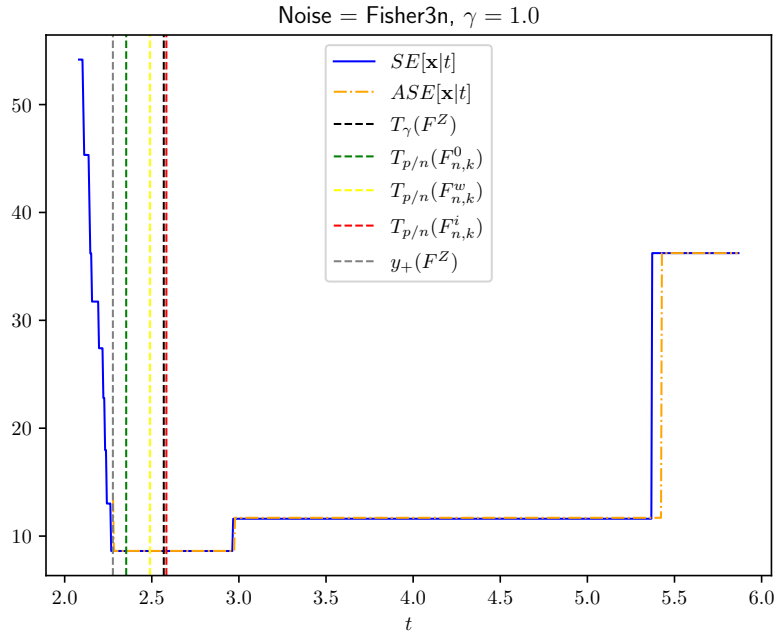
Fig 25: Experiment: **R0-vs-R1**Fig 26: Experiment: **SE-vs-ASE**

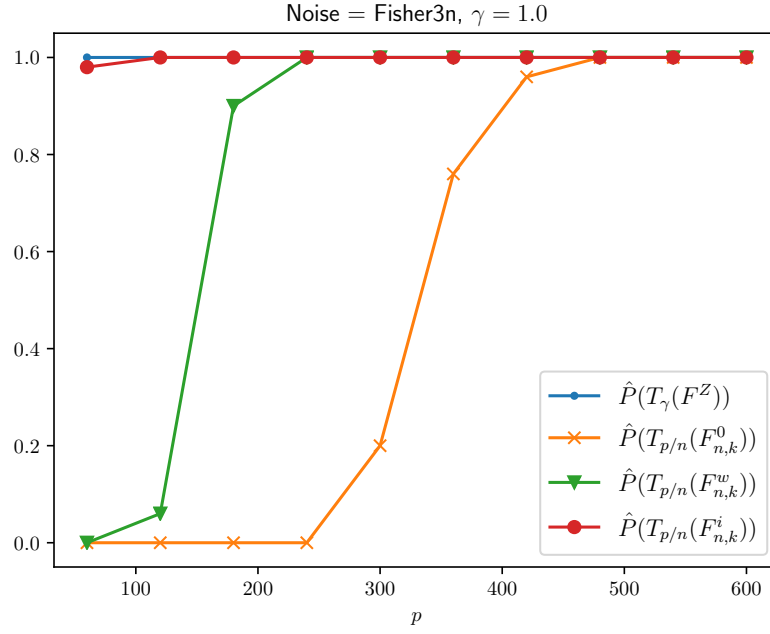
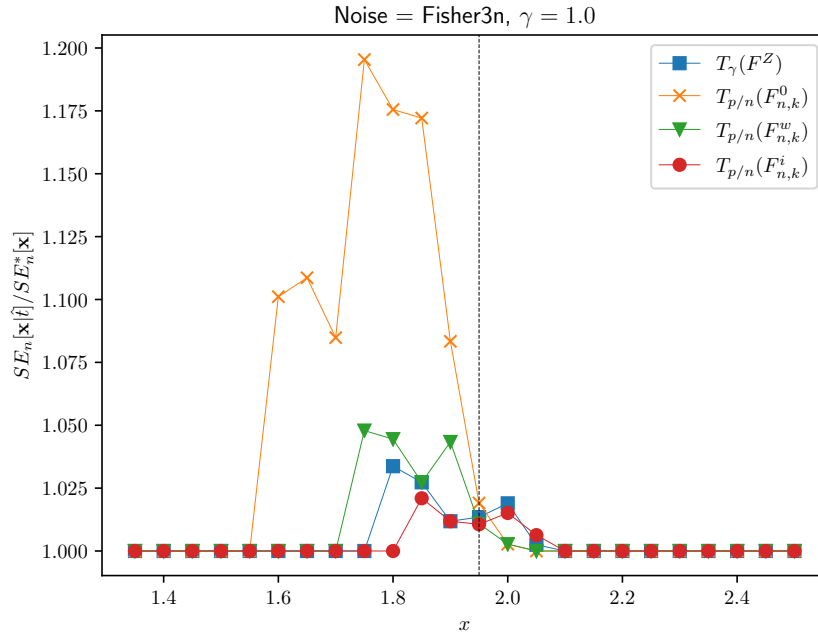
Fig 27: Experiment: **OracleAttainment**Fig 28: Experiment: **Regret**

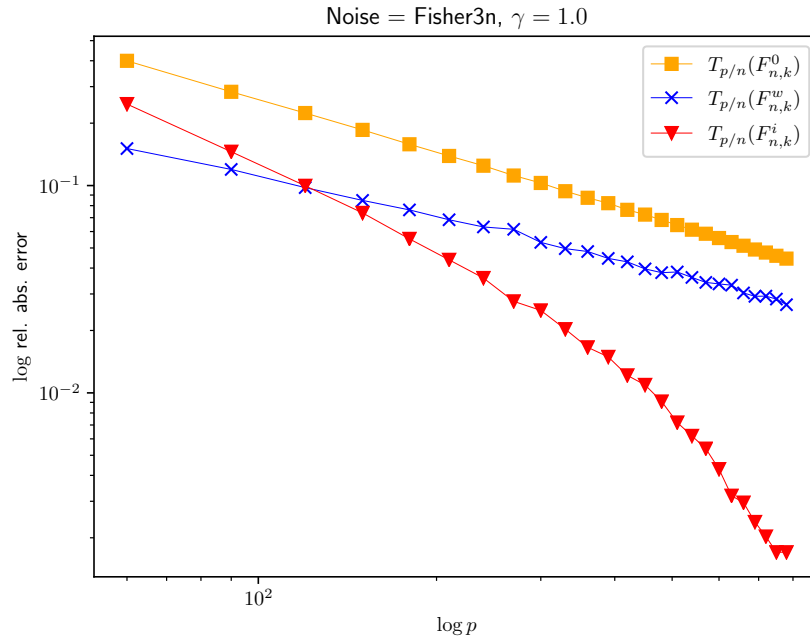
Fig 29: Experiment: **ConvergenceRate**

E.7. Distribution: Fisher3n, $\gamma = 1.0$

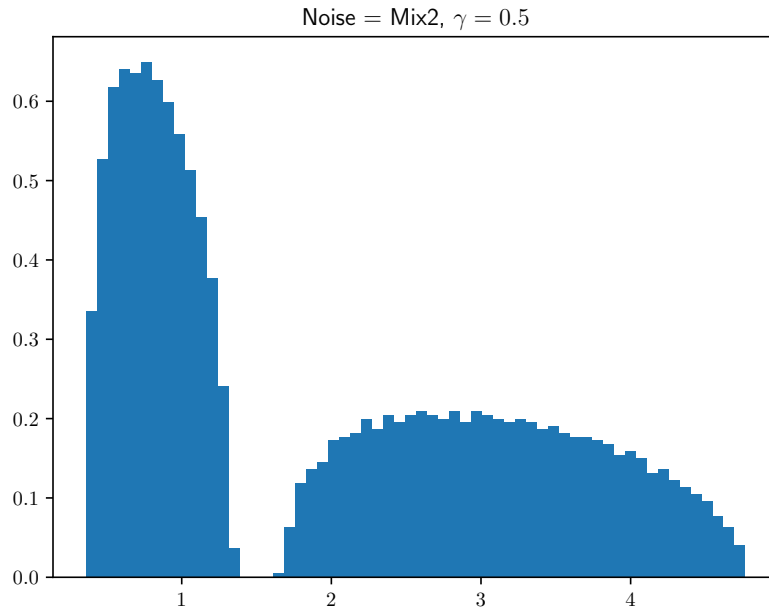
Fig 30: Experiment: **Hist**

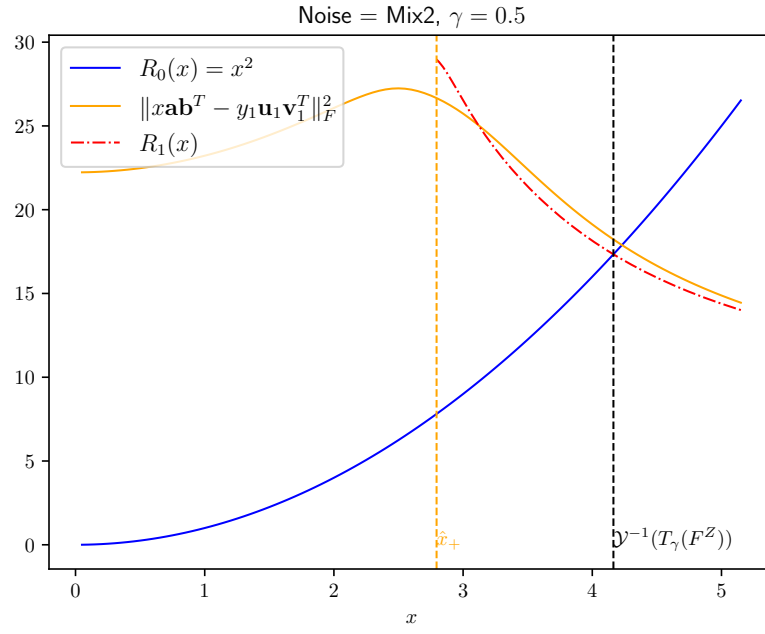
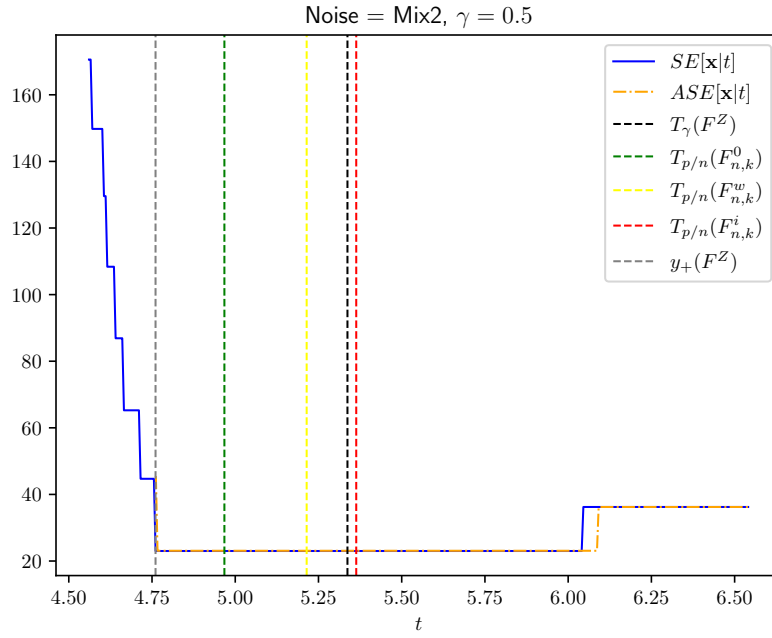
Fig 31: Experiment: **R0-vs-R1**Fig 32: Experiment: **SE-vs-ASE**

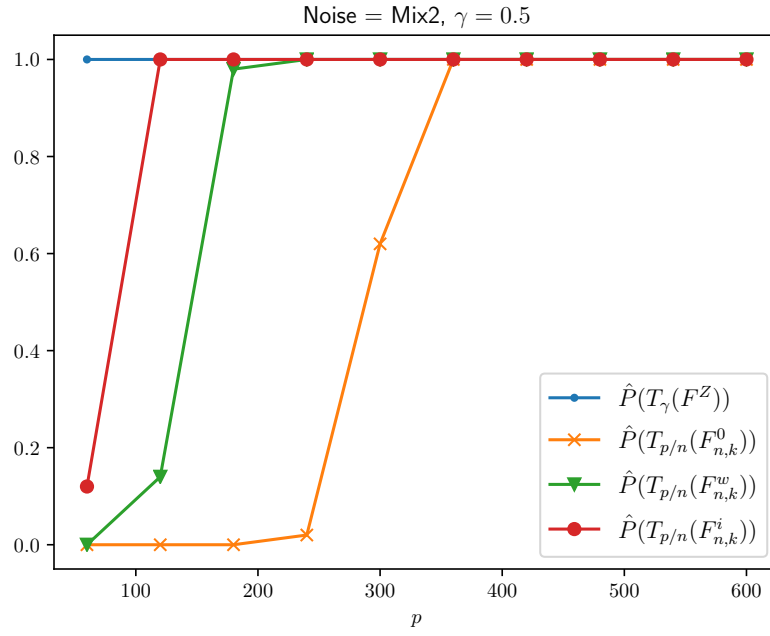
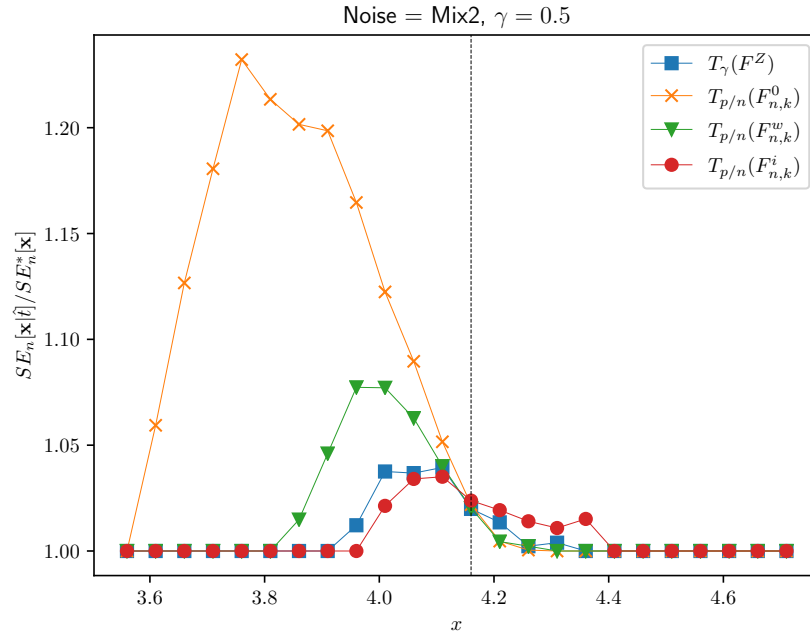
Fig 33: Experiment: **OracleAttainment**Fig 34: Experiment: **Regret**

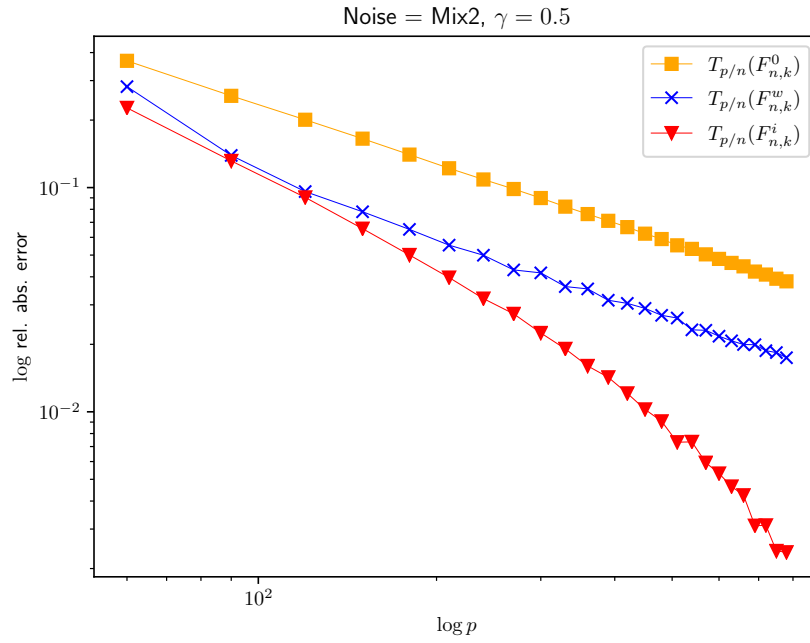
Fig 35: Experiment: **ConvergenceRate**

E.8. Distribution: Mix2, $\gamma = 0.5$

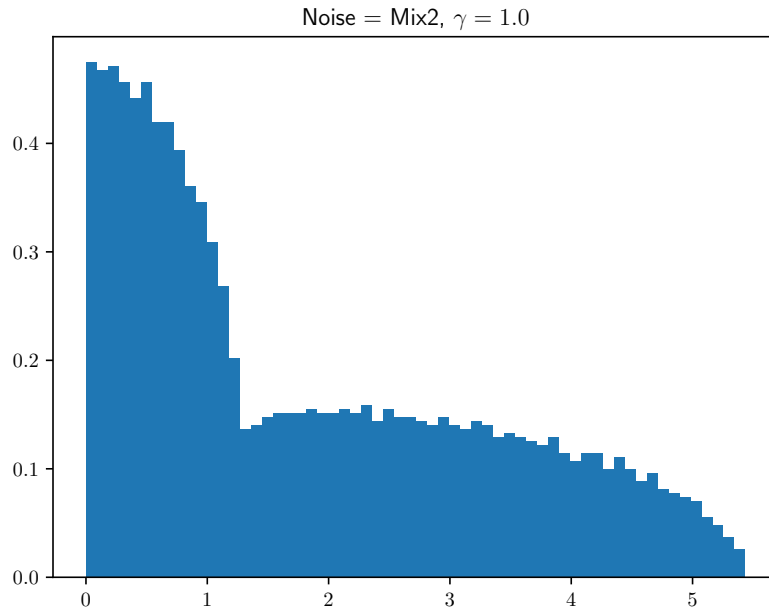
Fig 36: Experiment: **Hist**

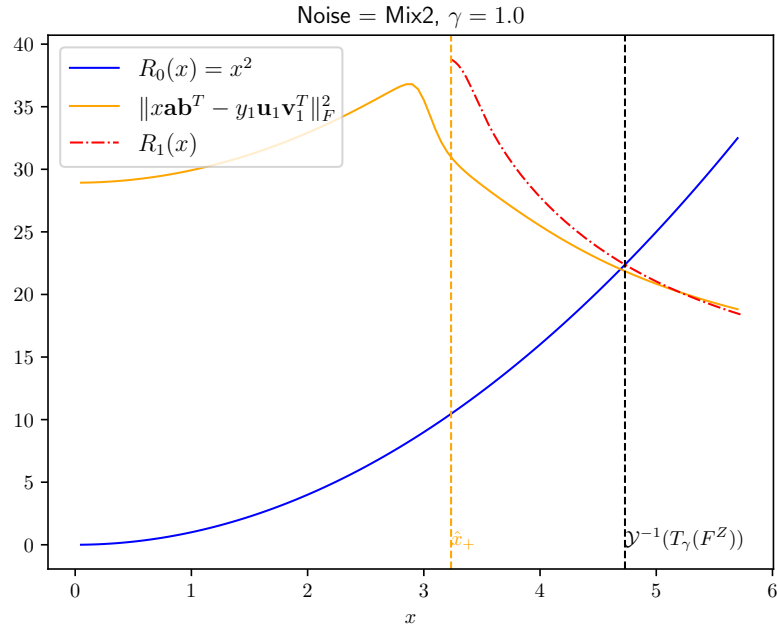
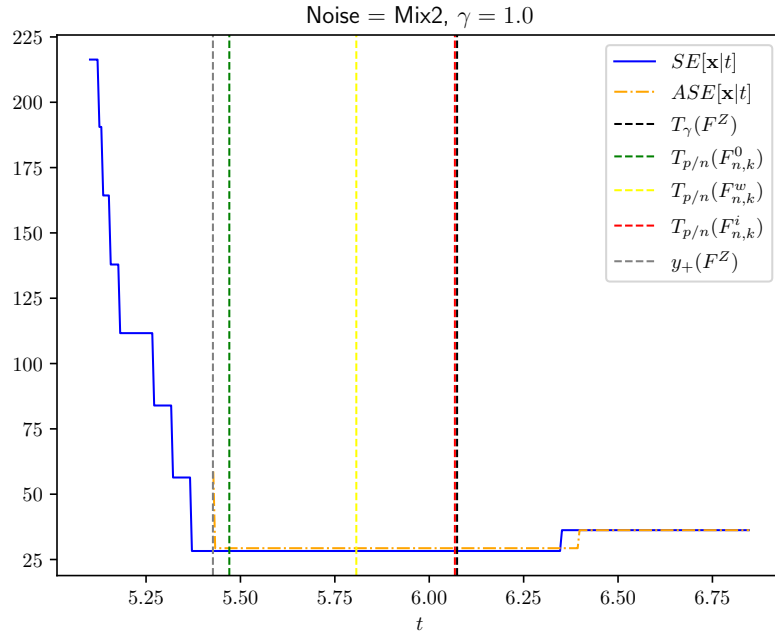
Fig 37: Experiment: **R0-vs-R1**Fig 38: Experiment: **SE-vs-ASE**

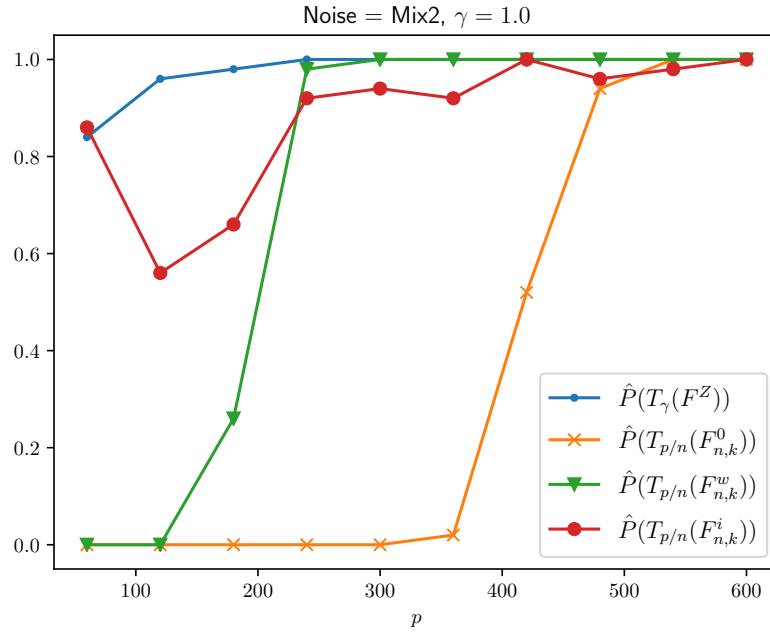
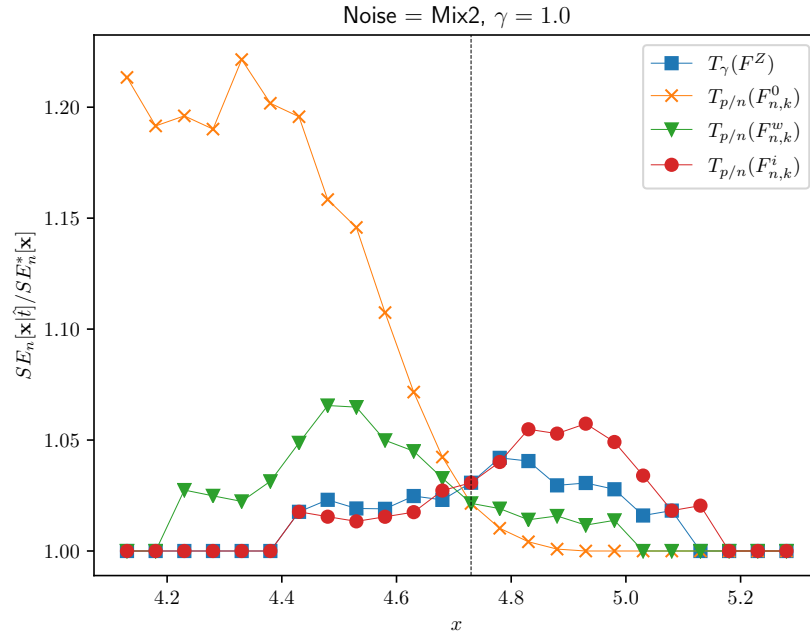
Fig 39: Experiment: **OracleAttainment**Fig 40: Experiment: **Regret**

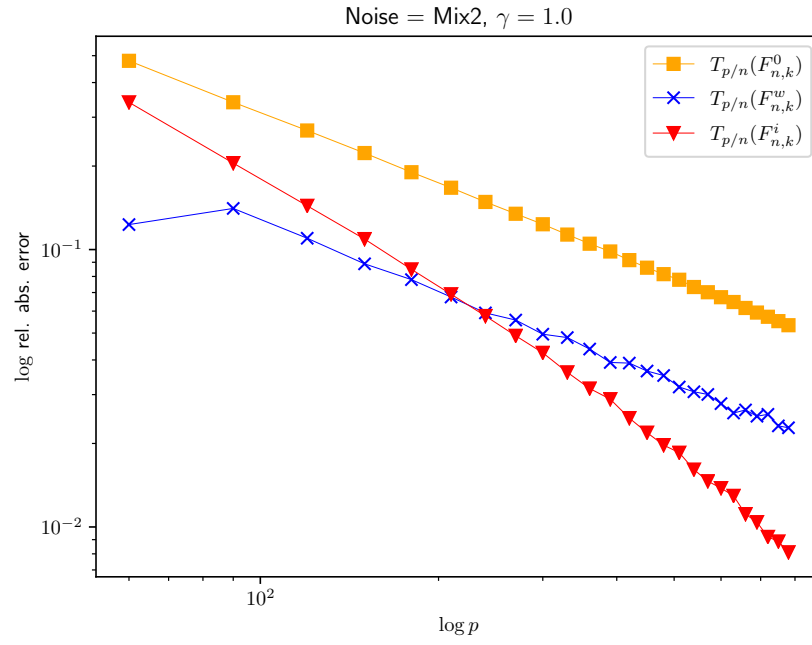
Fig 41: Experiment: **ConvergenceRate**

E.9. Distribution: Mix2, $\gamma = 1.0$

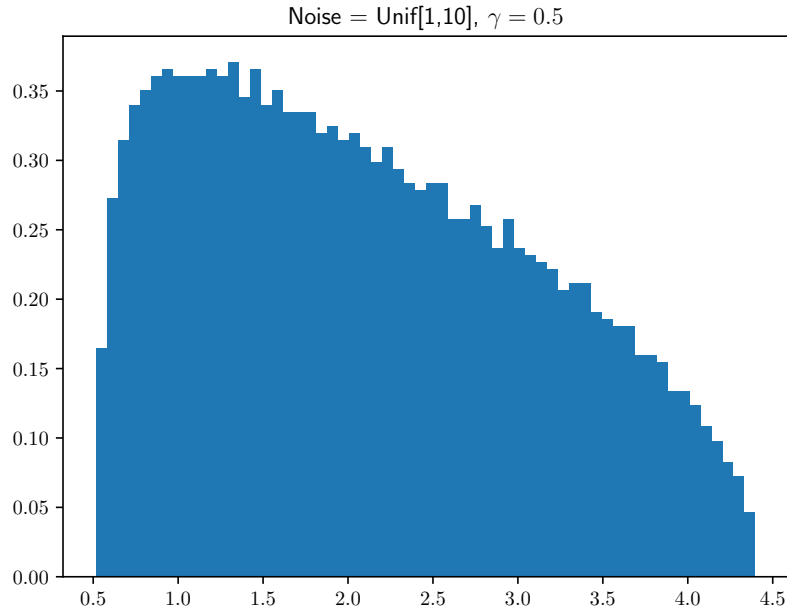
Fig 42: Experiment: **Hist**

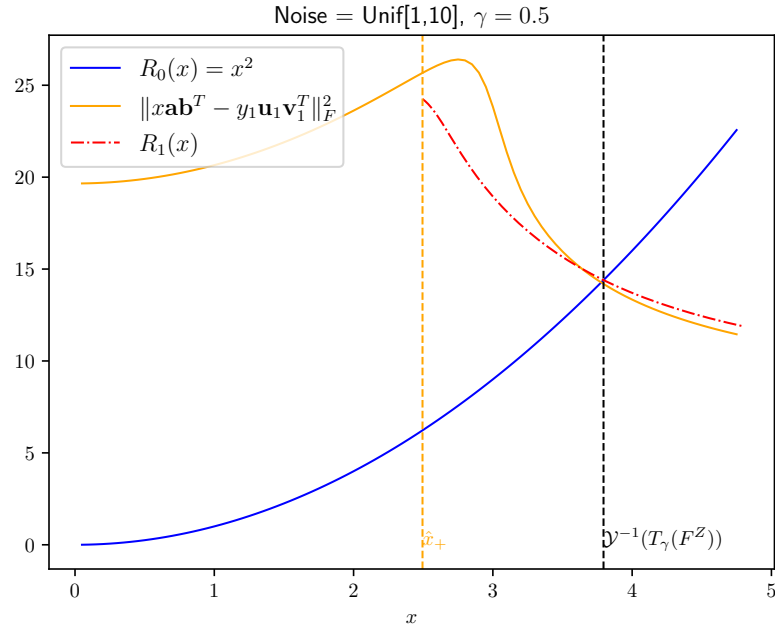
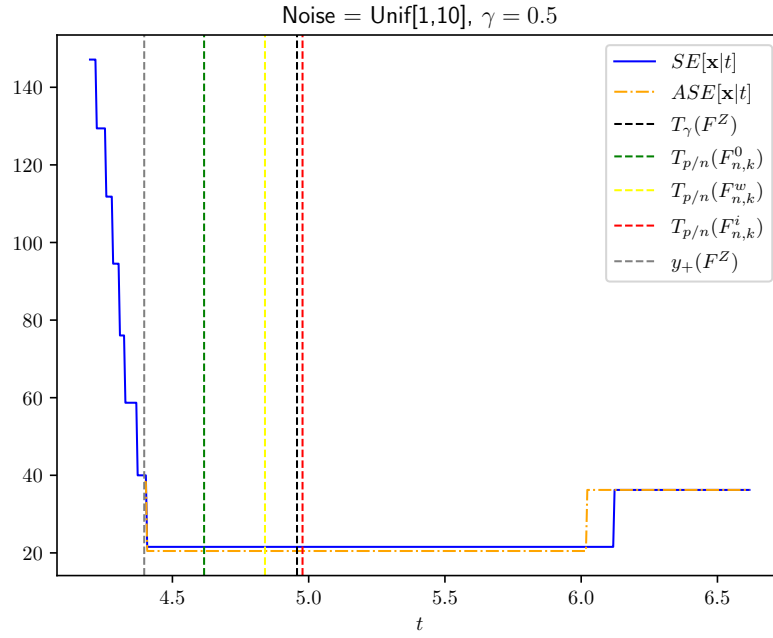
Fig 43: Experiment: **R0-vs-R1**Fig 44: Experiment: **SE-vs-ASE**

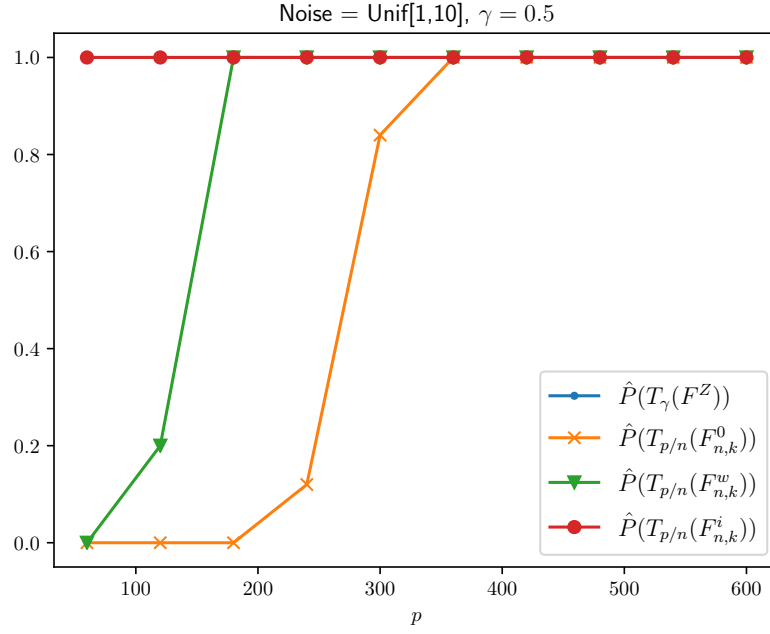
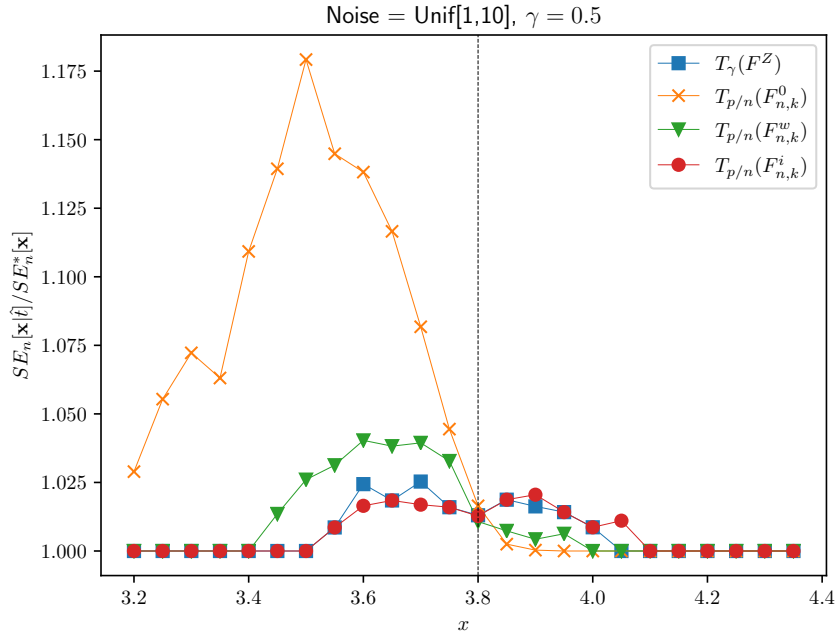
Fig 45: Experiment: **OracleAttainment**Fig 46: Experiment: **Regret**

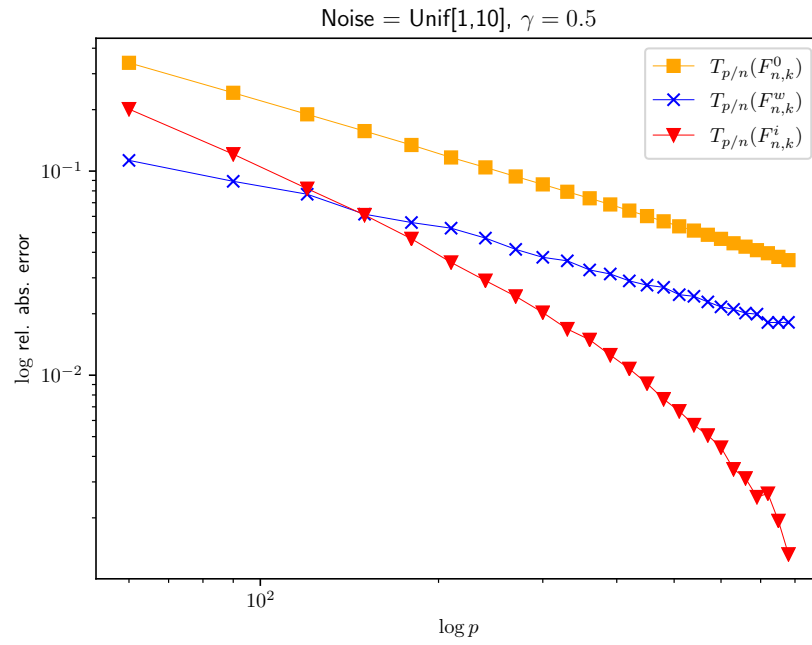
Fig 47: Experiment: **ConvergenceRate**

E.10. Distribution: Unif[1,10], $\gamma = 0.5$

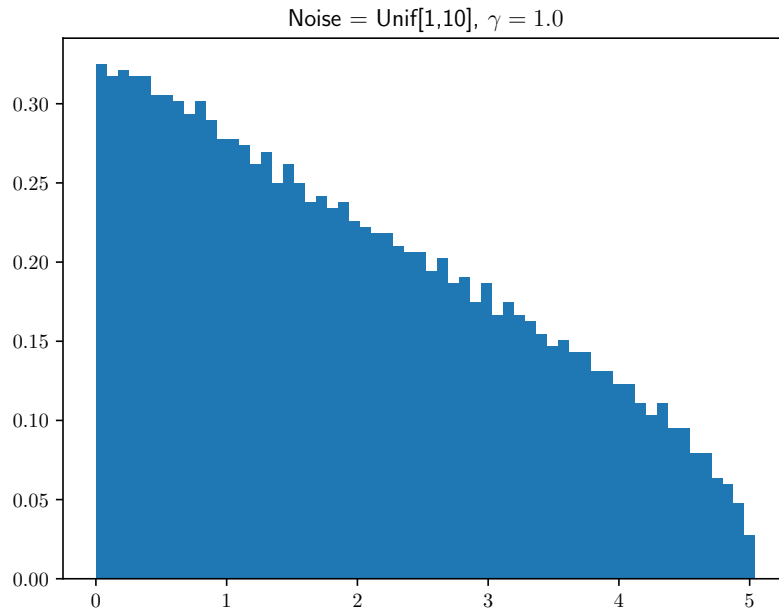
Fig 48: Experiment: **Hist**

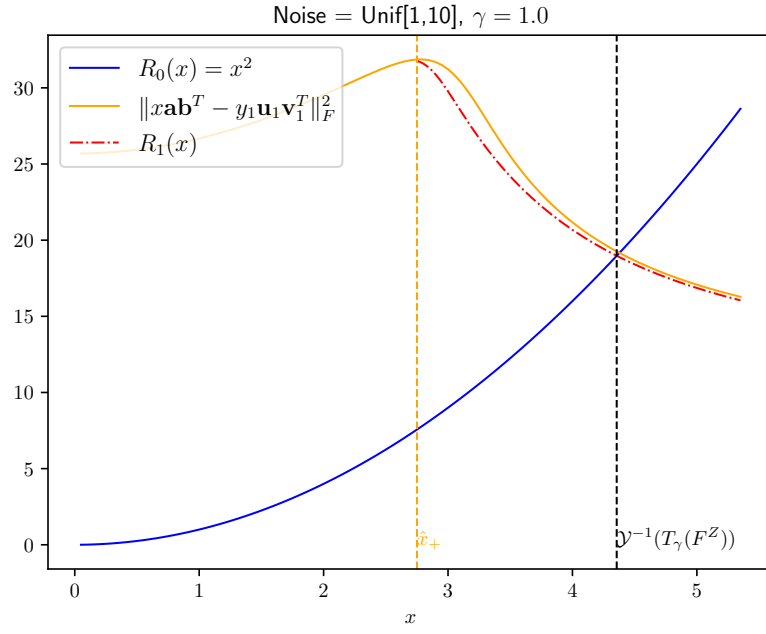
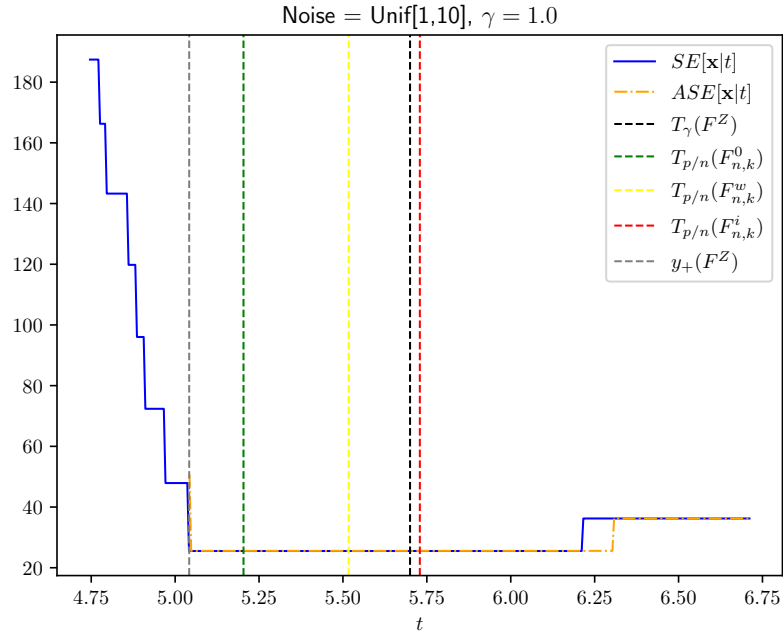
Fig 49: Experiment: **R0-vs-R1**Fig 50: Experiment: **SE-vs-ASE**

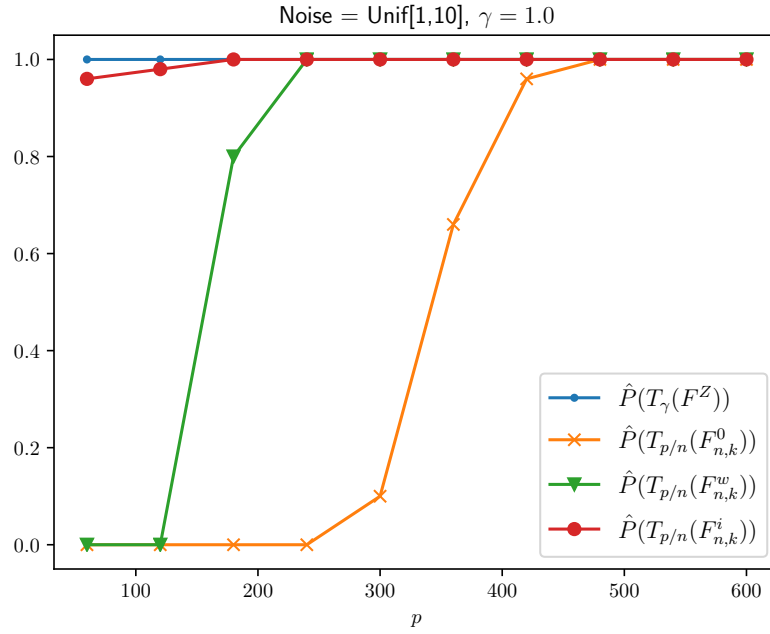
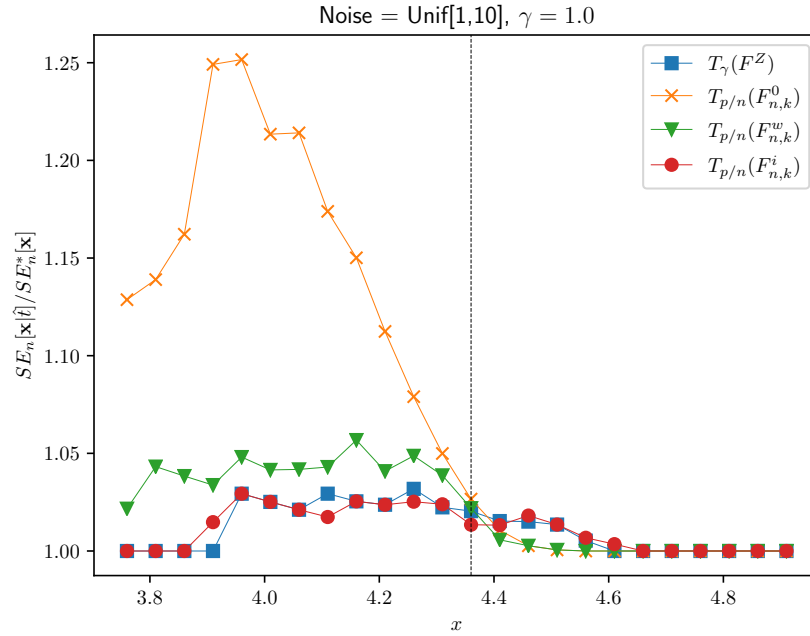
Fig 51: Experiment: **OracleAttainment**Fig 52: Experiment: **Regret**

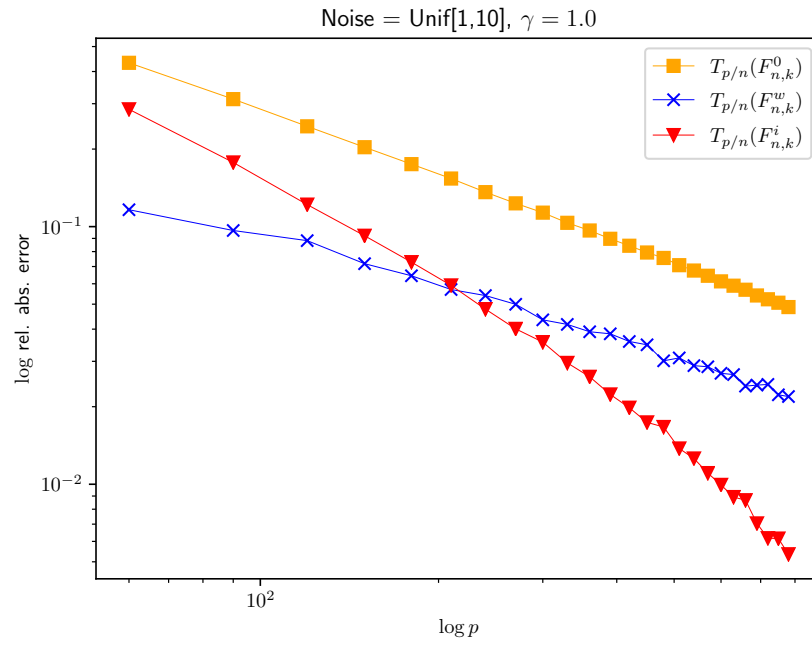
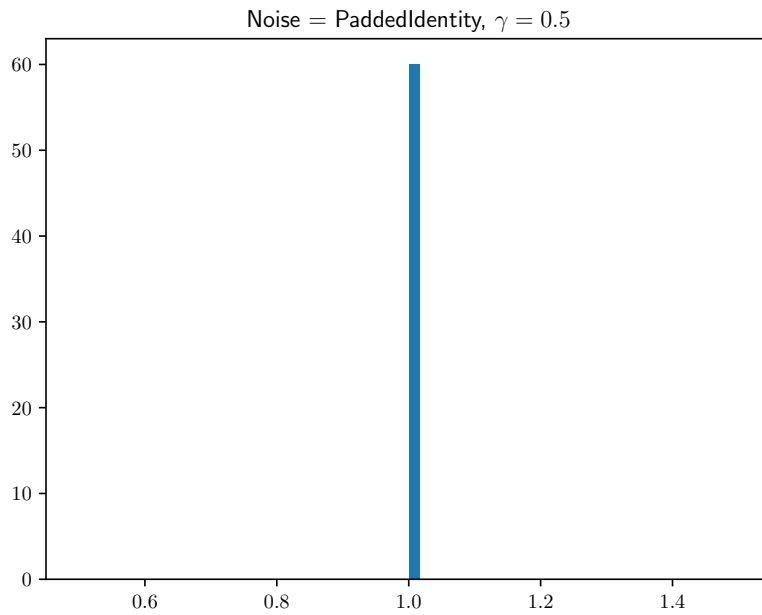
Fig 53: Experiment: **ConvergenceRate**

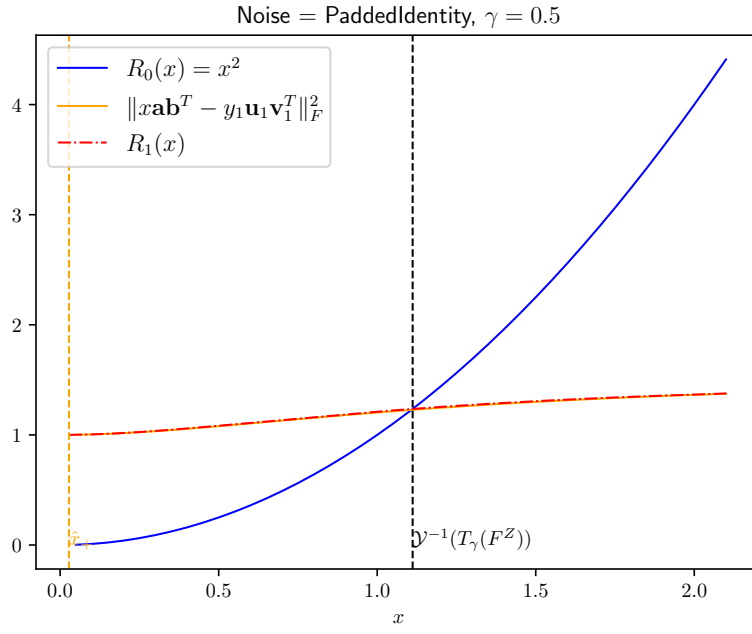
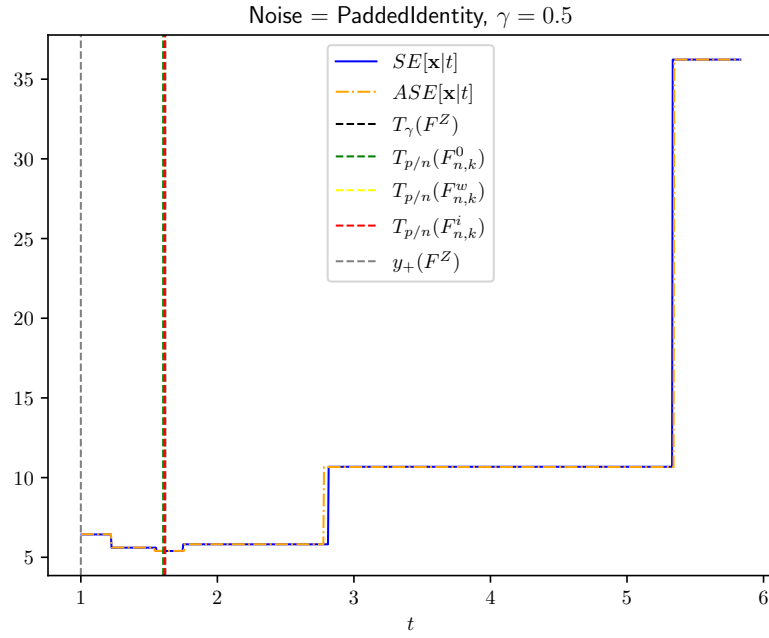
E.11. Distribution: Unif[1,10], $\gamma = 1.0$

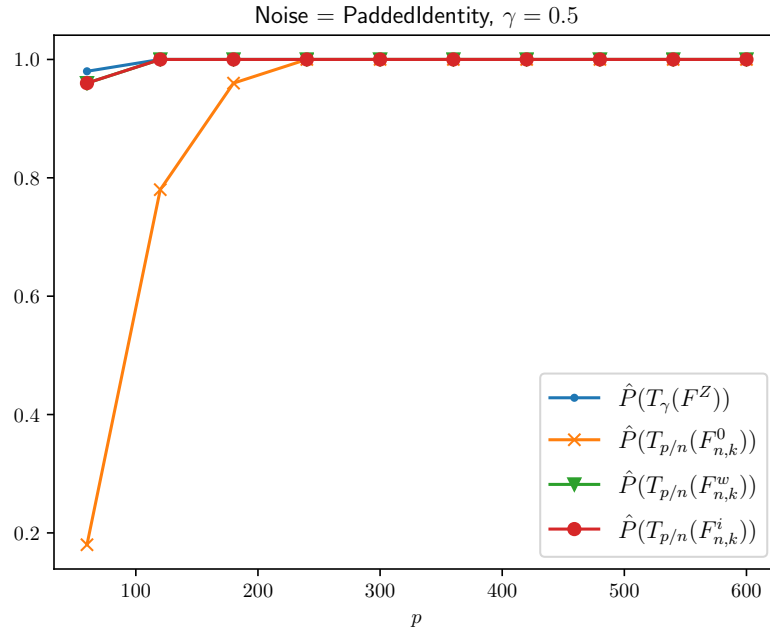
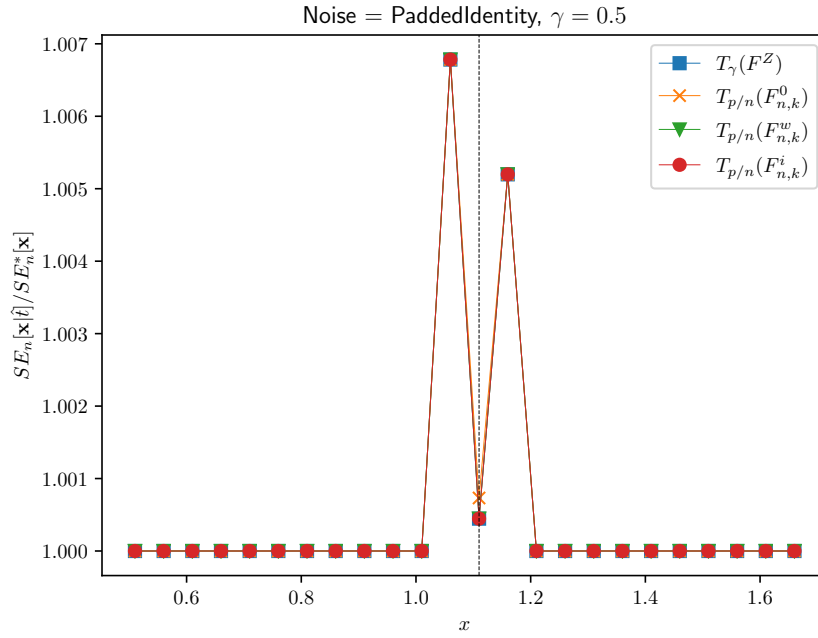
Fig 54: Experiment: **Hist**

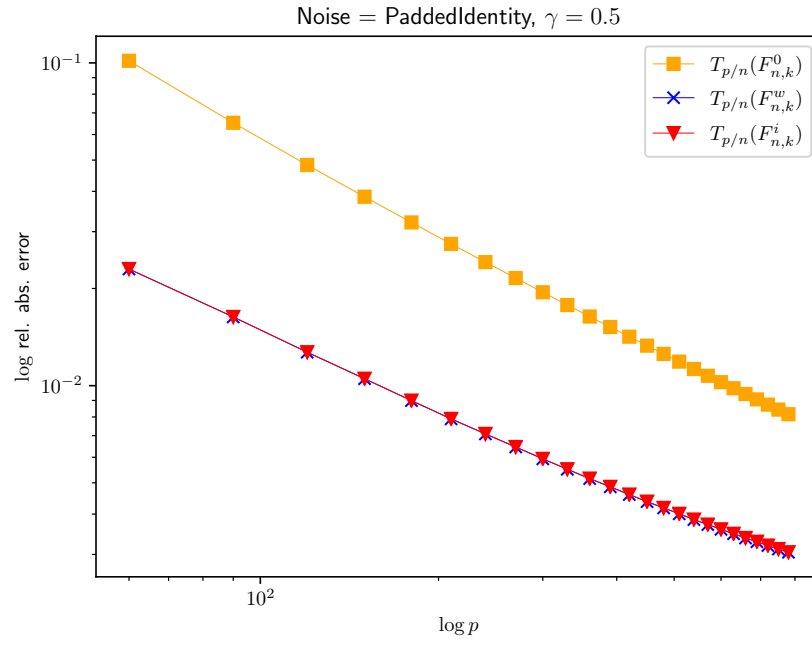
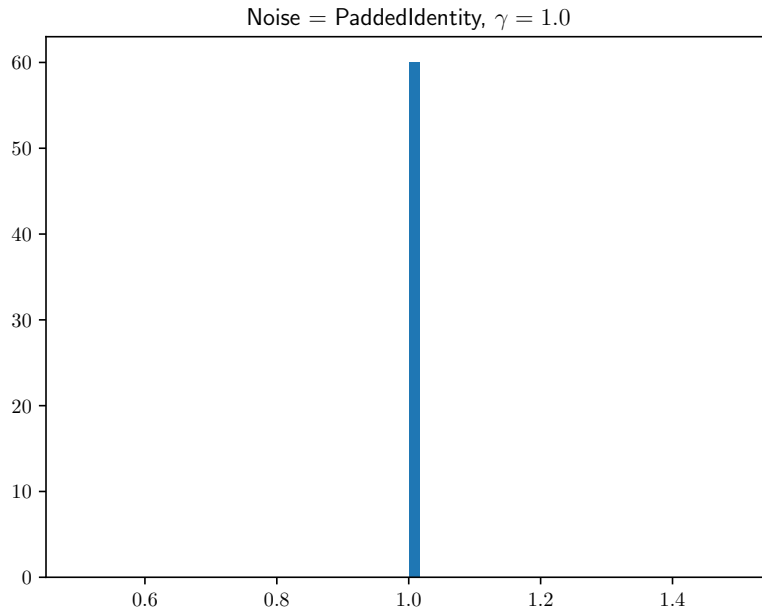
Fig 55: Experiment: **R0-vs-R1**Fig 56: Experiment: **SE-vs-ASE**

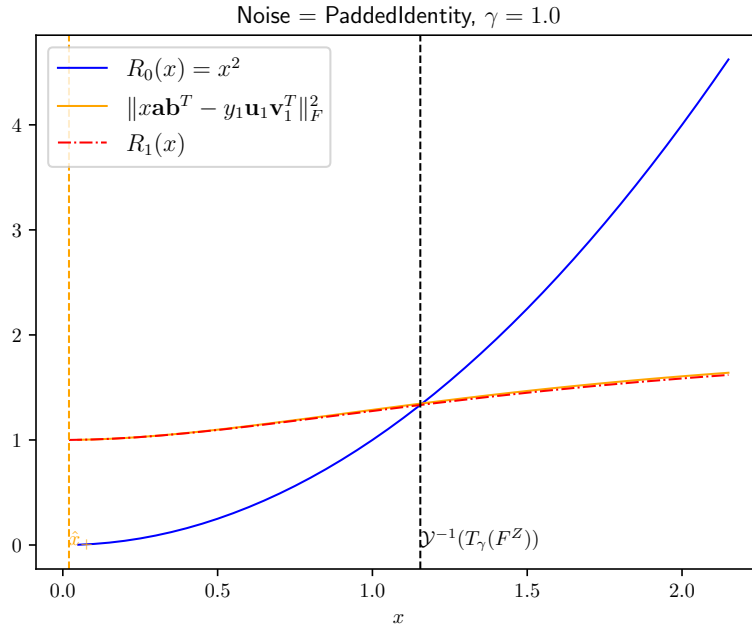
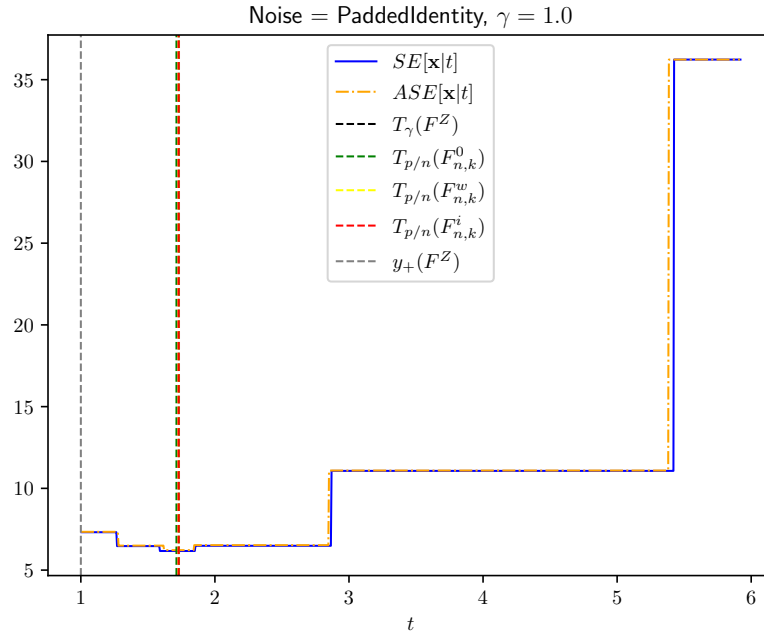
Fig 57: Experiment: **OracleAttainment**Fig 58: Experiment: **Regret**

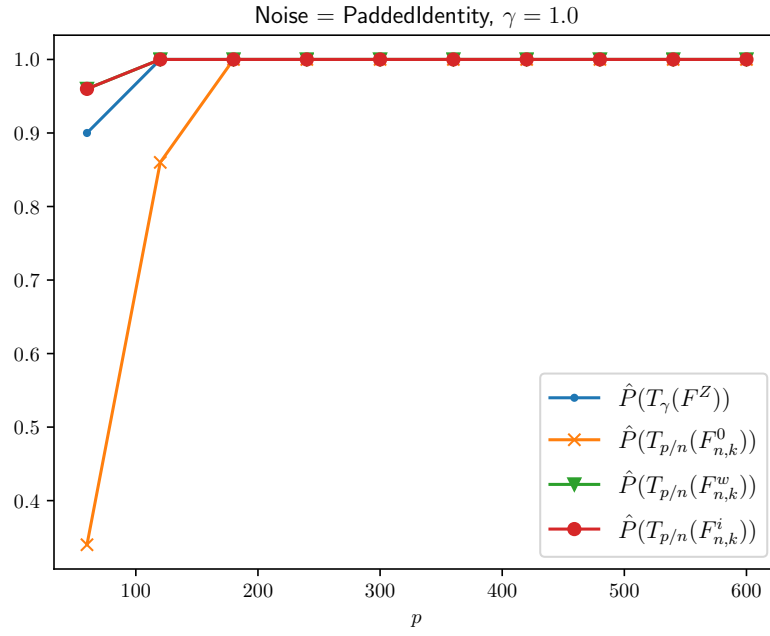
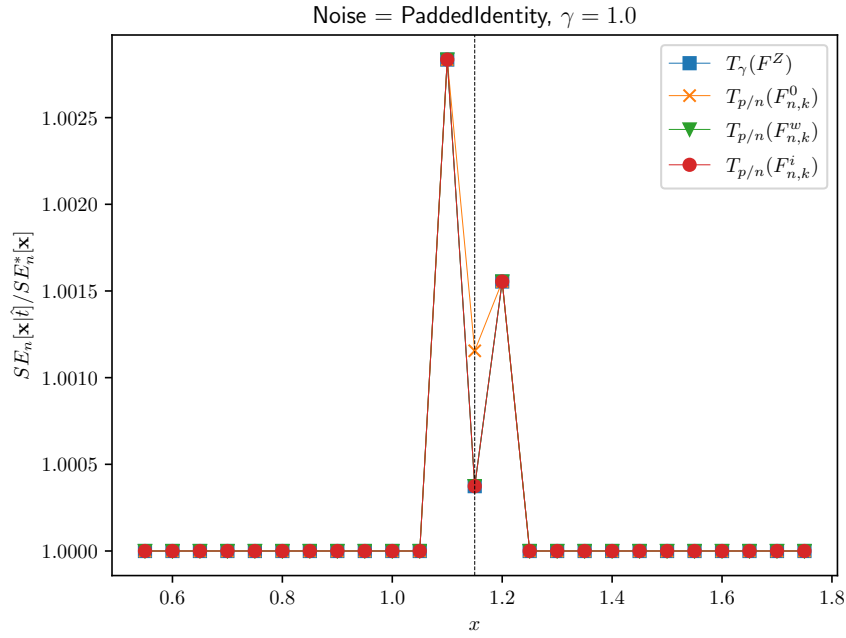
Fig 59: Experiment: **ConvergenceRate****E.12. Distribution: PaddedIdentity, $\gamma = 0.5$** Fig 60: Experiment: **Hist**

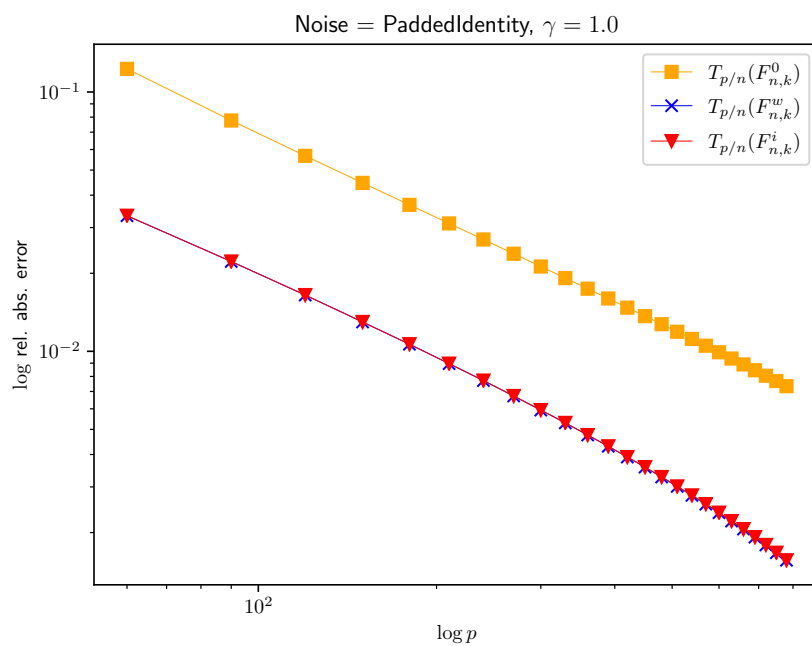
Fig 61: Experiment: **R0-vs-R1**Fig 62: Experiment: **SE-vs-ASE**

Fig 63: Experiment: **OracleAttainment**Fig 64: Experiment: **Regret**

Fig 65: Experiment: **ConvergenceRate****E.13. Distribution: PaddedIdentity, $\gamma = 1.0$** Fig 66: Experiment: **Hist**

Fig 67: Experiment: **R0-vs-R1**Fig 68: Experiment: **SE-vs-ASE**

Fig 69: Experiment: **OracleAttainment**Fig 70: Experiment: **Regret**

Fig 71: Experiment: **ConvergenceRate**